Topics in Multisensor Maneuvering Target Tracking

Except where reference is made to the work of others, the work described in this dissertation is my own or was done in collaboration with my advisory committee. This dissertation does not include proprietary or classified information.

Soonho Jeong

Certificate of Approval:

Stanley J. Reeves
Professor
Department of Electrical and Computer Engineering

Jitendra K. Tugnait, Chair
James B. Davis Professor
Department of Electrical and Computer Engineering

Thomas S. Denney Jr.
Associate Professor
Department of Electrical and Computer Engineering

Stephen L. McFarland
Dean
Graduate School

# Topics in Multisensor Maneuvering Target Tracking

Soonho Jeong

A Dissertation

Submitted to

the Graduate Faculty of

Auburn University

in Partial Fulfillment of the

Requirements for the

Degree of

Doctor of Philosophy

Auburn, Alabama
August 8, 2005

Topics in Multisensor Maneuvering Target Tracking

Soonho Jeong

Permission is granted to Auburn University to make copies of this thesis at its discretion, upon the request of individuals or institutions and at their expense. The author reserves all publication rights.

_____

Signature of Author

_____

Date

# Vita

Soonho Jeong, a Korean Army Major, was born on December 7, 1967 in Seoul, Republic of Korea (ROK), the third of four children of Wansuk Jeong and Jungja Hwang.

He graduated from Daewon High School, in Seoul, Korea, in 1986. He received the B.S. and M.S. degrees in electrical engineering from Korea Military Academy, Seoul, Korea, in 1990 and Naval Postgraduate School, Monterey, CA, in 1996, respectively. From 1999 to 2002 he served in the Weapons Systems Management Group (WSMG), Korea Army Headquarters as an Intelligence Technology Officer (ITO). He entered the graduate program in Electrical Engineering at Auburn University in August 2002.

He married Jeesoo Song, daughter of Kibok Song and Sunmoon Park, on June 13, 1993. He has two daughters, Seoin Jeong and Jahyun Jeong, who were born in November 16, 1994 and in August 26, 1997, respectively.

Dissertation Abstract

Topics in Multisensor Maneuvering Target Tracking

Soonho Jeong

Doctor of Philosophy, August 8, 2005
(M.S., Naval Postgraduate School, Monterey, CA, March 1996)
(B.S., Korea Military Academy, Republic of Korea, March 1990)

207 Typed Pages

Directed by Jitendra K. Tugnait

Tracking uses models of the real environment to estimate the past and present and even predict the future state of a moving object from noisy observations of uncertain origin. In a tracking scenario the most critical problem is that of data-association. This topic has received considerable attention in the literature and a number of solutions have been proposed. This dissertation considers the problem of tracking highly maneuvering target(s) using multiple sensors in the presence of clutter. A set of noble algorithms are developed to handle this problem.

First, the basic interacting multiple model (IMM) approach has been combined with probabilistic data association (PDA) to develop an IMMPDA (interacting multiple model probabilistic data association) algorithm with simultaneous measurement update (SMU) for tracking a maneuvering target in clutter with multiple sensors.

Second, we extend our noble SMU algorithm to a more practical tracking scenario, that of tracking a maneuvering target with asynchronous (in-sequence but time delayed) measurements. A state-augmented approach is developed to estimate the time delay

between a local sensor (assumed to be collocated and synchronized with a central processor) and a remote sensor (assumed to be separately located and not synchronized with a central processor).

Third, we address one of the most important issues for target tracking in a multisensor fusion network: out-of-sequence measurements (OOSM). However, this dissertation is not concerned with different sampling rate among sensors. Instead, we focus on a suboptimal filtering algorithm dealing with possibly time delayed, out-of-sequence measurements (OOSM) with a fixed relative time-delay (we assume that sampling rate are all the same for all sensors) among sensor measurements. A state-augmented approach is also developed to improve tracking performance with the possible presence of OOSM. The filtering algorithm is developed by OOSM updating with IMMPDA for the target.

Finally, we consider tracking of multiple highly maneuvering targets using multiple sensors with possibly unresolved measurement. When multiple targets move temporarily in close formation, it possibly gives rise to a single detection due to the resolution limitations of the sensor. Assuming that there are possibly unresolved measurements from at least two targets (i.e., measurement association with more than two targets simultaneously), any measurement therefore is either associated with a target, a group of merged targets, or caused by clutter. The filtering algorithm is developed by applying the basic IMM approach and the joint probabilistic data association with merged measurements (JPDAM) technique and coupled target state estimation.

## Acknowledgments

I would like to express my deep appreciation to Dr. Jitendra K. Tugnait for his guidance and encouragement throughout this work. During the course of this research, he has provided all the possible support for conducting my research with lasting patience. Thanks are due to my committee members, Dr. Stanley J. Reeves and Dr. Thomas S. Denney Jr., for their guidance and help. I would like to thank Dr. Dean G. Hoffman, Dr. Soo-Young Lee, and Dr. Scottedward A. Hodel for their advice and valuable discussions. I also would like to thank the Korea Army Headquarters and the Office of Naval Research for their support during this research. I also would like to thank Dr. Sang-Bum Lee, Dr. Junhak Song and Gen. Chi-Kyu Yang for their encouragement on my study. I also would like to acknowledge the immense support I received from my colleagues at Auburn University. I will thank them here under the socially acceptable convention of alphabetical order: Dr. Shuangchi He, Dr. Jung Hyun Jo, Dr. Moon Seong Kang, Dr. Hyungwook Kim, Dr. Xiaohong Meng, Dr. Sumedh P. Puranik, Mr. Shuying Qi, Dr. Junhak Song and Dr. Daesub Yoon.

Finally, I would never have been able to finish writing this dissertation without the support and understanding of my family. Many thanks to my children, Seoin and Jahyun, for giving Daddy time to work on the research. My hearty thanks to my wife, Jeesoo, whose love, support, encouragement and patience during the past three years have made it possible for me to complete my education.

Style manual or journal used Journal of Approximation Theory (together with the style known as "auphd"). Bibliograpy follows van Leunen's *A Handbook for Scholars*.

Computer software used The document preparation package TEX (specifically LATEX) together with the departmental style-file `auphd.sty`.

Table of Contents

List of Tables xii

List of Figures xiii

1 Introduction 1
1.1 Overview of Target Tracking Problems . . . 3
1.1.1 Data Association Techniques . . . 3
1.1.2 Estimation Algorithms . . . 5
1.1.3 Combination of IMM and PDA . . . 7
1.2 The Main Issues of Target Tracking Problem . . . 9
1.2.1 Tracking a Maneuvering Target . . . 9
1.2.2 Tracking a Target in Presence of Clutter . . . 10
1.2.3 Tracking a Target using Multiple Sensors . . . 12
1.2.4 Tracking Multiple Targets . . . 15
1.3 Contributions . . . 18
1.4 Organization of the Dissertation . . . 20

2 Basic Target Tracking Algorithms 22
2.1 Kalman Filter . . . 22
2.1.1 Discrete-Time Kalman Filter . . . 23
2.1.2 Extended Kalman filter . . . 28
2.2 Interactive Multiple Model . . . 34
2.2.1 Optimal Solution . . . 34
2.2.2 Basic IMM Algorithm . . . 38
2.2.3 Target Dynamic Models . . . 42
2.3 Probabilistic Data Association Filter . . . 48
2.3.1 Measurement Validation . . . 49
2.3.2 PDA approach combined with Kalman filter . . . 51
2.3.3 Summary . . . 53

3 Multisensor Tracking of a Maneuvering Target in Clutter using IMMPDA Filtering with Simultaneous Measurement Update 54
3.1 Introduction . . . 54
3.2 Simultaneous measurement update . . . 57
3.3 Problem Formulation for the Multiple Model System . . . 64
3.4 IMM/MSPDAF Algorithm for Simultaneous Measurement Update . . . 66
3.5 Simulation Example . . . 74
3.6 Conclusions . . . 79

4 Multisensor Tracking of a Maneuvering Target in Clutter with Asynchronous Measurements using Augmented State IMMPDA Filtering and Simultaneous Measurement Update 83
4.1 Introduction . . . 84
4.2 Problem Formulation for Asynchronous measurements . . . 85
4.3 State-Augmented System . . . 87
4.4 AS-IMM/MSPDAF Algorithm for Asynchronous Measurements . . . 88
4.5 Simulation Example . . . 94
4.6 Conclusions . . . 105

5 Multisensor Tracking of a Maneuvering Target in Clutter with Asynchronous and Possibly Out-of-Sequence Measurements using Augmented State IMMPDA Filtering and Simultaneous Measurement Update 106
5.1 Introduction . . . 106
5.2 Modeling Assumptions . . . 108
5.3 Problem Formulation . . . 110
5.3.1 Target Dynamics . . . 110
5.3.2 Measurements . . . 111
5.4 State-Augmented System . . . 114
5.5 IMM/MSPDAF Algorithm for Asynchronous and Possibly Out-of-Sequence Measurements . . . 116
5.6 Simulation Example . . . 127
5.7 Conclusions . . . 135

6 Tracking of Multiple Maneuvering Targets in Clutter with Possibly Merged Measurements using IMM and JPDAM Coupled Filtering 136
6.1 Introduction . . . 136
6.2 Problem Formulation . . . 140
6.2.1 Target Dynamics . . . 140
6.2.2 Measurements . . . 142
6.3 Modeling for the Merged Measurements . . . 144
6.3.1 Modeling Assumptions . . . 144
6.3.2 Measurement Model . . . 145
6.3.3 Sensor Resolution Model . . . 147
6.4 IMM/JPDAM Coupled Filtering Algorithm . . . 148
6.5 Simulation Example . . . 167
6.6 Conclusions . . . 173

7 Conclusions and Future Work 174
7.1 Conclusions . . . 174
7.2 Suggested Future Work . . . 176

7.2.1 Unresolved Measurements with Simultaneous Measurement Update . . . . . 176
7.2.2 Track Initialization . . . . . 177

Bibliography 178

Appendices 183

A Derivation of the mode-conditioned association event probability Eqn. (3.46) 184

B Derivation of Eqn. (6.62) 188

## List of Tables

4.1 Simulation Results: No. of lost tracks obtained from 100 Monte Carlo runs for fixed-but-unknown $d_k$ . . . . . 105

6.1 Simulation results summery based on 1000 runs . . . . . 172

## List of Figures


1.1 An outline of the components of a tracking system [12, page 5] . . . . . 2

1.2 A mathematical view of the state estimation problem [12, page 2] . . . . . 2

1.3 An example of origin uncertainties and validation regions: $\hat{Z}_k^1$ and $\hat{Z}_k^2$ are predicted measurements from target 1 and target 2 at time $k$, respectively. The parameters of the ellipses are determined by the covariance matrices of $\hat{Z}_k^1$ and $\hat{Z}_k^2$. Measurement $Z_k^1$ originates from target 1 or clutter. $Z_k^3$ originates from target 2 or clutter. $Z_k^2$ originates from target 1 or target 2 or both (in case of merged measurement) or clutter. . . . . 16

2.1 The trajectory of the target (true vs. estimated) . . . . . 32

2.2 Performance of the Kalman filter (read top-to-bottom): (a) RMSE in velocity. (b) RMSE in position . . . . . 33

2.3 Optimal solution (circle) vs suboptimal solution (diamond: interacting multiple model (IMM) algorithm) in term of the number of filters required 38

2.4 An example of a set of kinematic models describing a maneuvering target using two models: 1) constant velocity model and 2) coordinate turn with constant acceleration model. . . . . 43

3.1 Target tracking example using synchronized measurements observed from multiple sensors . . . . . 67

3.2 Trajectory of the maneuvering target (read left to right, top to bottom). (a) Position in $xy$ plane. (b) $x$ and $y$ velocities. (c) $x$ and $y$ accelerations. (d) magnitude of accelerations . . . . . 80

3.3 Performance of the simultaneous measurement updating IMM/MSPDAF in terms of the RMSE (root mean square error) in position (read top to bottom). (a) proposed IMM/MSPDAF vs standard sequential IMM/MSPDAF [21] with collocated sensors (Case 2). (b) proposed IMM/MSPDAF vs standard sequential IMM/MSPDAF [21] with separated sensors (Case 1). . . . . 81

4.1 Target tracking with a fixed-but-unknown relative time delay $d_k$ between the remote sensor clock and the central processor clock at sample time $t_k$ 86

4.2 Trajectory of maneuvering target (read left to right, top to bottom). (a) Position in $xy$ plane. (b) $x$ and $y$ velocities. (c) $x$ and $y$ accelerations. (d) magnitude of accelerations . . . . . 101

4.3 Estimation of delay (given unknown but fixed timing mismatch between two separated sensors) based on 100 Monte Carlo runs (read left to right, top to bottom). (a) d = 0. (b) d = $0.1T$. (c) d = $0.3T$. (d) d = $0.5T$. (e) d = $0.7T$. (f) d = $0.9T$. ($T$ = sampling rate). Solid: estimated delay $\hat{d}$; dashed: fixed delay $d$. . . . . 102

4.4 Comparison of filtered and smoothed (lag = 1) estimate for various delay values (acceleration, velocity, and position RMS errors (3 rows each), read left to right, top to bottom). (a) d = 0. (b) d = $0.1T$. (c) d = $0.3T$. (d) d = $0.5T$. (e) d = $0.7T$. (f) d = 0.9T. ($T$ = sampling rate). In the figure legends, estimation refers to filtering, and smoothing is with lag = 1. Solid: filtered estimate; dash-dot: smoothed estimate. . . . . 103

4.5 RMSE in position using IMM/MSPDAF for various delay values (read left to right, top to bottom). (a) d = 0. (b) d = $0.1T$. (c) d = $0.3T$. (d) d = $0.5T$. (e) d = $0.7T$. (f) d = $0.9T$. Unless otherwise stated, the results are for filtering. Solid: proposed AS-IMM/MSPDAF; dotted: proposed AS-IMM/MSPDAF (smoothing); dash-dot: standard IMM/MSPDAF [38]; dashed: proposed AS-IMM/MSPDAF with the knowledge of $d_k$. . . . . 104

5.1 Asynchronous measurements: In-sequence but delayed measurements and out of sequence measurements (OOSM) in multisensor tracking system . . 112

5.2 Trajectory of maneuvering target (read left to right, top to bottom). (a) Position in $xy$ plane. (b) $x$ and $y$ velocities. (c) $x$ and $y$ accelerations. (d) magnitude of accelerations. . . . . 133

5.3 AS-IMM/MSPDA comparison (RMSE in position, read top to bottom) for various probabilities of delayed measurement, $P_d = 0.25$ and 0.4: (a) $P_d$=0.25. (b) $P_d$=0.4. Solid: proposed AS-IMM/MSPDAF algorithm dealing with OOSM; dashed: AS-IMM/MSPDAF algorithm [50] with OOSM discarding; dotted: AS-IMM/MSPDAF algorithm applied to the hypothetical case of $P_d = 0$. . . . . 134

6.1 The true trajectories of the maneuvering targets (read left to right, top to bottom): (a) Position in $xy$ plane, (b) $x$ and $y$ velocities, (c) $x$ and $y$ accelerations, (d) distance between the targets. . . . . 170

6.2 Performance (RMSE in position) of the proposed IMM/JPDAMCF and the IMM/JPDACF of [25] based on successful runs (read left to right): (a) proposed IMM/JPDAMCF, (b) standard IMM/JPDACF [25]. . . . . 171

# Chapter 1

# Introduction

Target tracking is the estimation (the process of selecting the value of interest from indirect, inaccurate and uncertain observations) of the states (position, velocity, acceleration, etc.) of moving objects (plane, missile, submarine, etc.) both at the current time (filtering) and at any point in the future (prediction) based on remote measurements obtained from sensor(s). The objective of target tracking is to collect sensor data from a field of view (FOV) containing potential target information and then to partition the sensor data into sets of observations or tracks that are originated from the same sources. Different types of sensors can be employed to obtain remote measurements. Active sensors observe objects by illuminating them with an energy source and measuring the reflected energy. On the other hand, passive sensors observe objects by measuring characteristic emissions of the object. The sensors may be located at a fixed location or on moving platforms. The system block diagram of target tracking and the corresponding mathematical view of state estimation are shown in Fig. 1.1 and Fig. 1.2, respectively. Note that, in Figs. 1.1 and 1.2, the measurements are the only variables to which the estimator has access and are affected by the error sources in the form of *measurement noise* [12].

Solution of the target tracking problem requires the simultaneous completion of two tasks: *estimation* and *data association*. Estimation can be viewed as the process of finding the best model parameters to describe the observed data. The process of assigning observations to each target track is referred to as data association. There are many

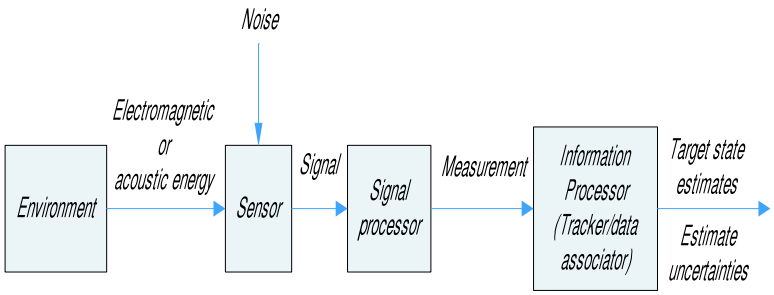


Figure 1.1: An outline of the components of a tracking system [12, page 5]

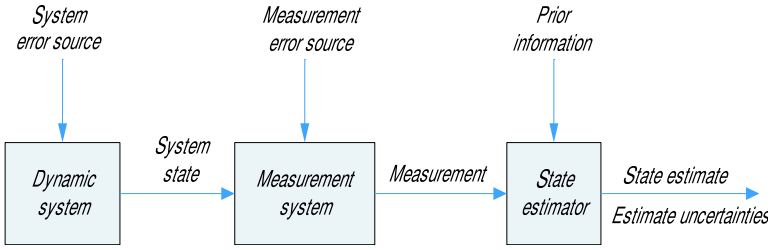


Figure 1.2: A mathematical view of the state estimation problem [12, page 2]

different approaches to both estimation and data association, and these are generally the distinguishing features that give rise to different tracking algorithms. Details of these tasks are discussed in Chapter 2. In this chapter we present an overview of general target tracking problems, some specific issues of target tracking problem, and main contributions of our works.

## 1.1 Overview of Target Tracking Problems

### 1.1.1 Data Association Techniques

Target tracking algorithms have continued to receive significant attention over the past fifty years. The problem of target tracking dealing with noise corrupted measurements has attracted significant attention since World War II. In 1955, Wax [1] formulated the problem of track formation, track maintenance, and track rejection based on the problem of detecting the path of a particle in a bubble chamber, but this paper was written before the adoption of Kalman filtering techniques for recursive target state estimation. In 1960, Kalman published his famous paper [2] describing a recursive solution to the discrete-data linear filtering problem. Since then, the Kalman filter has been the subject of extensive research and application, particularly in the area of autonomous or assisted navigation. It was recognized by Sittler [3] in 1964 that there can be an uncertainty associated with the origin of the measurements in target tracking. This is called the data association problem; a measurement may not have originated from the target of interest.

In the early 70's papers by Bar-Shalom [4, 5] and Singer [6, 7] began the development of the modern tracking systems which combined the data association and Kalman

filtering theory. In 1975, the paper by Bar-Shalom and Tse [5] introduced a suboptimal, computationally-bounded extension of the Kalman filter to cases where measurements were not always available or multiple measurements were simultaneously returned from the sensor. This extension was termed the probabilistic data association filter (PDAF). The PDAF is a Bayesian technique that incorporates clusters of measurements that could have originated from a single target into an updated state estimate for the target. It led to fewer lost tracks in the presence of clutter when compared to the nearest neighbor (NN) technique of data association where only the closest measurement to the predicted measurement was considered to have originated from the target and used to update the state estimate of the target [5]. Two years later from [5], the multiple hypothesis testing (MHT) technique was introduced by Reid [8, 9]. This approach splits an existing track into multiple tracks when more than one measurement is available for the target. However, in this dissertation we are not concerned with the MHT technique, but instead we focus on the PDAF technique because it has been recognized as one of the best suboptimal data association approaches in terms of combined accuracy and computational cost [27]. The theory behind the PDAF is discussed in Chapter 2.

In the early 1980's, as an extension of PDAF, the joint probabilistic data association filter (JPDAF) was introduced by Fortmann et al. [10] to deal with the multiple target tracking situation. The JPDAF is identical to the PDAF except for the extra computation of the association probabilities for all observations and all tracks. The JPDAF was fairly successful in simulations at tracking multiple targets travelling in close proximity. However, when two targets are "closely" spaced, they may give rise to a single detection due to the resolution limitations of the sensor. For instance, in radar ranging, returns

from multiple targets could fall in the same range cell, resulting in one unresolved detection only. This violates a principal assumption of the JPDAF: a measurement can originate from at most one target. Standard tracking algorithms that ignore such a phenomenon can lead to poor performance in multiple target tracking. As a consequence of the study of this problem, Chang and Bar-Shalom [11] introduced the joint probabilistic data association with merged measurements (JPDAM) technique in 1984. Under the Bayesian framework, there are two basic methods of track estimation with merged measurements in multiple target environments [12]: JPDAM and MHT. The MHT filter associates feasible measurements to track and forms multiple hypotheses for track extension. It is a measurement-oriented approach whereas JPDAM is a target-oriented approach. Moreover, MHT is a multiscan approach utilizing several scans of measurements to make data association decisions. MHT makes hard decisions where highly improbable hypotheses are pruned to reduce the computational burden. On the other hand, the JPDAM filter is a single scan approach which does not make hard decisions; rather it updates a track with a weighed sum of the measurements which could have originated from the target in track. The basic theory and simulation of the JPDAM are developed in Chapter 6. Looking ahead in this dissertation, the JPDAM technique has better performance than JPDAF especially in terms of the track estimation accuracy and the loss of tracks when two targets are "closely" spaced and may give rise to a single detection.

### 1.1.2 Estimation Algorithms

Optimal techniques, such as the Kalman filter, provide accurate results during certain motions but also cause large errors during target motions which are not modeled in

the Kalman filter. Moreover, the discrete-time Kalman filter requires sensor measurements at every time step, which is not always possible in target tracking scenario. After the data association problem had been first addressed by the PDAF, several multiple model tracking methods appeared in the early 1980's. The idea behind a multiple-model approach versus a traditional adaptive filter such as the Kalman filter was that traditional techniques would respond too slowly in abruptly changing environments [12, 13]. Optimal multiple model techniques were replaced by suboptimal techniques as memory requirements and computational time grew exponentially for the optimal approaches. The suboptimal estimation techniques introduced included the generalized pseudo-Bayesian (GPB1), second-order generalized pseudo-Bayesian (GPB2), detection-estimation algorithm (DEA), random sampling algorithm (RSA), and the interacting multiple model (IMM). The differences in these estimation approaches were how and when the multiple models were combined (also known as hypothesis pruning).

The GPB1 and GPB2 algorithms were introduced to combine the history of target models by Ackerson and Fu [14] in 1970. In the GPB methods, the hypothesis pruning was performed after the filtering step. The GPB2 differed from the GPB1 by including knowledge of the previous possible mode transitions, as modeled by a Markov chain. In the late 1970's, both DEA and RSA approaches were proposed for the switching environment problem and well detailed in [15] and [16], respectively. Tugnait [17] provided good overviews where suboptimal hypothesis pruning techniques, including the GPB, DEA, and RSA methods, are compared. These pruning techniques involved approximating sums of Gaussian distributions by a single Gaussian distribution, but were presented before the widespread adoption of IMM techniques.

The IMM algorithm was introduced by Blom [18] in 1984. He and Bar-Shalom [19, 20] further developed the idea of IMM in a couple of papers in the late 1980's. Differing from the GPB techniques, the hypothesis pruning was performed before each filtering step after information was shared among the various filters. Thus, like the GPB2 method, the IMM considers the previous possible mode transitions, but unlike the GPB2 method, the IMM requires not $n^2$ but $n$ filters, where $n$ is the number of models being considered. It was shown in [19] that the GPB2 and IMM produced slightly smaller tracking errors than the GPB1 during non-maneuvering target motion, but achieved significantly smaller tracking errors during maneuvering motion. In view of the fact that the IMM is conceptually similar to the GPB2 but its computational load is similar to that of the GPB1 [19], the IMM is superior to both the GPB1 and GPB2 when considering computational complexity and tracking accuracy. The basic theory behind the IMM is discussed in Sec. 2.2.

### 1.1.3 Combination of IMM and PDA

In the process of tracking a maneuvering target, for cases when measurements are not always available for the Kalman filter, or multiple measurements for a target exist, Houles and Bar-Shalom [21] introduced the combination of the IMM and the PDAF in the late 1980's. In [21] the IMM algorithm is combined with the PDA filter in a multiple sensor scenario to propose a combined IMM/MSPDAF (interacting multiple model/ multisensor probabilistic data association filter) algorithm. This algorithm considers an estimation of the target state at present time $k$ given measurements up to time $k$ (on state filtering). This combination is detailed in [21].

In [10, 22] multiple targets in clutter (but without using switching multiple models) have been considered using JPDA filter which, unlike the PDA filter, accounts for the interference from other targets. Most recently, various versions of IMM/JPDA filters for multiple target tracking using switching multiple models have been presented in [23, 24, 25, 26]. While [24, 26] present *uncoupled* filters (i.e., assumes that different target states are mutually independent conditioned on the past measurements), [23, 25] present *coupled* filters (i.e., assume that there exists "shared" measurements, yielding cross-covariances which reflect the correlation between the targets' state estimation errors). In addition, while Blom and Bloem [23] presented an "exact" JPDA coupled filter for non-switching models using the framework of a linear descriptor system, for switching models, they also presented IMM/JPDA uncoupled filter approximations [24]. In [25], Tugnait presented an IMM/JPDA coupled filtering algorithm where a simulation example resulted in fewer target swapping compared with uncoupled IMM/JPDA. As noted in [27], IMMPDA filter is in general superior to IMM/MHT filter when the associated computational cost and performance are considered. Therefore, our emphasis will be on IMM/JPDA techniques. Neither [11] nor [28] consider multiple switching kinematic models for maneuvering targets; rather they are limited to single (non-switching) kinematic models per target to achieve much enhanced performance.

When two targets are "closely" spaced, they may give rise to a single detection due to the resolution limitations of the sensor. For instance, in radar ranging, returns from multiple targets could fall in the same range cell, resulting in one unresolved detection only [11, 28]. Standard tracking algorithms that ignore such a phenomenon can lead to poor performance in multiple target tracking [11, 28]. Despite its importance, prior work on tracking with unresolved measurements and modeling of resolution capability of

a sensor in particular is sparse. Prior work includes [11] and [28] and references therein. In [11] the resolution phenomena related to tracking have been treated on the basis of a grid of resolution cells "frozen" in space. In [28] the resolution capability of the event that two targets are unresolved is conditioned on the relative distance between the two targets in terms of the measured variables (range, azimuth, etc.). A simple Gaussian shape is assumed which captures the sensor behavior in a mathematically tractable way. While [11] considers JPDA for data association, [28] exploits MHT.

In Chapter 6, we propose to use sensor resolution modeling of [28] in conjunction with JPDAM coupled filtering and IMM approach (see [25] for tracking with resolved measurements scenario).

## 1.2 The Main Issues of Target Tracking Problem

The main issues of target tracking problem discussed in this dissertation can be summarized as follows.

### 1.2.1 Tracking a Maneuvering Target

Traditional target tracking assumes that the states of the target of interest satisfy a certain kinematic model. However target model uncertainty typically exists because generally the target of interest is not a cooperating target in that it does not follow a predefined trajectory [27]. Basically the uncertainty in the model can be modeled by additive noise which compensates for the modeling inaccuracy. This approach works fairly well when the target kinematics can be closely approximated by a single model.

Therefore, if a certain model truly describes the kinematics of the target, a Kalman filter gives the optimal solution for tracking in the sense of minimizing the mean-square error in state estimation. The optimal Kalman filter yields large errors when the target is moving with nearly-constant speed and the noise variance is very high. However, in some cases, a target can maneuver and can exhibit different kinematic characteristics from time to time. For example, a military aircraft can perform many kinds of abrupt maneuvers. In that case, a single model cannot describe completely the behavior of the target, and the estimates based on a single model often lead to poor performance of the state estimates or loss of track.

The idea of using multiple models for describing the different motion phases of the target comes from the above impracticality of the filter. For instance, if a constant velocity model is used to describe the behavior of the target all the time, the selection of additive noise variance which models the uncertainty in the model is difficult. If the variance of the noise is small and the target undergoes rapid acceleration or sharp turn, this model suffers the loss of track of the target because the small noise variance can not cover properly those maneuvers. On the other hand, if the variance of the noise is large, it would be able to track those maneuvers but estimation accuracy would be degraded.

The interacting multiple model (IMM) estimator has become well accepted in the literature [12, 22, 29, 30, 33] as the best approach for tracking a maneuvering target.

### 1.2.2 Tracking a Target in Presence of Clutter

In target tracking, there exist various kind of "undesired" measurements (clutter) obtained from the sensor which are not generated from the actual target of interest.

This clutter (e.g., interfering radar echoes caused by objects such as clouds, sea waves, etc.) can degrade the tracking accuracy severely. Ideally, this measurement uncertainty can be described by a random model. However, in practice, there exists clutter that is persistent or somewhere between random and persistent [12]. We will only consider random clutter in the sequel. In the worst case, there exists no true measurement detected by the sensor, and only clutter may be present as measurement data. This cluttered environment complicates the target tracking problem by introducing uncertainty in the measurement origin. As a consequence of this measurement uncertainty, errors can be made in association of measurements to existing tracks. Hence one has to consider data association techniques to determine whether the true measurement originated from the target (Does a given measurement come from the target of interest, or is it a clutter or interference from the nearby target?).

The simplest way to deal with multiple measurements is to use NN (nearest neighbor) filters which, at any given moment, use the NN measurement as if it were the measurement coming from the target of interest. Thus it discards all other measurements for the final state estimation of the target of interest. But sometimes NN measurement may not originate from the target of interest and could be clutter. This happens when clutter density is high. So it is not a robust approach, as it often leads to loss of track [12]. The other way to deal with multiple measurements is to associate each measurement with a weight according to the probability that a given measurement could have originated from the target of interest. This is a Bayesian approach. More specifically, a validation region (hypersphere) centered at the predicted measurement (based on previous state estimate) is established. A validation process of all the measurements in the current scan is carried out. Only those measurements falling within the validation region are considered so that

this process eliminates highly improbable measurements. The validation process needs an appropriate model to describe the clutter. Once the clutter model is established, a data association process can be developed accordingly. An effective data association approach in a Bayesian framework is that of probabilistic data association (PDA) [22, 33] which is discussed in Sec. 2.3.

### 1.2.3 Tracking a Target using Multiple Sensors

The objective of using multiple sensors for target tracking is to improve the accuracy of tracking (i.e., infrared sensors only measures the direction of arrival, hence radar can be used together to measure the distance of the target, or at least two infrared sensors at different locations can be used to obtain the position of a target). In this dissertation, we restrict our attention to radar and infrared sensors.

- Radar Sensors

  Radar (radio detection and ranging) sensor is mostly used as an active sensor since it initiates the energy and detects the target reflections. It is well known that radar's all-weather performance and excellent kinematic measurement capabilities allow it to play a dominant role in any multisensor tracking system. This active nature of the radar is the primary factor that makes it such an effective sensor. Since the source of the energy is the radar itself, the nature of the returned target signal is at least partially under control of the radar operator. The range resolution and aperture size of the radar is primarily determined by the frequency band used by the radar. It is also possible to use the sensor in a passive mode, searching for targets emitting radar signals which is often referred as radar warning

receivers (RWR). The measurement model for a 2-D radar sensor considered in this dissertation is

$$z = h(x) = \begin{bmatrix} R \\ \\ \theta \end{bmatrix} + w$$

where $x$ is the system state, $z$ is the (true) measurement vector, $w$ is the measurement noise, $R$ is the range, and $\theta$ is the azimuth angle. A common model for the measurement noise is to assume an additive white Gaussian noise model.

- Infrared Sensors

  The passive nature of the infrared (IR) sensors leads to distinct advantages and disadvantages. The excellent measurement accuracy of the IR sensors makes them an important element of any multiple sensor tracking system. Emphasis in military applications on reduced target signatures places new emphasis on the development of IR system in mainly two ways. First, use of active sensors must be minimized since the use of active sensors potentially uncovers one's existence (e.g., the enemy can easily detect radar tracking by using RWR). Second, the enemy's efforts at reduced RCS (radar cross section) signature and advanced ECM (electronic countermeasures) increase the need to exploit other target signatures such as its infrared emissions. In addition, the use of IR sensors enhances resolution capability for closely spaced targets, accurate angle measurements, and resistance to ECM. The measurement model for this sensor considered in this dissertation is

$$z = h(x) = \begin{bmatrix} \theta \\ \\ \phi \end{bmatrix} + w$$

where $\theta$ is the azimuth angle and $\phi$ is the elevation angle.

Unlike single sensor case, multiple sensors introduce the problems of temporal and spatial characteristics of the measurement data. Sensors may not always be located at the same place. Hence measurements available at the sensors could be at different time instants. So sensors may be either synchronous (ideal case), which means that the sampling times of all sensors are the same and there is no delay (timing mismatch) among sensors, or asynchronous, which means that the sampling times may vary or there is delay (timing mismatch) from each other. This gives rise to architectural issues of the sensor network, and one may carry out the estimation process in a centralized way (estimation at one central node, called the master node) or in a decentralized way (estimation at each sensor locally and then obtain global estimate by track fusion) [27].

If sensors are distant from each other, then there could be delay in the estimation due to data transmission time and channel bandwidth issues. So one has to deal with synchronous as well as asynchronous measurement data to obtain the estimate. Usually if synchronous measurement data is available from all the sensors then either 'parallel updating' (updating state by processing data from all the sensors simultaneously at the same time) or 'sequential updating' (updating state based on the available measurement data from that particular sensor) can be carried out. In [34], it has been shown that those two schemes are equivalent (for linear models) if provided sensors are synchronized and measurement noise across the sensors are uncorrelated (a realistic assumption). But parallel updating is computationally more expensive than sequential updating. On the other hand, if the sensors are not synchronized, then one has to deal with possible OOSM (*out of sequence measurements*). This asynchronous measurements case has been

considered in [12, 35, 36, 37] and a noble state-augmented algorithm to deal with OOSM is presented in Chapter 5.

### 1.2.4 Tracking Multiple Targets

The presence of multiple targets in the detection range of sensors (also called the scope) makes the target tracking very complicated by introducing the additional uncertainty in the origin of the measurement. One has to solve the data association problem to determine whether the available measurement is generated from one of the targets present in the scope and from which target it originated. Data association in a multiple target scenario is carried out by considering all the targets simultaneously.

Since each target can constitute a "persistent" interference to other targets, it is a great challenge to track multiple targets moving close to each other. The merged measurement case arise when two (or more) targets are so "close" that the sensor detects them as one target due to a lack of resolution (see Fig. 1.3). The objective of the multitarget tracking is to partition the sensor data into sets of observations, or tracks, produced by the same source (target). Once tracks are formed and confirmed, the task is to maintain each track. All of the above target tracking issues have already been studied by numerous researchers and, as a consequence, many effective solutions have been provided for these problems. However, more effective and cheap algorithms are still required to improve the estimation accuracy and to reduce the computational cost. Compared to single target tracking, multitarget tracking is a very complicated and computationally intensive process. When there are $n$ targets in the detection range (scope) of the sensors, the measurement origin uncertainty problem is the worst one as the

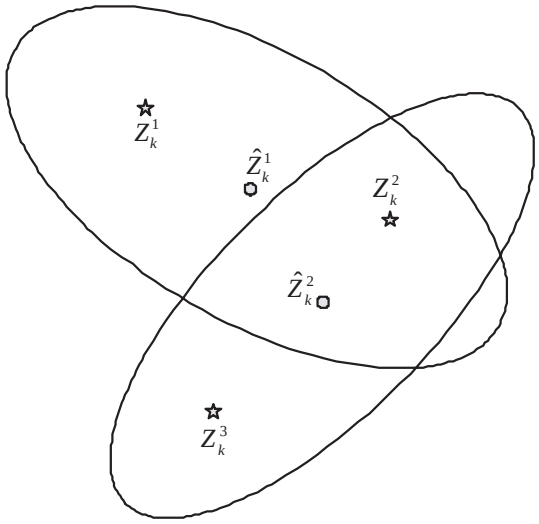


Figure 1.3: An example of origin uncertainties and validation regions: $\hat{Z}_k^1$ and $\hat{Z}_k^2$ are predicted measurements from target 1 and target 2 at time $k$, respectively. The parameters of the ellipses are determined by the covariance matrices of $\hat{Z}_k^1$ and $\hat{Z}_k^2$. Measurement $Z_k^1$ originates from target 1 or clutter. $Z_k^3$ originates from target 2 or clutter. $Z_k^2$ originates from target 1 or target 2 or both (in case of merged measurement) or clutter.

number of combinations of association of measurement and target increases dramatically. An objective of our research is to develop advanced signal processing algorithms for multiple target tracking by exploiting filtering theory and data association techniques.

There are mainly two approaches to deal with the merged measurement problem.

- Multiple hypothesis tracker (MHT)

  No prior knowledge is needed about the number of targets. One has to consider simultaneously all the targets and also consider simultaneously all the scans of measurements. The main theme of MHT is that it evaluates the probabilities that there is a target from which a sequence of measurements have originated. It is

called a *measurement-oriented* approach. The more complex MHT provides improved performance, but it is difficult to implement and in cluttered environments a large number of hypotheses may have to be maintained, which requires extensive computational resources.

- Joint probabilistic data association(JPDA)

  The JPDA techniques are based on PDA (probabilistic data association), which uses a weighted average of all the measurements falling inside a track's validation region (i.e., gating) at the current time to update the track state. In this approach, it is assumed that the number of targets is known already. The tracks of these targets have already been formed. The task is to evaluate the measurement-to-target association probabilities for the latest set of measurements and then obtain the state estimates by combining those measurements. It is called a *target-oriented approach*. These techniques give much better performance than the simpler data association techniques (i.e., NN filter) and requires less computational resources than MHT approach.

- JPDA with merged measurements (JPDAM)

  When multiple targets are close enough in the measurement range, they will give merged (unresolved) measurement due to the resolution limitation of sensor. Since the JPDA algorithm can track targets with measurements originating from one of the targets in track or clutter, additional data association for the merged measurements needs to be done in JPDA technique. To deal with the possibility that a

measurement originated from more than one target, JPDAM can be applied. JPDAM uses a probabilistic model and corresponding data association for the merged measurements.

## 1.3 Contributions

Our contributions in this dissertation are:

**IMMPDA simultaneous measurement update for a maneuvering target tracking using multiple sensors**

We present a noble suboptimal filtering algorithm for tracking a highly maneuvering target in a cluttered environment using multiple sensors. The filtering algorithm is developed by applying the basic IMM approach and the PDA technique to a two sensor (radar and infrared) problem for state estimation for the target. A simultaneous measurement update approach is followed where the raw sensor measurements are passed to a fusion node and fed directly to the target tracker. A multisensor (MS) PDA is developed for parallel sensor processing for target tracking under clutter. The algorithm is illustrated via a highly maneuvering target tracking simulation example where two sensors, a radar and an infrared sensor, are used. Compared with an existing IMMPDA filtering algorithm with sequential sensor processing, the proposed algorithm achieves significant improvement in the accuracy of track estimation.

**IMMPDA simultaneous measurement update for a maneuvering target tracking with delayed but in-sequence measurements**

We extend IMMPDA simultaneous measurement update algorithm to possibly asynchronous (in-sequence but time delayed) measurements. A state augmented approach is

developed to estimate the time delay between local and remote sensors. A multisensor probabilistic data association filter (PDAF) is developed for parallel sensor processing for target tracking under clutter. Compared with an existing IMMPDA filtering algorithm with the assumption of synchronous measurements sensor processing, the proposed algorithm achieves considerable improvement (especially in the case of larger delays) in the accuracy of track estimation.

**IMMPDA simultaneous measurement update with possibly out-of-sequence measurements**

We propose a suboptimal filtering algorithm dealing with possibly time delayed, out-of-sequence measurements (OOSM) with a fixed relative time-delay among sensor measurements. The filtering algorithm is developed by applying the basic IMM approach, the PDA technique, and OOSM updating for the target. A state augmented approach is developed to improve tracking performance with the presence of OOSM. A multisensor PDA filter is developed for parallel sensor processing for target tracking under clutter. The algorithm is illustrated via a highly maneuvering target tracking simulation example where two sensors, a radar and an infrared sensor, are used. Compared with an existing IMMPDA filtering algorithm with in-sequence only sensor processing, the proposed algorithm achieves considerable improvement in the accuracy of track estimation.

**Multitarget tracking with possibly merged measurements**

We propose a noble suboptimal filtering algorithm for tracking multiple maneuvering targets in a cluttered environment using multiple sensors. This algorithm is an extension of IMM/JPDA filtering algorithm [25] to deal with possibly merged measurements. We

concentrate on the case of two targets which temporarily move in close formation. The filtering algorithm is developed by applying the basic IMM approach and the joint probabilistic data association with merged measurements (JPDAM) technique and coupled target state estimation to a Markovian switching system. The algorithm is illustrated via a simulation example involving tracking of two highly maneuvering, at times closely spaced, targets with possibly unresolved measurements. Compared with an existing IMM/JPDA filtering algorithm developed without allowing for merged measurements [25], the proposed algorithm achieves significant improvement in the accuracy of track estimation during target merging period.

### 1.4 Organization of the Dissertation

The remainder of this dissertation is organized as follows:

In Chapter 2, we elaborate on some basic target tracking algorithms, mainly the Kalman filter, IMM filter, and PDA filter. Theory associated with those algorithms serves as the foundation for our contributions. Chapter 3 presents a noble suboptimal filtering algorithm for tracking a highly maneuvering target in a cluttered environment using multiple sensors. We develop a noble algorithm "simultaneous measurement update using IMMPDA filtering". The proposed algorithm provides significant improvement over an existing standard IMMPDA filtering algorithm with sequential sensor processing especially tracking a maneuvering target. In Chapter 4, we extend the proposed filtering algorithm to the asynchronous measurement case. Compared with an existing IMMPDA filtering algorithm with the assumption of synchronous (no delay) measurements sensor processing, the proposed algorithm achieves considerable improvement (especially

in the case of larger delays) in the accuracy of track estimation. A suboptimal filtering algorithm dealing with possibly time delayed, out-of-sequence measurements (OOSM) with a fixed relative time-delay among sensor measurements is presented in Chapter 5. In Chapter 6, we focus on multitarget tracking problem with possibly merged measurements. The simulation example shows significant improvement in the position estimate compared to the multisensor tracking by IMM/JPDA coupled filtering algorithm of [25]. Finally, Chapter 7 presents the future work that we would like to continue in the area.

# Chapter 2

## Basic Target Tracking Algorithms

In this chapter we review some basic algorithms. We divide the problem of tracking into *state estimation* and *data association*. We briefly describe some existing state estimation algorithms: Kalman filter, extended Kalman filter, and interacting multiple model (IMM) algorithms. For data association, the probabilistic data association filter (PDAF) is briefly described in this chapter. This is background work and is quite useful in later chapters where we discuss our contributions.

### 2.1 Kalman Filter

Kalman filter theory is fundamental for the development of target tracking algorithms. Given a collection of sensor measurements, it is often possible to determine several optimal state estimates based on different optimality conditions which can be stated in terms of the probability density function (pdf) of the states given the observation. Hence, the problem of state estimation can be formulated by calculating the probability density of the state. Under general conditions, it is not possible to obtain a closed-form solution to the problem of state estimation. However, when the system is linear and the random variables are assumed to be Gaussian, a closed-form solution can be obtained. Under this conditions, the optimal estimator is the Kalman filter and it is usually specified as a finite length algorithm based on a recursion of the mean and covariance of the state. It can be applied to both continuous and discrete linear systems. The target of interest, which is being tracked, is continuous by nature, but the

processor, which runs the tracking algorithm, is discrete. The original Kalman filter [2] was defined in continuous-time, but a discrete version also derived after [2]. Since the discrete Kalman filter is only used in this dissertation, we briefly describe the steps for implementing a Kalman filter in discrete time domain.

### 2.1.1 Discrete-Time Kalman Filter

Consider a discrete time linear dynamic system with additive white Gaussian noise that models the disturbances. The discrete time index is denoted by $k$. A general time-varying state space model for the Kalman filter is

$$x_{k+1} = F_k x_k + G_k u_k + v_k \tag{2.1}$$

where

$x_k$ = the state vector of dimension $n_x$ at time $k$

$F_k = n_x \times n_x$ transition matrix

$G_k = n_x \times n_u$ input distribution matrix

$u_k$ = a known input vector of dimension $n_u$

$v_k$ = the random process noise vector of dimension $n_x$.

It is assumed that $v_k$ is the sequence of zero-mean white Gaussian process noise with covariance

$$E\{v_j v_k'\} = Q_{jk} = Q\delta_{jk} \tag{2.2}$$

where $E\{.\}$ denotes the expectation, $'$ denotes the transpose operation and $\delta_{jk}$ is the Dirac delta function. The statistical model of the measurement is described by

$$z_k = H_k x_k + w_k \tag{2.3}$$

where $z_k$ is the $m_x$-dimensional measurement vector, $H_k$ is the $m_x \times n_x$ observation matrix, and $w_k$ is zero mean white Gaussian measurement noise with covariance

$$E\{w_j w_k'\} = R_{jk} = R\delta_{jk}. \tag{2.4}$$

Since a complete knowledge of the statistical model constitutes the knowledge of $F_k$, $G_k$, $Q_k$, $H_k$, and $R_k$, these system matrices are assumed known and can be time varying. The initial condition of the state $x_0$ is a random variable with known mean $\bar{x}_0$ and covariance $P_0$. Process noise $v_k$, measurement noise $w_k$, and initial state $x_0$ are assumed to be mutually independent. Define $\hat{x}_{k|j}$ $(:= E\{x_k|Z^j\})$ as an estimate of the state vector $x_k$ based upon the knowledge of the measurements up to time $j$ where $Z^j := \{z_1, z_2, \cdots, z_j\}$. Specially, $k > j$ denotes a predicted estimate, $k < j$ denotes a smoothed estimate, and $k = j$ denotes a filtered estimate. The goal is to estimate the state $x_k$ based on all the available measurements up to time $k$. If the mean square error is chosen as the cost criterion, then Kalman [2] has shown that the estimate of the state $x_k$ minimizing its cost is

$$\hat{x}_{k|k} := E\{x_k|Z^k\} \tag{2.5}$$

where

$$Z^k := \{z_1, z_2, \cdots, z_k\} \tag{2.6}$$

is the measurement sequence up to the current time $k$. The uncertainty in the estimate is indicated by the state covariance, which is computed as covariance of the estimation error

$$P_{k|k} := E\{[x_k - \hat{x}_{k|k}][x_k - \hat{x}_{k|k}]'|Z^k\}. \tag{2.7}$$

Note from (2.5) that, under the Gaussian assumption for the initial state and all the noise signals entering the system, the Kalman filter is the optimal MMSE (minimum mean-square error) state estimator:

$$\hat{x}_k^{MMSE} = \arg\min_{\hat{x}_k} E\left\{(\hat{x}_k - x_k)^T (\hat{x}_k - x_k) \,|Z^k\right\}. \tag{2.8}$$

The solution to this problem is obtained by differentiating the expected value with respect to the estimate $\hat{x}_k$:

$$\begin{aligned} &\tfrac{\partial}{\partial \hat{x}_k}\left[E\left\{(\hat{x}_k - x_k)^T (\hat{x}_k - x_k) \,|Z^k\right\}\right] \\ &= \tfrac{\partial}{\partial \hat{x}_k}\left[\int_{-\infty}^{\infty} (\hat{x}_k - x_k)^T (\hat{x}_k - x_k)\, p\left(x_k|Z^k\right) dx_k\right] \\ &= 2\int_{-\infty}^{\infty} (\hat{x}_k - x_k)\, p\left(x_k|Z^k\right) dx_k. \end{aligned} \tag{2.9}$$

From the last line of Eqn. (2.9), it can be derived as

$$\int_{-\infty}^{\infty} (\hat{x}_k - x_k)\, p\left(x_k|Z^k\right) dx_k \Big|_{\hat{x}_k = \hat{x}_k^{MMSE}} = 0. \tag{2.10}$$

Thus the MMSE-estimate can be obtained as (from the fact that $\int_{-\infty}^{\infty} p(x_k|Z^k)dx_k = 0$)

$$\hat{x}_k^{MMSE} = \int_{-\infty}^{\infty} x_k p\left(x_k|Z^k\right) dx_k = E\left\{x_k|Z^k\right\} \tag{2.11}$$

which is equal to the Kalman filter equation of (2.5). The derivation of the Kalman filter can be found in [39, 40, 41]. Since the Kalman filter updates the state whenever a measurement arrives and is a recursive algorithm, we only list one cycle of the Kalman filter in this dissertation. Assume that, at time $k$, the following are available: the state estimate $\hat{x}_{k-1|k-1}$ and the associated error covariance $P_{k-1|k-1}$. Now when measurement $z_k$ is available at time $k$, the estimate update at time $k$ is obtained as follows.

**Prediction**

The state estimates and its covariance estimates are first predicted from time $k-1$ to time $k$. The state prediction is

$$\hat{x}_{k|k-1} := E\{x_k|Z^{k-1}\} = F_{k-1}\hat{x}_{k-1|k-1} + G_{k-1}u_{k-1}. \tag{2.12}$$

The state prediction covariance is

$$\begin{aligned} P_{k|k-1} &:= E\{[x_k - \hat{x}_{k|k-1}][x_k - \hat{x}_{k|k-1}]'|Z^{k-1}\} \\ &= F_{k-1}P_{k-1|k-1}F'_{k-1} + Q_{k-1}. \end{aligned} \tag{2.13}$$

The measurement prediction is

$$\hat{z}_{k|k-1} := E\{z_k|Z^{k-1}\} = H_k\hat{x}_{k|k-1}. \tag{2.14}$$

**Update**

When the measurement at time $k$ is obtained, the measurement residual or *innovation* is first computed as

$$\nu_k := z_k - \hat{z}_{k|k-1}. \tag{2.15}$$

This measurement residual is a Gaussian random variable with zero mean and covariance

$$S_k := E\{\nu_k \nu_k' | Z^{k-1}\} = H_k P_{k|k-1} H_k' + R_k. \tag{2.16}$$

The state estimate is updated as

$$\hat{x}_{k|k} = \hat{x}_{k|k-1} + W_k \nu_k \tag{2.17}$$

where $W_k$ is the filter gain defined as

$$W_k := P_{k|k-1} H_k' S_k^{-1}. \tag{2.18}$$

Finally, the covariance of updated state estimate can be obtained as

$$\begin{aligned} P_{k|k} &:= E\{[x_k - \hat{x}_{k|k}][x_k - \hat{x}_{k|k}]' | Z^k\} = P_{k|k-1} - P_{k|k-1} H_k' S_k^{-1} H_k P_{k|k-1} \\ &= [I - W_k H_k] P_{k|k-1} = P_{k|k-1} - W_k S_k W_k'. \end{aligned} \tag{2.19}$$

That is, one may notice from (2.19) that the predicted covariance described in (2.13) is now reduced because the new information brought to the system allows a more accurate estimate. Note from (2.18) that the Kalman gain $W_k$ is (from a simplistic scalar point

of view) "proportional" to the state prediction variance and "inversely proportional" to the innovation variance. Hence, the Kalman gain is "large" if the state prediction is inaccurate (has a large variance) and the measurement is accurate (has a relatively small variance). This "large" Kalman gain indicates a "rapid" response to the measurement in updating the state, while a "small" gain yields a "slower" response to the measurement. In the frequency domain a large/small Kalman gain properties correspond to a higher/lower bandwidth of the Kalman filter [13].

### 2.1.2 Extended Kalman filter

One of the main problems with the standard Kalman filter is the requirement of a linear measurement equation (2.3). This problem makes the standard Kalman filter impractical in most tracking situations. Typically the measurements do not contain the target position in Cartesian coordinates. For instance, a radar can measure the range and the azimuth angle, and a passive sensor such as infrared sensor might give the azimuth and elevation angles only. Therefore, when tracking problems are not linear so the Kalman filter cannot be used directly, one can approximate the nonlinear equation by linearizing around a point and solving for the linearized system with a Kalman filter. This approach is referred to as the extended Kalman filter (EKF). It is basically an extension of the linear Kalman filter described in the previous section and allows nonlinear state transition and measurement equations. Unfortunately, this filter is no longer optimal. Hence, in complex tracking circumstances the performance may be degraded significantly.

**One Cycle of the EKF**

The update equation for the EKF is nearly the same as the linear Kalman filter (LKF). The state prediction (2.12) and measurement predictions (2.14) are replaced by the corresponding nonlinear equations. That is, the state is predicted as

$$\hat{x}_{k|k-1} = f(\hat{x}_{k-1|k-1}) + G_{k-1}u_{k-1}. \tag{2.20}$$

When the measurement equation is nonlinear, i.e., the predicted equation (2.14) is replaced by

$$\hat{z}_{k|k-1} = h(\hat{x}_{k|k-1}). \tag{2.21}$$

In the covariance equations the nonlinear function cannot be used. Therefore, the functions are to be linearized first. It would also be possible to compute the Taylor series of the functions and use the desired number of terms [13]. The linearization corresponds to taking only the first term of each series. Details are well explained in [13]. The Jacobian of the state transformation function $f(\cdot)$ is evaluated at the previous estimate:

$$F_k = \left.\frac{\partial f(x)}{\partial x}\right|_{x=\hat{x}_{k-1|k-1}}. \tag{2.22}$$

Similarly, the Jacobian of the measurement function is computed. It is evaluated at the predicted state:

$$H_k = \left.\frac{\partial h(x)}{\partial x}\right|_{x=\hat{x}_{k|k-1}}. \tag{2.23}$$

The above linearizations in (2.22) and (2.23) may degrade the performance of the filter significantly. Especially in passive (i.e., infrared sensor) tracking, valuable information

can be lost when equation (2.23) applied. If more terms of the Taylor were used, the accuracy could be improved with extra computations.

Note from the EKF equations that the Kalman gain computation and the resulting update of the state estimates to form $\hat{x}_{k|k}$ are dependent on the initial estimates $\hat{x}_{k|k-1}$. Therefore, there may be a tendency for the EKF to diverge if the initial estimate is inaccurate. It means that in the case where several quantities are measured, the order of processing measurements should be considered for better estimate. This is in contrast to the LKF where all measurements can be processed simultaneously or in any order with no effect on the resultant accuracy.

**Example: Tracking a target moving at constant velocity using EKF**

Consider a system with the following state space model

$$\mathbf{x}_{k+1} = F_k \mathbf{x}_k + G_k v_k \tag{2.24}$$

with the state vector consisting of position $[x_k \ y_k \ z_k]^T$ in Cartesian coordinates in meters where $\dot{x}_k := \frac{dx_k}{dt}$ and

$$\mathbf{x}_k = [x_k \ \dot{x}_k \ y_k \ \dot{y}_k \ z_k \ \dot{z}_k]^T. \tag{2.25}$$

If a target is moving at constant velocity, the corresponding system matrices would be [12]

$$F_k = \begin{bmatrix} 1 & T & 0 & 0 & 0 & 0 \\ 0 & 1 & 0 & 0 & 0 & 0 \\ 0 & 0 & 1 & T & 0 & 0 \\ 0 & 0 & 0 & 1 & 0 & 0 \\ 0 & 0 & 0 & 0 & 1 & T \\ 0 & 0 & 0 & 0 & 0 & 1 \end{bmatrix}, \quad G_k = \begin{bmatrix} T^2/2 & 0 & 0 \\ T & 0 & 0 \\ 0 & T^2/2 & 0 \\ 0 & T & 0 \\ 0 & 0 & T^2/2 \\ 0 & 0 & T \end{bmatrix} \tag{2.26}$$

where $T$ is the sampling rate (in second). Assuming a 2-D radar being used for target tracking, the sensor measurement of range ($R$) and azimuth angle ($\phi$) can be defined as

$$z_k = h(\mathbf{x}_k) + w_k = \begin{bmatrix} R \\ \phi \end{bmatrix} = \begin{bmatrix} \sqrt{x_k^2 + y_k^2 + z_k^2} \\ \tan^{-1}(y_k/x_k) \end{bmatrix} + w_k \tag{2.27}$$

where $w_k$ is zero-mean Gaussian noises with the covariance matrix of measurement noise

$$R_k = \begin{bmatrix} \sigma_R^2 & 0 \\ 0 & \sigma_\phi^2 \end{bmatrix}. \tag{2.28}$$

The linearized measurement matrix $H_k$ can be obtained as

$$H_k = \frac{\partial h(\mathbf{x})}{\partial \mathbf{x}}\Big|_{\mathbf{x}=\hat{\mathbf{x}}_{k|k-1}} = \begin{bmatrix} \frac{\partial R}{\partial x_k} & \frac{\partial R}{\partial \dot{x}_k} & \frac{\partial R}{\partial y_k} & \frac{\partial R}{\partial \dot{y}_k} & \frac{\partial R}{\partial z_k} & \frac{\partial R}{\partial \dot{z}_k} \\ \frac{\partial \phi}{\partial x_k} & \frac{\partial \phi}{\partial \dot{x}_k} & \frac{\partial \phi}{\partial y_k} & \frac{\partial \phi}{\partial \dot{y}_k} & \frac{\partial \phi}{\partial z_k} & \frac{\partial \phi}{\partial \dot{z}_k} \end{bmatrix}_{\mathbf{x}_k=\hat{\mathbf{x}}_{k|k-1}}$$

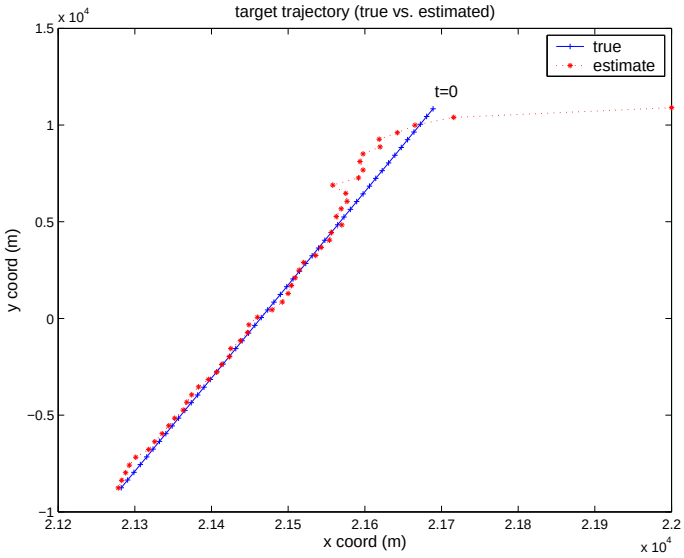


Figure 2.1: The trajectory of the target (true vs. estimated)

$$= \begin{bmatrix} cos\hat{\theta}cos\hat{\phi} & 0 & cos\hat{\theta}sin\hat{\phi} & 0 & sin\hat{\theta} & 0 \\ -\frac{sin\hat{\phi}}{\hat{R}cos\hat{\theta}} & 0 & \frac{cos\hat{\phi}}{\hat{R}cos\hat{\theta}} & 0 & 0 & 0 \end{bmatrix} \tag{2.29}$$

where

$$\hat{R} = \sqrt{\hat{x}^2_{k|k-1} + \hat{y}^2_{k|k-1} + \hat{z}^2_{k|k-1}} \tag{2.30}$$

$$\hat{\phi} = \tan^{-1}\left(\frac{\hat{y}_{k|k-1}}{\hat{x}_{k|k-1}}\right) \tag{2.31}$$

$$\hat{\theta} = \tan^{-1}\left(\frac{\hat{z}_{k|k-1}}{\sqrt{(\hat{x}^2_{k|k-1} + \hat{y}^2_{k|k-1})}}\right). \tag{2.32}$$

The target trajectories of both true and estimated target state are shown in Fig. 2.1. The true target is flying with constant velocity from the upper right corner to lower left corner. Position measurements (range and bearing) of the target are sampled with period

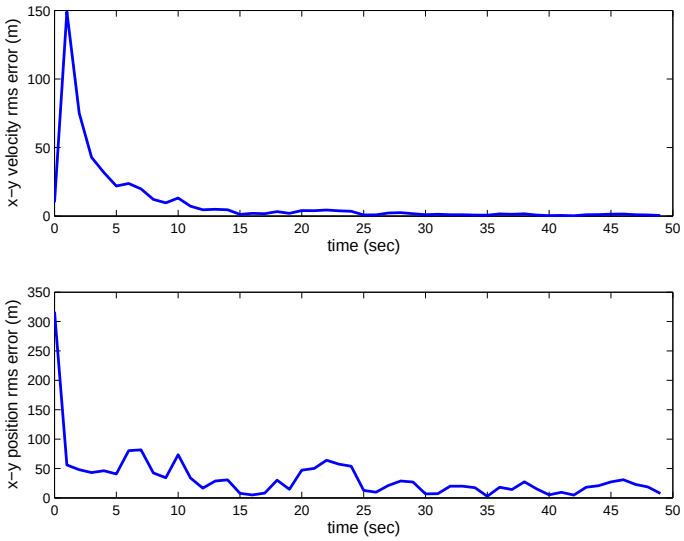


Figure 2.2: Performance of the Kalman filter (read top-to-bottom): (a) RMSE in velocity. (b) RMSE in position

$T$=1s, and measurements (range and bearing) error variance of $\sigma_R^2 = (20\text{m})^2$ and $\delta_\phi^2 = (0.002\text{rad})^2$. The results for tracking a non-maneuvering target in terms of the root mean square errors (RMSE) in velocity and position are presented in Fig. 2.2 based on 100 Monte Carlo runs. Fig. 2.2 shows that EKF works well in tracking of a non-maneuvering target. As seen from above example, traditional target tracking problems can be solved using EKF. However, in case of tracking a maneuvering target, since the Kalman filter uses permanently a large process noise to cover the maneuver, it would respond too slowly in abruptly changing environments [13]. To handle maneuvering targets, multiple models can be used for the possible hypotheses. Bar-Shalom et al. [12, 13] provided good overviews where the Kalman filter and interacting multiple model (IMM) filter are compared. In the following section, the IMM approach to state estimation is presented.

## 2.2 Interactive Multiple Model

As mentioned above, a single model sometimes cannot describe the dynamics of a system very well. Hence it is useful to introduce multiple models to describe complete behavior of the target motion. One important issue for a multiple model is to reduce the number of hypotheses. This can be done by pruning or merging techniques. For example, if the number of models is $n$, there are $n^{k+1}$ different model paths available at time $k$. Since the number of model paths for the optimal estimation grows exponentially in time, it is not feasible in real applications. To solve this computational cost problem, a suboptimal algorithm is needed. As one of the most efficient suboptimal algorithms, the IMM algorithm has continued to receive increasing attention over the past twenty years. There are many sources that provide a detailed discussion of IMM algorithms [12, 13, 21, 33, 42]. In the following discussion, an optimal solution for the multiple model approach to state estimation is given and then some practical suboptimal solutions are presented.

### 2.2.1 Optimal Solution

In the multiple model (MM) approach it is assumed that the dynamics of the system at any time can be described by one of a finite number of given models. Such systems are called *hybrid*, since there exist both the discrete (modeling) uncertainties and continuous (noise) uncertainties. If it is assumed that the mode switching occurs only at the sampling time (state update time), the model switching of the whole system can be described as a Markovian switching system. Suppose that there are $n$ hypothesized models, $M^1, M^2, \cdots, M^n$ for the system and the event that model $M^j$ is in effect during

the sampling period ending at time $t_k$ (i.e., the sampling period $(t_{k-1}, t_k]$) is denoted by $M_k^j$. When event $M_k^j$ is effective, the system is modeled as

$$x_k = F_{k-1}^j x_{k-1} + v_{k-1}^j \tag{2.33}$$

and

$$z_k = H_k^j x_k + w_k^j. \tag{2.34}$$

When the $j$th model is correct (the system is in mode $M^j$), the initial (prior) mode probability is denoted by (i.e., at $k$=0)

$$P[M_0^j] = \mu_0^j \quad \text{for} \quad j = 1, 2, \cdots, n \tag{2.35}$$

with

$$\sum_{j=1}^{n} \mu_0^j = 1 \tag{2.36}$$

is assumed to be known. The switching of the model is governed by a Markov chain with known model transition probabilities

$$p_{ij} := P[M_k^j | M_{k-1}^i]. \tag{2.37}$$

The $l$-th possible model history (sequence of models) through time $k$ is denoted as

$$\widetilde{M}_k^l = \{M_0^{j_0}, M_1^{j_1}, \cdots, M_k^{j_k}\} \quad \text{for} \quad l = 1, 2, \cdots, n^{k+1} \tag{2.38}$$

where $1 \leq j_i \leq n$ for $i = 0, 1, \cdots, k$. Note that the number of histories ($n^{k+1}$) increases exponentially with time $k$. By the total probability theorem, it follows that the conditional pdf of the state at time $k$ is obtained as a Gaussian sum with exponentially increasing number of terms

$$p(x_k|Z^k) = \sum_{l=1}^{n^{k+1}} p(x_k|\widetilde{M}_k^l, Z^k) P[\widetilde{M}_k^l|Z^k]. \tag{2.39}$$

Since $p(x_k|\widetilde{M}_k^l, Z^k)$ is Gaussian with mean $E(x_k|\widetilde{M}_k^l, Z^k)$, which can be obtained via a Kalman filter, it follows that

$$E(x_k|Z^k) = \sum_{l=1}^{n^{k+1}} E(x_k|\widetilde{M}_k^l, Z^k) P[\widetilde{M}_k^l|Z^k]. \tag{2.40}$$

Noticing that (2.40) is the optimal solution for the state estimate, it is clear that the number of filters needed to implement (2.40) increases exponentially with time $k$, which makes the optimal approach impractical. In order to develop a computationally feasible approach, consider the conditional probability of each model history $\widetilde{M}_k^l$. It follows from Bayes' formula that

$$\begin{aligned} \tilde{\mu}_k^l &:= P[\widetilde{M}_k^l|Z^k[= P[\widetilde{M}_k^l|z_k, Z^{k-1}] \\ &= \frac{1}{c} p(z_k|Z^{k-1}, \widetilde{M}_k^l) P[\widetilde{M}_k^l|Z^{k-1}] \end{aligned} \tag{2.41}$$

where $c$ is a normalization constant such that $\sum_{l=1}^{n^{k+1}} \tilde{\mu}_k^l = 1$. Equation (2.41) can be rewritten as

$$\tilde{\mu}_k^l = \frac{1}{c} p(z_k|Z^{k-1}, \widetilde{M}_k^l) P[M_k^j, \widetilde{M}_{k-1}^s|Z^{k-1}]$$

$$
\begin{aligned}
&= \frac{1}{c} p(z_k|Z^{k-1}, \widetilde{M}_k^l) P[M_k^j|\widetilde{M}_{k-1}^s, Z^{k-1}] P[\widetilde{M}_{k-1}^s|Z^{k-1}] \\
&= \frac{1}{c} p(z_k|Z^{k-1}, \widetilde{M}_k^l) P[M_k^j|\widetilde{M}_{k-1}^s] \tilde{\mu}_{k-1}^s
\end{aligned} \tag{2.42}
$$

If the current model $M_k^{j_k}$ depends only on the previous model $M_{k-1}^{j_{k-1}}$, (2.42) can be simplified further as

$$
\tilde{\mu}_k^l = \frac{1}{c} p\left(z_k|Z^{k-1}, \widetilde{M}_k^l\right) p_{ij} \tilde{\mu}_{k-1}^s \tag{2.43}
$$

where $M_{k-1}^i$ is the last model of the sequence $\widetilde{M}_{k-1}^s$.

According to [13], the advantage of an optimal estimator is that the best utilization of the data and the knowledge of the system and the disturbances can be guaranteed, but on the other hand, the disadvantages of the estimator are that it is possibly sensitive to modeling errors and requires higher computational cost compared to a suboptimal estimator. Therefore optimal multiple model techniques need to be replaced by suboptimal techniques as memory requirements and computational time grow exponentially for the optimal approaches. The main idea of suboptimal multiple model techniques is to combine the multiple models (also known as hypothesis pruning). Fig. 2.3 presents a comparison of the number of filters required between optimal and suboptimal solutions (i.e., interacting multiple model (IMM) algorithm). As shown in Fig. 2.3, the number of filters needed to implement the optimal estimator increases exponentially with time $k$ (see (2.40)) while the number of filters needed to implement the suboptimal estimator increases linearly with time $k$ (see (2.59)), which makes the suboptimal solution approach more practical.

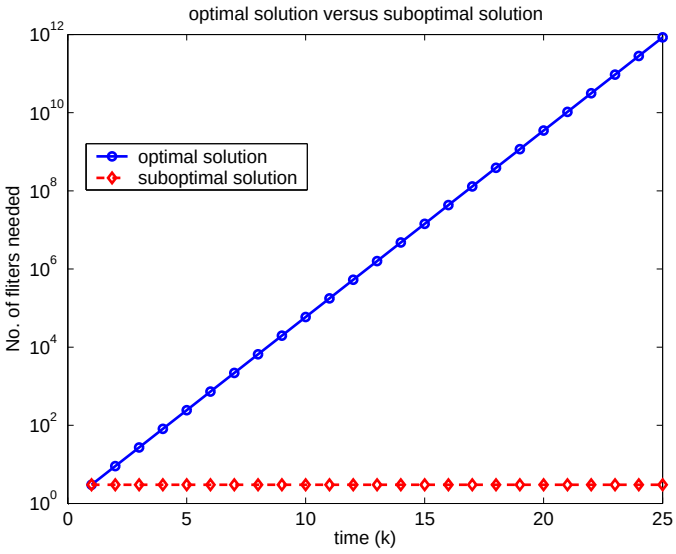


Figure 2.3: Optimal solution (circle) vs suboptimal solution (diamond: interacting multiple model (IMM) algorithm) in term of the number of filters required

### 2.2.2 Basic IMM Algorithm

The IMM algorithm of [30], has been found to offer a good compromise between the computational and storage requirements and estimation accuracy [29, 43]. Our future work is also based on the IMM approach. So in the following section we describe the basic IMM algorithm. The IMM algorithm [30] for state filtering is based on running $n$ "mode-matched" state estimation filters which exchange information (interact) at each sampling instant. It assumes that the conditional probability density $p(x_k|M_k^j, Z^k)$ is a Gaussian with mean $\hat{x}_{k|k}^j := E\{x_k|M_k^j, Z^k\}$ and the covariance $P_{k|k}^j := E\{[x_k - \hat{x}_{k|k}^j][x_k - \hat{x}_{k|k}^j]'|M_k^j, Z^k\}$. In reality, the density $p(x_k|M_k^j, Z^k)$ is Gaussian sum containing $n^k$ terms.

As the algorithm is well explained in [29, 30, 43], we briefly outline the basic steps in 'one cycle' (i.e., processing needed to update the new measurement) of the IMM filtering algorithm. We follow Table I of [29] for the most part.

*Assumed available*: It is assumed that following is available at the beginning of the state estimate update cycle ending at time $k$: the state estimate $\hat{x}^j_{k-1|k-1} := E\{x_{k-1}|M^j_{k-1}, Z^{k-1}\}$, the associated covariance $P^j_{k-1|k-1}$, and the conditional mode probability $\mu^j_{k-1} := P[M^j_{k-1}|Z^{k-1}]$ at time $k-1$ for each $j \in \mathcal{M}_n := \{1, 2, \cdots, n\}$. For $k = 1$, we take initial condition $\hat{x}^j_{0|0} = \bar{x}^j_0$, $P^j_{0|0} = P^j_0$ and $\mu^j_0 = P[M^j_0]$.

**Step 1: Interaction – mixing of the estimate from the previous time**

In this stage, the main objective is to reduce the number of hypotheses from $n^2$ to $n$. At the end of the interaction stage, $n$ conditioned state estimates $\hat{x}^{0j}_{k-1|k-1} := E\{x_{k-1}|M^j_k, Z^{k-1}\}$ ($j \in \mathcal{M}_n$) and the associated covariances are obtained. The details are as given below :

predicted mode probability:

$$\mu^{j-}_k := P[M^j_k|Z^{k-1}] = \sum_{i=1}^{n} p_{ij}\mu^i_{k-1} \tag{2.44}$$

mixing probability:

$$\mu^{i|j} := P[M^i_{k-1}|M^j_k, \mathcal{Z}^{k-1}] = p_{ij}\mu^i_{k-1}/\mu^{j-}_k \tag{2.45}$$

mixed estimate:

$$\hat{x}^{0j}_{k-1|k-1} := E\{x_{k-1}|M^j_k, Z^{k-1}\} = \sum_{i=1}^{n} \hat{x}^i_{k-1|k-1}\mu^{i|j} \tag{2.46}$$

covariance of the mixed estimate:

$$\begin{aligned} P^{0j}_{k-1|k-1} &:= E\{[x_{k-1} - \widehat{x}^{0j}_{k-1|k-1}][x_{k-1} - \widehat{x}^{0j}_{k-1|k-1}]'|M^j_k, Z^{k-1}\} \\ &= \sum_{i=1}^{n}\{P^i_{k-1|k-1} + [\widehat{x}^i_{k-1|k-1} - \widehat{x}^{0j}_{k-1|k-1}][\widehat{x}^i_{k-1|k-1} - \widehat{x}^{0j}_{k-1|k-1}]'\}\mu^{i|j} \end{aligned} \tag{2.47}$$

**Step 2: Prediction and Filtering** $(\forall j \in \mathcal{M}_n)$:

While the mixed state estimate is the estimate of the state at time $k-1$, the predicted state is the estimate of the state at time $k$ without the current measurement $z_k$ being available. The details of this stage are given below:

state prediction:

$$\hat{x}^j_{k|k-1} := E\{x_k|M^j_k, Z^{k-1}\} = F^j_{k-1}\hat{x}^{0j}_{k-1|k-1} \tag{2.48}$$

covariance of state prediction:

$$\begin{aligned} P^j_{k|k-1} &:= E\{[x_k - \hat{x}^j_{k|k-1}][x_k - \hat{x}^j_{k|k-1}]'|M^j_k, Z^{k-1}\} \\ &= F^j_{k-1}P^{0j}_{k-1|k-1}F^{j'}_{k-1} + G^j_{k-1}Q^j_{k-1}G^{j'}_{k-1} \end{aligned} \tag{2.49}$$

measurement prediction:

$$\hat{z}^j_{k|k-1} := H^j_k\hat{x}^j_{k|k-1} \tag{2.50}$$

measurement residual (innovations)

$$\nu^j_k := z_k - \hat{z}^j_{k|k-1} \tag{2.51}$$

measurement residual covariance (innovation covariance):

$$S_k^j := E\{\nu_k^j \nu_k^{j\prime} | Z^{k-1}\} = H_k^j P_{k|k-1}^j H_k^{j\prime} + R_k^j \tag{2.52}$$

Kalman gain:

$$W_k^j := P_{k|k-1}^j H_k^{j\prime} S_k^{j\,-1} \tag{2.53}$$

filtered state estimate:

$$\hat{x}_{k|k}^j = \hat{x}_{k|k-1}^j + W_k^j \nu_k^j \tag{2.54}$$

covariance of filtered state estimate:

$$\begin{aligned} P_{k|k}^j &:= E\{[x_k - \hat{x}_{k|k}^j][x_k - \hat{x}_{k|k}^j]' | Z^k\} \\ &= P_{k|k-1}^j - W_k^j S_k^j W_k^{j\prime} \end{aligned} \tag{2.55}$$

likelihood function:

$$\Lambda_k^j = \mathcal{N}\left(\nu_k^j; 0, S_k^j\right) \tag{2.56}$$

where

$$\mathcal{N}(x; y, P) = |2\pi P|^{-1/2} \exp\left[-\frac{1}{2}(x-y)' P^{-1} (x-y)\right] \tag{2.57}$$

and $|A|$ is the determinant of the matrix $A$.

Updating mode probability:

$$\mu_k^j = P[M_k^j | Z^k] = \frac{\mu_k^{j-} \Lambda_k^j}{\sum_{i=1}^{n} \mu_k^{i-} \Lambda_k^i}. \tag{2.58}$$

**Step 3: Combination of the mode-conditioned estimates**

In the combination stage, a single lumped state estimate given all measurements up to the current time is obtained as well as the associated covariance. The final state estimate update at time $k$ is given by

$$\hat{x}_{k|k} := E\{x_k|Z^k\} = \sum_{j=1}^{n} \hat{x}^j_{k|k}\mu^j_k \tag{2.59}$$

and its covariance is given by

$$\begin{aligned} P_{k|k} &:= E\{[x_k - \hat{x}_{k|k}][x_k - \hat{x}_{k|k}]'|Z^k\} \\ &= \sum_{j=1}^{n} \left\{P^j_{k|k} + [\widehat{x}^j_{k|k} - \widehat{x}_{k|k}][\widehat{x}^j_{k|k} - \widehat{x}_{k|k}]'\right\}\mu^j_k. \end{aligned} \tag{2.60}$$

### 2.2.3 Target Dynamic Models

We discuss important target tracking models to be used in the IMM algorithm. The main focus is on the state dynamics and process noise. An example of a set of kinematic models describing a maneuvering target is shown in Fig. 2.4. To describe the motion of the target as closely as possible, as shown in Fig. 2.4, it is essential to select the set of models properly. The motion of a target can be modeled with an accurate, high-order model if the type of target can be determined from the sensor measurements. The use of a small number of low-order models can effectively track many types of targets through various moving situations. In this section a class of widely used models derived from simple equations of motion (constant velocity and constant acceleration) are discussed. There are mainly two classes of discretized kinematic models: discretized continuous-time

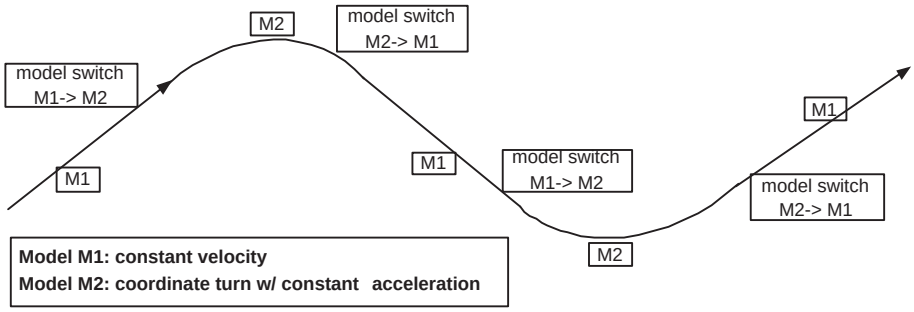


Figure 2.4: An example of a set of kinematic models describing a maneuvering target using two models: 1) constant velocity model and 2) coordinate turn with constant acceleration model.

kinematic models (discretized model is generated via a continuous-time white process noise) and direct discrete-time kinematic models (it is directly defined in discrete-time domain and the noise is a discrete-time process noise) [13]. We mainly focus on direct discrete-time kinematic models as follows:

**Piecewise Constant Wiener Process Acceleration Model**

Assume that there is an object moving in a 3-dimensional Cartesian space plane with non-zero acceleration. Let the state vector at time $kT$ ($T$ = sample period)

$$x_k = [\xi_k \;\; \dot{\xi}_k \;\; \ddot{\xi}_k \;\; \eta_k \;\; \dot{\eta}_k \;\; \ddot{\eta}_k \;\; \zeta_k \;\; \dot{\zeta}_k \;\; \ddot{\zeta}_k]' \tag{2.61}$$

where $\xi_k$, $\eta_k$ and $\zeta_k$ are the Cartesian position coordinates, and where the velocity components are denoted by $\dot{\xi}_k$, $\dot{\eta}_k$ and $\dot{\zeta}_k$, and where the acceleration components are denoted by $\ddot{\xi}_k$, $\ddot{\eta}_k$ and $\ddot{\zeta}_k$. The state dynamics for the piecewise constant Wiener process

acceleration model can be approximated using Taylor series expansion:

$$f(t) = f(t_0) + \dot{f}(t_0)(t - t_0) + \ddot{f}(t_0)\frac{(t - t_0)^2}{2!} + \cdots. \tag{2.62}$$

Let $t = (k+1)T$ and $t_0 = kT$. Then

$$\xi_{k+1} = \xi_k + \dot{\xi}_k T + \ddot{\xi}_k \tfrac{T^2}{2} + p_k^{\xi}, \tag{2.63}$$

$$\dot{\xi}_{k+1} = \dot{\xi}_k + \ddot{\xi}_k T + v_k^{\xi}, \tag{2.64}$$

$$\ddot{\xi}_{k+1} = \ddot{\xi}_k + a_k^{\xi}. \tag{2.65}$$

Define

$$x_k(\xi) := \begin{bmatrix} \xi_k \\ \dot{\xi}_k \\ \ddot{\xi}_k \end{bmatrix}, \quad x_k := \begin{bmatrix} x_k(\xi) \\ x_k(\eta) \\ x_k(\zeta) \end{bmatrix}, \quad w_k(\xi) := \begin{bmatrix} p_k^{\xi} \\ v_k^{\xi} \\ a_k^{\xi} \end{bmatrix}, \quad \text{and} \quad w_k := \begin{bmatrix} w_k(\xi) \\ w_k(\eta) \\ w_k(\zeta) \end{bmatrix}. \tag{2.66}$$

From Eqns. (2.62)-(2.66), the state dynamics for the piecewise constant Wiener process acceleration model can be written as in (2.67) [13]. (Note that, only in this section, we denote "$w_k$" (instead of "$v_k$") as the process noise at time $k$ to distinguish it from velocity components in (2.64) and (2.66).)

$$x_{k+1} = F_k x_k + G_k w_k \tag{2.67}$$

where

$$F_k = \begin{bmatrix} F_k(\xi) & 0 & 0 \\ 0 & F_k(\eta) & 0 \\ 0 & 0 & F_k(\zeta) \end{bmatrix}, \quad F_k(\xi) = F_k(\eta) = F_k(\zeta) = \begin{bmatrix} 1 & T & \frac{1}{2}T^2 \\ 0 & 1 & T \\ 0 & 0 & 1 \end{bmatrix} \tag{2.68}$$

and

$$G_k = \begin{bmatrix} G_k(\xi) & 0 & 0 \\ 0 & G_k(\eta) & 0 \\ 0 & 0 & G_k(\zeta) \end{bmatrix}, \quad G_k(\xi) = G_k(\eta) = G_k(\zeta) = \begin{bmatrix} \frac{1}{2}T^2 \\ T \\ 1 \end{bmatrix}. \tag{2.69}$$

**Piecewise Constant White Acceleration Model**

Assume that there is an object moving in a 3-dimensional Cartesian space plane with constant speed (zero acceleration). Let the state vector at time $kT$ ($T$ = sample period)

$$x_k = [\xi_k \quad \dot{\xi}_k \quad \eta_k \quad \dot{\eta}_k \quad \zeta_k \quad \dot{\zeta}_k]'. \tag{2.70}$$

Then similar to Eqns. (2.62)-(2.66),

$$\xi_{k+1} = \xi_k + \dot{\xi}_k T + p_k^{\xi}, \tag{2.71}$$

$$\dot{\xi}_{k+1} = \dot{\xi}_k + v_k^{\xi}. \tag{2.72}$$

Define

$$x_k(\xi) := \begin{bmatrix} \xi_k \\ \dot{\xi}_k \end{bmatrix}, \quad x_k := \begin{bmatrix} x_k(\xi) \\ x_k(\eta) \\ x_k(\zeta) \end{bmatrix}, \quad w_k(\xi) := \begin{bmatrix} p_k^{\xi} \\ v_k^{\xi} \end{bmatrix} \quad \text{and} \quad w_k := \begin{bmatrix} w_k(\xi) \\ w_k(\eta) \\ w_k(\zeta) \end{bmatrix}. \tag{2.73}$$

From Eqns. (2.70)-(2.73), the state dynamics for the piecewise constant Wiener process acceleration model can be written as [13]

$$x_{k+1} = F_k x_k + G_k w_k \tag{2.74}$$

where

$$F_k = \begin{bmatrix} F_k(\xi) & 0 & 0 \\ 0 & F_k(\eta) & 0 \\ 0 & 0 & F_k(\zeta) \end{bmatrix}, \quad F_k(\xi) = F_k(\eta) = F_k(\zeta) = \begin{bmatrix} 1 & T \\ 0 & 1 \end{bmatrix} \tag{2.75}$$

and

$$G_k = \begin{bmatrix} G_k(\xi) & 0 & 0 \\ 0 & G_k(\eta) & 0 \\ 0 & 0 & G_k(\zeta) \end{bmatrix}, \quad G_k(\xi) = G_k(\eta) = G_k(\zeta) = \begin{bmatrix} T \\ 1 \end{bmatrix}. \tag{2.76}$$

**Coordinated Turn Model**

Assume that there is an object moving in a $xy$ plane with constant speed and turning with a constant angular rate (i..e., *coordinated turn* in aviation language) [13, 44]. Let

the state vector

$$x_k = [\xi \;\; \dot{\xi} \;\; \eta \;\; \dot{\eta}]' \tag{2.77}$$

where $\xi$ and $\eta$ are the Cartesian position coordinates, and where the velocity components are denoted $\dot{\xi}$ and $\dot{\eta}$. If we assume a constant speed $\nu = \sqrt{\dot{\xi}^2 + \dot{\eta}^2}$ and a constant angular rate $\Omega = \dot{\phi}$ ($\Omega > 0$ implies a counterclockwise turn), where we have

$$\dot{\xi} = \nu\cos(\phi), \qquad \dot{\eta} = \nu\sin(\phi). \tag{2.78}$$

Now the acceleration (with $\dot{\nu} = 0$) components are

$$\ddot{\xi} = \frac{d}{dt}\dot{\xi} = -\nu\Omega\sin(\phi) = -\Omega\dot{\eta} \tag{2.79}$$

$$\ddot{\eta} = \frac{d}{dt}\dot{\eta} = -\nu\Omega\cos(\phi) = -\Omega\dot{\xi}. \tag{2.80}$$

The state equation can be expressed as

$$x(t) = \frac{d}{dt}\begin{bmatrix} \xi \\ \dot{\xi} \\ \eta \\ \dot{\eta} \end{bmatrix} = \begin{bmatrix} \dot{\xi} \\ -\Omega\dot{\eta} \\ \dot{\eta} \\ \Omega\dot{\xi} \end{bmatrix}. \tag{2.81}$$

By discretizing the system, it gives

$$x_{k+1} = \begin{bmatrix} 1 & \frac{\sin(\Omega T)}{\Omega} & 0 & -\frac{1-\cos(\Omega T)}{\Omega} \\ 0 & \cos(\Omega T) & 0 & -\sin(\Omega T) \\ 0 & \frac{1-\cos(\Omega T)}{\Omega} & 1 & \frac{\sin(\Omega T)}{\Omega} \\ 0 & \sin(\Omega T) & 0 & \cos(\Omega T) \end{bmatrix} x_k + G_k w_k. \tag{2.82}$$

This allows us to generate the state trajectories for such turns. These coordinated turns are very common for any flying objects.

## 2.3 Probabilistic Data Association Filter

The multiple model approach discussed above section is effective when we track a single target under the assumption that measurements of the target are available at all time steps from the sensor(s). This assumption means that we must be able to associate measurements from sensor(s) to each target of interest before we do any filtering. In addition, in the case of multiple radar returns received at the radar sensor, it is possible for sensor(s) to miss the radar return from the target of interest for several consecutive scans. Therefore, we must not only associate the available measurements with existing target tracks but also consider the cases when there is no measurement available for the target of interest.

The basic algorithms discussed so far in the previous section do not take into account the problem of measurement origin uncertainty. In this section we discuss the basic probabilistic data association filter (PDAF) that was proposed by Bar-Shalom in [5]. PDAF is a Bayesian technique that handles these two issues: measurement origin

uncertainty and no measurement available for the target. It is mainly used for tracking a single target in the presence of clutter. For tracking multiple targets, the same approach of PDA has been extended to JPDA (joint probabilistic data association) [10]. In JPDA one has to do data association jointly by considering simultaneously all the targets present in the surveillance region. Details about JPDA are given in Chapter 6. Here we give the basic PDA algorithm of [5]. PDA algorithm calculates the association probabilities of each validated measurement to the target at the current time. It is usually combined with a proper tracking filter to track a single target in clutter. Let us discuss now the validation of measurements.

### 2.3.1 Measurement Validation

Assume that there is a target whose track has been initialized. One can then set up a validation gate [12], based on predicted measurement and residual covariance obtained in the appropriate filter prediction stage. A key assumption is that the past information about the true target state conditioned on the past measurements is summarized approximately by

$$p(x_k|Z^{k-1}) = \mathcal{N}(x_k; \hat{x}_{k|k-1}, P_{k|k-1}). \tag{2.83}$$

In addition, the true measurement conditioned on the past measurements is also Gaussian distributed with probability density function given by

$$p(z_k|Z^{k-1}) = \mathcal{N}(z_k; \hat{z}_{k|k-1}, S_k). \tag{2.84}$$

The validation region is given by

$$\mathcal{V}(k,\gamma) := \left\{ z : [z - \hat{z}_{k|k-1}]' S_k^{-1} [z - \hat{z}_{k|k-1}] \leq \gamma \right\} \tag{2.85}$$

with gate threshold $\gamma$. The gate probability

$$P_G := P[z_k \in \mathcal{V}(k,\gamma)] \tag{2.86}$$

gives the probability that the true measurement will fall within the validation region. The probability $P_G$ is a function of $\gamma$ and the dimension of the measurement $n_z$. The volume $V$ of the validation region $\mathcal{V}$ corresponding to the threshold $\gamma$ is given by [12]

$$V_k = c_{n_z} \gamma^{\frac{n_z}{2}} |S_k|^{\frac{1}{2}} \tag{2.87}$$

where $c_{n_z}$ is the volume of the unit hypersphere of dimension $n_z$ ($c_1 = 2, c_2 = \pi, c_3 = 4\pi/3$, etc.). Therefore, an increase in the design parameter, $c_{n_z}$ or $S_k$, will increase the size of the validation area. Practically we take $\gamma = 16$ and the corresponding $P_G = 0.9989$ (or 0.9997) when $n_z = 3$ (or 2). The following assumptions are made [12]:

(AS1) Among the possibly several validated measurements, at most one of them can be target originated provided the target is detected and the corresponding measurement falls within the validation gate.

(AS2) All the remaining measurements are assumed to be due to clutter or false alarm and modeled as independent and identically distributed (i.i.d.) with uniform spatial distribution.

(AS3) Target detection occurs independently over time with known probability $P_D$.

### 2.3.2 PDA approach combined with Kalman filter

The following section discusses how to apply the PDA to a typical Kalman filter which tracks a single target in clutter. From among all the raw measurements at time $k$, i.e.,

$$Z_k := \{z_k^{(1)}, z_k^{(2)}, \cdots, z_k^{(m_k)}\}, \tag{2.88}$$

define the set of validated measurement at time $k$ as

$$Y_k := \{y_k^{(1)}, y_k^{(2)}, \cdots, y_k^{(\bar{m}_k)}\} \tag{2.89}$$

where $\bar{m}_k$ is total number of validated measurement at time $k$. And

$$y_k^{(i)} := z_k^{(j)} \quad 1 \leq i \leq j \leq m_k \tag{2.90}$$

where $1 \leq \bar{m}_k \leq m_k$ when $\bar{m}_k \neq 0$. The cumulative set of validated measurements is denoted by

$$Z^k := \{Y_1, Y_2, \cdots, Y_k\}. \tag{2.91}$$

We also define set of association events [12]

$$\begin{aligned} \theta_k^i &= y_k^i \text{ is originated from the target: } i = 1, \cdots, \bar{m}_k \\ \theta_k^0 &= \text{none of the measurements is originated from the target.} \end{aligned} \tag{2.92}$$

Note that the events $\{\theta_k^i\}_{i=0}^{\bar{m}_k}$ are mutually exclusive and exhaustive based on (AS1). Now the estimate of the state $x_k$ conditioned on the above events is obtained by the

total probability theorem as

$$\begin{aligned}\hat{x}_{k|k} &:= E\{x_k|Z^k\} \\ &= \sum_{i=0}^{\bar{m}_k} E\{x_k|\theta_k^i, Z^k\}P[\theta_k^i|Z^k] \\ &= \sum_{i=0}^{\bar{m}_k} \hat{x}_{k|k}^i \beta_k^i\end{aligned} \tag{2.93}$$

where $x_{k|k}^i := E\{x_k|\theta_k^i, Z^k\}$ is the updated state conditioned on the event that the $i$-th validated measurement is correct and $\beta_k^i := P[\theta_k^i|Z^k]$ is the association probability with this event. The conditional state estimate based on measurement $i$ being correct is

$$\hat{x}_{k|k}^i = \hat{x}_{k|k-1} + W_k\nu_k^i \quad i = 1, \cdots, \bar{m}_k \tag{2.94}$$

where the innovations

$$\nu_k^i := z_k^i - \hat{z}_{k|k-1} \tag{2.95}$$

and gain

$$W_k := P_{k|k-1}H_k'S_k^{-1}. \tag{2.96}$$

The final state update equation is

$$\hat{x}_{k|k} = \hat{x}_{k|k-1} + W_k\nu_k \tag{2.97}$$

where the combined innovations

$$\nu_k := \sum_{i=1}^{\bar{m}_k} \beta_k^i \nu_k^i. \tag{2.98}$$

For $i = 0$ (when no measurement is originated from the target of interest), we have $\hat{x}^0_{k|k} = \hat{x}_{k|k-1}$, where the updated state estimate is identical to the predicted state. The covariance associated with the updated state is [12]

$$P_{k|k} = P_{k|k-1} - (1 - \beta^0_k) W_k S_k W'_k + W_k (\sum_{i=1}^{\bar{m}_k} \beta^i_k \nu^i_k \nu^{i'}_k - \nu_k \nu'_k) W'_k. \tag{2.99}$$

### 2.3.3 Summary

In this chapter we briefly discussed the background work needed to understand the fundamentals of target tracking. The Kalman filter provides the optimum solution in the MMSE sense, but its application is limited to a single model. For the multiple model approach, suboptimal algorithms such as IMM filter are applicable. To tackle the measurement origin uncertainty, one has to combine the IMM filter with data association techniques like PDA. Tracking a target using multiple sensors can improve the tracking accuracy. With this background work we are ready to discuss our noble algorithms in the following chapters.

# Chapter 3

# Multisensor Tracking of a Maneuvering Target in Clutter using IMMPDA Filtering with Simultaneous Measurement Update

In this chapter, we present a suboptimal filtering algorithm for tracking a highly maneuvering target in a cluttered environment using multiple sensors. The filtering algorithm is developed by applying the basic interacting multiple model (IMM) approach and the probabilistic data association (PDA) technique to a two sensor (radar and infrared, for instance) problem for state estimation for the target. A simultaneous measurement update approach is followed where the raw sensor measurements are passed to a central processor and fed directly to the target tracker. A multisensor probabilistic data association filter is developed for simultaneous measurement update (SMU) for target tracking under clutter. A past approach using SMU has ignored certain data association probabilities leading to an inaccurate implementation. Another existing approach applies only to non-maneuvering targets. The algorithm is illustrated via a highly maneuvering target tracking simulation example where two sensors, a radar and an infrared sensor, are used. Compared with an existing IMMPDA filtering algorithm with sequential sensor processing, the proposed algorithm achieves significant improvement in the accuracy of track estimation.

## 3.1 Introduction

We consider the problem of tracking a maneuvering target in clutter. This class of problem has received considerable attention in the literature [5, 12, 21, 22, 44, 45]. We

develop a simultaneous measurement update technique by applying the basic interacting multiple model (IMM) algorithm and probabilistic data association (PDA) technique. The switching multiple model approach has been found to be quite effective in modeling highly maneuvering targets [12, 14, 21, 29, 30, 33, 45]. In this approach various "modes" of target motion are represented by distinct kinematic models, and in a Bayesian framework, the target maneuvers are modeled by switching among these models controlled by a Markov chain. To accommodate the fact that the target can be highly maneuvering, we will follow a switching multiple model formulation as in [12, 21, 29, 30, 33] and references therein. It is assumed that a track has been formed (initiated) and our objective is that of track maintenance. In [21] such a problem has been considered using multiple sensors, PDA and switching multiple models. The optimal solution (in the minimum mean-square error sense) to target state estimation, given sensor measurements and absence of clutter, requires exponentially increasing (with time) computational complexity; therefore, one has to resort to suboptimal approximations. For the switching multiple model approach, the IMM algorithm of [30] has been found to offer a good compromise between the computational and storage requirements and estimation accuracy [29]. In the presence of clutter, the measurements at the sensors may not all have originated from the target of interest. Therefore, one has to account for measurements of uncertain origin (target or clutter?). In this case one has to solve the problem of data association. An effective approach in a Bayesian framework is that of PDA [12, 22]. Here too, in a Bayesian framework, one has to resort to approximations to reduce the computational complexity, resulting in the PDA filter [5, 12, 21, 22, 45].

In [21] the IMM algorithm has been combined with the PDA filter in a multiple sensor scenario to propose a combined IMM/MSPDAF (interacting multiple model/

multisensor probabilistic data association filter) algorithm. While [21] uses *sequential updating* of the state estimates with measurements (i.e., updating the state estimates sequentially with measurements from different sensors), the multisensor approach of [45] falls in the category of simultaneous measurement update, or *parallel sensor processing*, where the raw measurements from all sensors are passed to a central processor to be processed simultaneously (i.e., updating the state estimates with all the measurements at the same time as if they were from a single sensor). Sequential updating results in computational savings but this approach is not necessarily the best. For linear systems, both sequential and parallel updating methods are algebraically equivalent but the parallel updating is computationally more expensive [12]. Ref. [45] uses SMU but has some errors: during data association, all measurements at the same time from different sensors are assumed to be either from clutter or from the target. The possibility that a measurement from sensor 1 may be from target while the measurement from sensor 2 may be clutter-induced (and vice-versa) is implicitly not allowed in [45] - this is clearly incorrect. Ref. [46] allows for such distinctions (hypotheses), but it is limited to non-maneuvering targets.

In this chapter, we extend the multisensor approach of [46] to maneuvering targets. "Standard" assumptions are used for PDA filtering [12, 22]: a measurement can have only one source; among the possibly several validated measurements, at most one of them can be target-originated and the remaining validated measurements are assumed to be due to false alarms or clutter, and are modeled as independently and identically distributed (i.i.d) with uniform spatial distribution over the entire validation region.

The remainder of this chapter is organized as follows. Sec. 3.2 presents the basic implementation of simultaneous measurement update technique. Sec. 3.3 presents

the problem formulation for multiple model system. Sec. 3.4 describes the proposed IMM/MSPDAF algorithm with simultaneous measurement update to multiple model system. Simulation results using the proposed algorithm for a realistic problem are given in Sec. 3.5. Finally, concluding remarks may be found in Sec. 3.6.

### 3.2 Simultaneous measurement update

In the simultaneous measurement update procedure, the state can be updated simultaneously with all the synchronized measurements observed from multiple sensors. We consider a system of a 2-D radar and an infrared sensor located separately at $[x_1, y_1, z_1]$ and $[x_2, y_2, z_2]$, respectively, and covering a common cluttered surveillance region that is being traversed by a single non-maneuvering target. Assume that the target dynamic equation can be described as

$$x_k = F_{k-1}x_{k-1} + G_{k-1}v_{k-1}. \tag{3.1}$$

Assume that there are $q$ *synchronized* sensors. At a given sampling time $k$, there are $m_l$ measurements from each sensor $l$. The measurement from sensor $l$ at time $k$ is

$$z_k^l = H_k^l x_k + w_k^l \quad \text{for } \; l = 1, \cdots, q, \tag{3.2}$$

where $x_k$ is the system state at $t_k$ and of dimension $n_x$, $z_k^l$ is the (true) measurement vector (i.e., due to the target) from sensor $l$ at $t_k$ and of dimension $n_{zl}$, where $H_k^l$ is the Jacobian matrix of $h^l$ evaluated at some value of the estimate of state $x_k$. The process noise $v_{k-1}$ and the measurement noise $w_k^l$ are mutually uncorrelated zero-mean white

Gaussian processes with covariance matrices $Q_{k-1}$ and $R_k^l$, respectively. Note that, in general, at any time $k$, some measurements may be due to clutter and some due to the target, i.e., there can be more than a single measurement at time $k$ at sensor $l$. The measurement set (not yet validated) generated by sensor $l$ at time $k$ is denoted as

$$Z_k^l := \{z_k^{l(1)}, z_k^{l(2)}, \cdots, z_k^{l(m_l)}\} \tag{3.3}$$

where $m_l$ is the number of measurements generated by sensor $l$ at time $k$. Variable $z_k^{l(i)}$ $(i = 1, \cdots, m_l)$ is the $i$th measurement within the set. The cumulative set of measurements (not yet validated) from sensor $l$ up to time $k$ is denoted as $Z^{k(l)} := \{Z_1^l, Z_2^l, \cdots, Z_k^l\}$. In heavily cluttered environment, validation gates can be applied to reduce the number of unwanted measurements for further processing. Following [12, 21], one sets up a validation gate for sensor $l$ centered at the predicted measurement, $\hat{z}_k^l$. Then measurement $z_k^{l(i)}$ ($i$=1,2,$\cdots$,$m_l$) is validated if and only if

$$[z_k^{l(i)} - \hat{z}_k^l]'[S_k^l]^{-1}[z_k^{l(i)} - \hat{z}_k^l] < \gamma \tag{3.4}$$

where $\gamma$ is an appropriate threshold. The volume of the validation region with the threshold $\gamma$ is

$$V_k^l := c_{n_{zl}} \gamma^{n_{zl}/2} |S_k^l|^{1/2} \tag{3.5}$$

where $n_{zl}$ is the dimension of the measurement and $c_{n_{zl}}$ is the volume of the unit hypersphere of this dimension ($c_1$=2, $c_2$=$\pi$, $c_3$=$4\pi/3$, etc.). Choice of $\gamma$ is discussed in more detail in [12, Sec. 2.3.2]. From among all the raw measurements from sensor $l$ at time $k$, i.e., $Z_k^l := \{z_k^{l(1)}, z_k^{l(2)}, \cdots, z_k^{l(m_l)}\}$, define the set of validated measurement for sensor

$l$ at time $k$ as

$$Y_k^l := \{y_k^{l(1)}, y_k^{l(2)}, \cdots, y_k^{l(\bar{m}_l)}\} \tag{3.6}$$

where $\bar{m}_l$ is total number of validated measurement for sensor $l$ at time $k$, and

$$y_k^{l(i)} := z_k^{l(l_i)} \tag{3.7}$$

where $1 \leq l_1 < l_2 < \cdots < l_{\bar{m}_l} \leq m_l$ when $\bar{m}_l \neq 0$. The validated set of measurements of sensor $l$ at time $k$, which passed the validation gates will be denoted by $Y_k^l$, containing $\bar{m}_l$ ($\leq m_l$) measurement vectors. The cumulative set of validated measurements from sensor $l$ up to time $k$ is denoted as

$$Y^{k(l)} := \{Y_1^l, Y_2^l, \cdots, Y_k^l\}. \tag{3.8}$$

The cumulative set of validated measurements from all sensors up to time $k$ is denoted as

$$Z^k := \{Y^{k(1)}, Y^{k(2)}, \cdots, Y^{k(q)}\}. \tag{3.9}$$

After measurement validation processing, there still exists uncertainty regarding the measurements' origins. Define the association events (hypotheses) $\theta_k^{a,b}$ ($a$ and $b$ are integers) as follows (here we follow [46]).

- $\theta_k^{0,0}$: none of the measurements in $Y_k^1$ or $Y_k^2$ is target originated,
- $\theta_k^{0,b}$: only $y_k^{2(b)}$ in $Y_k^2$ is a target measurement, all other measurements in $Y_k^1$ or $Y_k^2$ are clutter, $a = 0$, $b = 1, \cdots, \bar{m}_2$,

- $\theta_k^{a,0}$: only $y_k^{1(a)}$ in $Y_k^1$ is a target measurement, all other measurements in $Y_k^1$ or $Y_k^2$ are clutter, $a = 1, \cdots, \bar{m}_1$, $b = 0$,

- $\theta_k^{a,b}$: $y_k^{1(a)}$ and $y_k^{2(b)}$ in $Y_k^1$ and $Y_k^2$, respectively, are target measurements, all other measurements are clutter, $a = 1, \cdots, \bar{m}_1$, $b = 1, \cdots, \bar{m}_2$.

Therefore, there are a total of $\bar{m}_1\bar{m}_2+\bar{m}_1+\bar{m}_2+1$ possible association hypotheses, each of which has an association probability. Define the innovations $\nu_k^{a,b}$ as

$$\begin{aligned}
\nu_k^{0,0} &= \begin{bmatrix} 0_{n_{z1}\times 1} \\ \\ 0_{n_{z2}\times 1} \end{bmatrix}, \quad a = 0, \quad b = 0 \\
\nu_k^{0,b} &= \begin{bmatrix} 0_{n_{z1}\times 1} \\ \\ \nu_k^{2(b)} \end{bmatrix}, \quad a = 0, \quad b = 1, \cdots, \bar{m}_2 \\
\nu_k^{a,0} &= \begin{bmatrix} \nu_k^{1(a)} \\ \\ 0_{n_{z2}\times 1} \end{bmatrix}, \quad a = 1, \cdots, \bar{m}_1, \quad b = 0 \\
\nu_k^{a,b} &= \begin{bmatrix} \nu_k^{1(a)} \\ \\ \nu_k^{2(b)} \end{bmatrix}, \quad a = 1, \cdots, \bar{m}_1, \quad b = 1, \cdots, \bar{m}_2.
\end{aligned} \tag{3.10}$$

The covariance of the residual, $\nu_k^{l(i)} := z_k^{l(i)} - \hat{z}_k^l$, is given by (assume $q$=2, the case of 2 sensors)

$$S_k^1 := E\{\nu_k^{1(i)}\nu_k^{1(i)'}|Z^{k-1}\} = H_k^1 P_{k|k-1} H_k^{1'} + R_k^1 \tag{3.11}$$

$$S_k^2 := E\{\nu_k^{2(i)}\nu_k^{2(i)'}|Z^{k-1}\} = H_k^2 P_{k|k-1} H_k^{2'} + R_k^2 \tag{3.12}$$

where $H_k^l$ is the first order derivative (Jacobian matrix) of $h^l(.)$ evaluated at the state prediction $\hat{x}_{k|k-1}$. Note that (3.11) and (3.12) assume that $z_k^{l(i)}$ originates from the target. Since our approach to the problem deals with the multiple simultaneous measurements arising from two separate sensors that are tracking a single target through a common surveillance region, a method for combination of multiple measurements has to be devised. In order to do this, the combined covariance $S_k$ of the residual obtained from (3.11) and (3.12), also need to be considered as follows:

$$\begin{aligned} S_k &:= E\left\{ \begin{bmatrix} \nu_k^{1(i)} \\ \nu_k^{2(i)} \end{bmatrix} \begin{bmatrix} \nu_k^{1(i)'} & \nu_k^{1(i)'} \end{bmatrix} | Z^{k-1} \right\} \\ &= \begin{bmatrix} H_k^1 \\ H_k^2 \end{bmatrix} P_{k|k-1} \begin{bmatrix} H_k^{1'} & H_k^{2'} \end{bmatrix} + \begin{bmatrix} R_k^1 & 0 \\ 0 & R_k^2 \end{bmatrix}. \end{aligned} \tag{3.13}$$

Define the association event probabilities as

$$\beta_k^{a,b} := P[\theta_k^{a,b} | Y_k^1, Y_k^2, Z^{k-1}]. \tag{3.14}$$

Exploiting the diffuse model for clutter in [12, 21], it turns out that

$$\begin{aligned} \beta_k^{0,0} &= C \frac{\left(1-P_{D_1}P_{G_1}\right)\left(1-P_{D_2}P_{G_2}\right)}{(V_k^1)^{\bar{m}_1}(V_k^2)^{\bar{m}_2}}, \quad a=0, b=0 \\ \beta_k^{0,b} &= C \frac{P_{D_2}\left(1-P_{D_1}P_{G_1}\right)\mathcal{N}\left[\nu_k^{2(b)};0,S_k^2\right]}{(V_k^2)^{\bar{m}_2-1}\bar{m}_2}, \quad a=0, \quad b=1,\cdots,\bar{m}_2 \\ \beta_k^{a,0} &= C \frac{P_{D_1}\left(1-P_{D_2}P_{G_2}\right)\mathcal{N}\left[\nu_k^{1(a)};0,S_k^1\right]}{(V_k^1)^{\bar{m}_1-1}\bar{m}_1}, \quad a=1,\cdots,\bar{m}_1, \quad b=0 \\ \beta_k^{a,b} &= C \frac{P_{D_1}P_{D_2}\mathcal{N}\left[\nu_k^{a,b};0,S_k\right]}{\bar{m}_1\bar{m}_2(V_k^1)^{\bar{m}_1-1}(V_k^2)^{\bar{m}_2-1}}, \quad a=1,\cdots,\bar{m}_1, \quad b=1,\cdots,\bar{m}_2 \end{aligned} \tag{3.15}$$

where $P_{D_1}$ and $P_{D_2}$ are the detection probabilities that the sensors 1 and 2 detect the target, respectively, $P_{G_1}$ and $P_{G_2}$ are the probabilities that the target is in the validation region observed from sensors 1 and 2, respectively, $C$ is a normalization constant such that $\sum_{a=0}^{\bar{m}_1}\sum_{b=0}^{\bar{m}_2}\beta_k^{a,b}=1$. The related likelihood function is

$$\Lambda_k := p\left(Y_k^1, Y_k^2|Z^{k-1}\right) = \sum_{a=0}^{\bar{m}_1}\sum_{b=0}^{\bar{m}_2} p\left(Y_k^1, Y_k^2, \theta_k^{a,b}|Z^{k-1}\right) \tag{3.16}$$

where using the Bayes' formula, we obtain

$$p\left(Y_k^1, Y_k^2, \theta_k^{a,b}|Z^{k-1}\right) = p\left(Y_k^1, Y_k^2|\theta_k^{a,b}, Z^{k-1}\right) P[\theta_k^{a,b}]$$

$$= \begin{cases} \frac{\left(1-P_{D_1}P_{G_1}\right)\left(1-P_{D_2}P_{G_2}\right)}{\left[V_k^1\right]^{\bar{m}_1}\left[V_k^2\right]^{\bar{m}_2}}, & a=0,\ b=0 \\ \frac{\left(1-P_{D_1}P_{G_1}\right)\left(P_{D_2}P_{G_2}\right)/\bar{m}_2}{P_{G_2}\left[V_k^2\right]^{\bar{m}_2-1}} \times \mathcal{N}\left[\nu_k^{2(b)}; 0, S_k^2\right], & a=0,\ b=1,\cdots,\bar{m}_2 \\ \frac{\left(P_{D_1}P_{G_1}\right)\left(1-P_{D_2}P_{G_2}\right)/\bar{m}_1}{P_{G_1}\left[V_k^1\right]^{\bar{m}_1-1}} \times \mathcal{N}\left[\nu_k^{1(a)}; 0, S_k^1\right], & a=1,\cdots,\bar{m}_1,\ b=0 \\ \frac{\left(P_{D_1}P_{G_1}\right)\left(P_{D_2}P_{G_2}\right)/(\bar{m}_1\bar{m}_2)}{P_{G_1}\left[V_k^1\right]^{\bar{m}_1-1}P_{G_2}\left[V_k^2\right]^{\bar{m}_2-1}} \times \mathcal{N}\left[\nu_k^{a,b}; 0, S_k\right], & a=1,\cdots,\bar{m}_1,\ b=1,\cdots,\bar{m}_2. \end{cases} \tag{3.17}$$

Using state prediction $\hat{x}_{k|k-1}$ and its covariance $P_{k|k-1}$ at time $k-1$ (see Eqns. (2.12) and (2.12), respectively), one computes the partial update $\hat{x}_{k|k}$ and its covariance $P_{k|k}$ according to the standard PDAF [21] except that the augmented state is conditioned on $\theta_k^{a,b}$ with data combination from sensors 1 and 2.

Define the combined mode-conditioned innovations

$$\nu_k := \sum_{\substack{a=0 \\ (a,b)\neq(0,0)}}^{\bar{m}_1}\sum_{b=0}^{\bar{m}_2} \beta_k^{a,b}\nu_k^{a,b}. \tag{3.18}$$

Therefore, partial update of the state estimate is given by

$$\hat{x}_{k|k}^{a,b} := E\left\{x_k|\theta_k^{a,b}, Z^{k-1}, Y_k^1, Y_k^2\right\} = \hat{x}_{k|k-1} + W_k^{a,b}\nu_k^{a,b} \tag{3.19}$$

where Kalman gains, $W_k^{a,b}$, are computed as

$$W_k^{a,b} = \begin{cases} W_k^{0,0} = 0, & \text{for} \quad a = 0,\ b = 0 \\ W_k^{a,0} = P_{k|k-1}[H_k^{1'}[S_k^1]^{-1} \ \ 0], & \text{for} \quad a \neq 0,\ b = 0 \\ W_k^{0,b} = P_{k|k-1}[0 \ \ H_k^{2'}[S_k^2]^{-1}], & \text{for} \quad a = 0,\ b \neq 0 \\ W_k^{a,b} = P_{k|k-1}H_k'[S_k]^{-1}, & \text{for} \quad a \neq 0,\ b \neq 0, \end{cases} \tag{3.20}$$

and $H_k' = \left[H_k^{1'} \ \ H_k^{2'}\right]$. Despite the fact that here we follow [46] for the association events (hypotheses) $\theta_k^{a,b}$ to deal with existing uncertain measurements' origins, there are "oversights" in [46, Sec. 2.1]. When both sensor measurements are associated with the target, [46] states (p. 62, 2nd para., [46, Sec. 2.1]) that $W[k] = [W_1[k] \ \ W_2[k]]$ where $W[k]$ = Kalman filter gain for the "overall" filter and $W_i[k]$ = Kalman filter gain corresponding to the measurements from sensor $i$ ($i = 1, 2$). This is NOT true. Since the two sensors observe the same state, there is "cross-coupling" as described in Eqn. (3.20).

The mode-conditioned update of the state estimate is

$$\hat{x}_{k|k} := E\left\{x_k|M_k, Z^{k-1}, Y_k^1, Y_k^2\right\} = \sum_{a=0}^{\bar{m}_1}\sum_{b=0}^{\bar{m}_2}\beta_k^{a,b}\hat{x}_{k|k-1}^{a,b} \tag{3.21}$$

and the covariance of $\hat{x}_{k|k}$ is (follow the steps in [12, 22] for the standard PDAF)

$$\begin{aligned} P_{k|k} := P_{k|k-1} - \sum_{\substack{a=0 \\ (a,b)\neq(0,0)}}^{\bar{m}_1} \sum_{b=0}^{\bar{m}_2} \beta_k^{a,b} W_k^{a,b} S_k^{a,b} W_k^{a,b'} + \sum_{a=0}^{\bar{m}_1} \sum_{b=0}^{\bar{m}_2} \beta_k^{a,b} W_k^{a,b} \nu_k^{a,b} \nu_k^{a,b'} W_k^{a,b'} \\ - \left[ \sum_{a=0}^{\bar{m}_1} \sum_{b=0}^{\bar{m}_2} \beta_k^{a,b} W_k^{a,b} \nu^{a,b} \right] \left[ \sum_{a=0}^{\bar{m}_1} \sum_{b=0}^{\bar{m}_2} \beta_k^{a,b} W_k^{a,b} \nu^{a,b} \right]'. \end{aligned} \tag{3.22}$$

Now we are ready to extend the above simultaneous measurement update technique to a multiple model scenario.

### 3.3 Problem Formulation for the Multiple Model System

Assume that the target dynamics can be modeled by one of $n$ hypothesis models. The model set is denoted as $\mathcal{M}_n := \{1, \cdots, n\}$ and there are total $q$ sensors from which $q$, or fewer (if the probability of target detection is less than one) or more (due to clutter), measurement vectors are generated at a time. The event that model $j$ is in effect during the sampling period $(t_{k-1}, t_k]$ is denoted by $M_k^j$. For the $j$-th hypothesized model(mode), the state dynamics and measurements, respectively, are modeled as

$$x_k = F_{k-1}^j x_{k-1} + G_{k-1}^j v_{k-1}^j \tag{3.23}$$

and

$$z_k^l = h^l(x_k) + w_k^{j,l} \quad \text{for} \;\; l = 1, \cdots, q, \tag{3.24}$$

where $x_k$ is the system state at $t_k$ and of dimension $n_x$, $z_k^l$ is the (true) measurement vector (i.e., due to the target) from sensor $l$ at $t_k$ and of dimension $n_{zl}$, $F_{k-1}^j$ and $G_{k-1}^j$ are the system matrices when model $j$ is in effect over the sampling period $(t_{k-1}, t_k]$, and $h^l$ is the nonlinear transformation of $x_k$ to $z_k^l$ $(l = 1, \cdots, q)$ for model $j$. Henceforth,

time $t_k$ will be denoted by $k$. A first-order linearized version of (3.24) is given by

$$z_k^l = H_k^{j,l} x_k + w_k^{j,l} \quad \text{for} \;\; l = 1, \cdots, q, \tag{3.25}$$

where $H_k^{j,l}$ is the Jacobian matrix of $h^l$ evaluated at some value of the estimate of state $x_k$. The process noise $v_{k-1}^j$ and the measurement noise $w_k^{j,l}$ are mutually uncorrelated zero-mean white Gaussian processes with covariance matrices $Q_{k-1}^j$ and $R_k^{j,l}$, respectively. At the initial time $t_0$, the initial conditions for the system state under each model $j$ are assumed to be Gaussian random variables with the known mean $\bar{x}_0^j$ and the known covariance $P_0^j$. The probability of model $j$ at $t_0$, $\mu_0^j = P[M_0^j]$, is also assumed to be known. The switching from model $M_{k-1}^i$ to model $M_k^j$ is governed by a finite-state stationary Markov chain with known transition probabilities $p_{ij} = P[M_k^j | M_{k-1}^i]$.

The following notations and definitions are used regarding the measurements at sensor $l$. Note that, in general, at any time $k$, some measurements may be due to clutter and some due to the target, i.e., there can be more than a single measurement at time $k$ at sensor $l$. The measurement set (not yet validated) generated by sensor $l$ at time $k$ is denoted as

$$Z_k^l := \{z_k^{l(1)}, z_k^{l(2)}, \cdots, z_k^{l(m_l)}\} \tag{3.26}$$

where $m_l$ is the number of measurements generated by sensor $l$ at time $k$. Variable $z_k^{l(i)}$ $(i = 1, \cdots, m_l)$ is the $i$th measurement within the set. The cumulative set of measurements (not yet validated) from sensor $l$ up to time $k$ is denoted as $Z^{k(l)} := \{Z_1^l, Z_2^l, \cdots, Z_k^l\}$ and the cumulative set of measurements (not yet validated) from all sensors up to time $k$ is denoted as $Z^k := \{Z^{k(1)}, Z^{k(2)}, \cdots, Z^{k(q)}\}$ where $q$ is the number of sensors. The validated set of measurements of sensor $l$ at time $k$ will be denoted

by $Y_k^l$, containing $\bar{m}_l$ ($\leq m_l$) measurement vectors. The cumulative set of validated measurements from sensor $l$ up to time $k$ is denoted as

$$Y^{k(l)} := \{Y_1^l, Y_2^l, \cdots, Y_k^l\}. \tag{3.27}$$

The cumulative set of validated measurements from all sensors up to time $k$ is denoted as

$$Z^k := \{Y^{k(1)}, Y^{k(2)}, \cdots, Y^{k(q)}\}. \tag{3.28}$$

Our goal is to find the state estimate

$$\hat{x}_{k|k} := E\{x_k | Z^k\} \tag{3.29}$$

and the associated error covariance matrix

$$P_{k|k} := E\{[x_k - \hat{x}_{k|k}][x_k - \hat{x}_{k|k}]' | Z^k\} \tag{3.30}$$

where $x_k'$ denotes the transpose of $x_k$.

### 3.4 IMM/MSPDAF Algorithm for Simultaneous Measurement Update

We now modify the IMMPDA algorithms of [21] and [47] to derive the proposed IMM/MSPDAF with simultaneous measurement update system. We confine our attention to the case of 2 sensors; however, the algorithm can be easily adapted to the case of arbitrary $q$ sensors. We assume that all measurements observed from sensors are synchronized with the same sampling rate (see Fig. 3.1). We will only briefly outline the basic

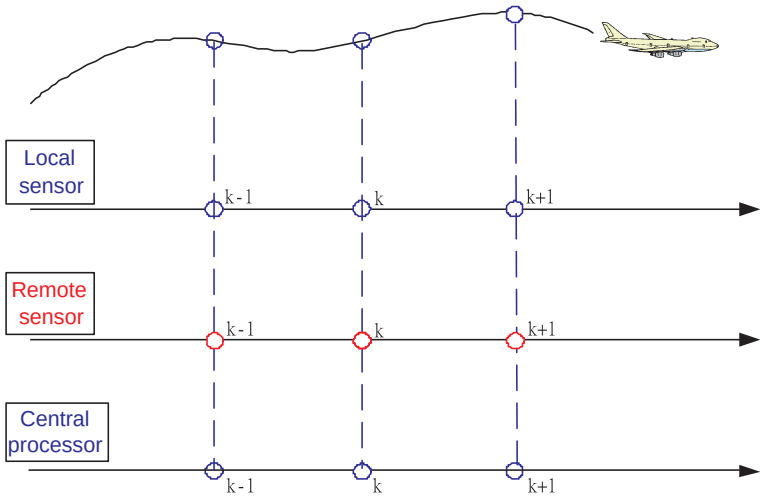


Figure 3.1: Target tracking example using synchronized measurements observed from multiple sensors

steps in 'one cycle' (i.e., processing needed to update for a new set of measurements) of the IMM/MSPDA filter.

**Assumed available** : Given the state estimate $\hat{x}^j_{k-1|k-1} := E\{x_{k-1}|M^j_{k-1}, Z^{k-1}\}$, the associated covariance $P^j_{k-1|k-1}$, and the conditional mode probability $\mu^j_{k-1} := P[M^j_{k-1}|Z^{k-1}]$ at time $k-1$ for each mode $j \in \mathcal{M}_n$.

**Step 1. Interaction - mixing of the estimate from previous time** ($\forall j \in \mathcal{M}_n$):

predicted mode probability:

$$\mu^{j-}_k := P[M^j_k|Z^{k-1}] = \sum_{i=1}^{n} p_{ij}\mu^i_{k-1}. \tag{3.31}$$

mixing probability:

$$\mu^{i|j} := P[M^i_{k-1}|M^j_k, Z^{k-1}] = p_{ij}\mu^i_{k-1}/\mu^{j-}_k. \tag{3.32}$$

mixed estimate:

$$\hat{x}^{0j}_{k-1|k-1} := E\{x_{k-1}|M^j_k, Z^{k-1}\} = \sum_{i=1}^{n} \hat{x}^i_{k-1|k-1}\mu^{i|j}. \tag{3.33}$$

covariance of the mixed estimate:

$$\begin{aligned} P^{0j}_{k-1|k-1} &:= E\{[x_{k-1} - \hat{x}^{0j}_{k-1|k-1}][x_{k-1} - \hat{x}^{0j}_{k-1|k-1}]'|M^j_k, Z^{k-1}\} \\ &= \sum_{i=1}^{n}\{P^i_{k-1|k-1} + [\hat{x}^i_{k-1|k-1} - \hat{x}^{0j}_{k-1|k-1}][\hat{x}^i_{k-1|k-1} - \hat{x}^{0j}_{k-1|k-1}]'\}\mu^{i|j}. \end{aligned} \tag{3.34}$$

**Step 2. Predicted state and measurements for sensors 1 and 2 ($\forall j \in \mathcal{M}_n$) :**

state prediction:

$$\hat{x}^j_{k|k-1} := E\{x_k|M^j_k, Z^{k-1}\} = F^j_{k-1}\hat{x}^{0j}_{k-1|k-1}. \tag{3.35}$$

state prediction error covariance:

$$\begin{aligned} P^j_{k|k-1} &:= E\{[x_k - \hat{x}^j_{k|k-1}][x_k - \hat{x}^j_{k|k-1}]'|M^j_k, Z^{k-1}\} \\ &= F^j_{k-1}P^{0j}_{k-1|k-1}F^{j'}_{k-1} + G^j_{k-1}Q^j_{k-1}G^{j'}_{k-1}. \end{aligned} \tag{3.36}$$

The mode-conditioned predicted measurement for sensor $l$ is

$$\hat{z}^{j,l}_k := h^l(\hat{x}^j_{k|k-1}). \tag{3.37}$$

Using the linearized version (3.25), the covariance of the mode-conditioned residual

$$\nu_k^{j,l(i)} := z_k^{l(i)} - \hat{z}_k^{j,l}$$

is given by (assume $q$=2, the case of 2 sensors)

$$S_k^{j,1} := E\{\nu_k^{j,1(i)} \nu_k^{j,1(i)'} | M_k^j, Z^{k-1}\} = H_k^{j,1} P_{k|k-1}^j H_k^{j,1'} + R_k^{j,1} \tag{3.38}$$

$$S_k^{j,2} := E\{\nu_k^{j,2(i)} \nu_k^{j,2(i)'} | M_k^j, Z^{k-1}\} = H_k^{j,2} P_{k|k-1}^j H_k^{j,2'} + R_k^{j,2} \tag{3.39}$$

where $H_k^{j,l}$ is the first order derivative (Jacobian matrix) of $h^l(.)$ evaluated at the state prediction $\hat{x}_{k|k-1}^j$ (see (3.37)). Note that (3.38) and (3.39) assume that $z_k^{l(i)}$ originates from the target.

As we mentioned earlier, since our approach to the problem deals with the multiple simultaneous measurements arising from two separate sensors that are tracking a single target through a common surveillance region, a method for combination of multiple measurements has to be devised. In order to do this, the combined covariance $S_k^j$ of the mode-conditioned residual obtained from (3.38) and (3.39) also needs to be considered as follows:

$$\begin{aligned} S_k^j &:= E\left\{ \begin{bmatrix} \nu_k^{j,1(i)} \\ \nu_k^{j,2(i)} \end{bmatrix} \begin{bmatrix} \nu_k^{j,1(i)'} & \nu_k^{j,1(i)'} \end{bmatrix} | M_k^j, Z^{k-1} \right\} \\ &= \begin{bmatrix} H_k^{j,1} \\ H_k^{j,2} \end{bmatrix} P_{k|k-1}^j \begin{bmatrix} H_k^{j,1'} & H_k^{j,2'} \end{bmatrix} + \begin{bmatrix} R_k^{j,1} & 0 \\ 0 & R_k^{j,2} \end{bmatrix}. \end{aligned} \tag{3.40}$$

**Step 3. Measurement validation for sensors 1 and 2 ($\forall j \in \mathcal{M}_n$):**

Since the measurement validation process was well explained in Sec. 3.2 for non-maneuvering target tracking scenario, we briefly describe the difference between non-maneuvering target tracking and maneuvering target tracking in this step. Following [12, 21], one sets up a validation gate for sensor $l$ centered at the mode-conditioned predicted measurement, $\hat{z}_k^{j,l}$. Let ($|A| = \det(A)$)

$$j_a := \arg \left\{ \max_{j \in \mathcal{M}_n} \left| S_k^{j,l} \right| \right\}. \tag{3.41}$$

Then measurement $z_k^{l(i)}$ ($i$=1,2,$\cdots$,$m_l$) is validated if and only if

$$[z_k^{l(i)} - \hat{z}_k^{j_a,l}]' [S_k^{j_a,l}]^{-1} [z_k^{l(i)} - \hat{z}_k^{j_a,l}] < \gamma. \tag{3.42}$$

The volume of the validation region with the threshold $\gamma$ is

$$V_k^l := c_{n_{zl}} \gamma^{n_{zl}/2} |S_k^{j_a,l}|^{1/2} \tag{3.43}$$

where $n_{zl}$ is the dimension of the measurement and $c_{n_{zl}}$ is the volume of the unit hyper-sphere of this dimension ($c_1$=2, $c_2$=$\pi$, $c_3$=4$\pi$/3, etc.). Choice of $\gamma$ is discussed in more detail in [12, Sec. 2.3.2].

**Step 4. State estimation with validated measurement from sensors 1 and 2 ($\forall j \in \mathcal{M}_n$) :**

Using the definition of the association events (hypotheses) $\theta_k^{a,b}$ (see Sec. 3.2), define the mode-conditioned association event probabilities as

$$\beta_k^{j,a,b} := P[\theta_k^{a,b} | M_k^j, Y_k^1, Y_k^2, Z^{k-1}]. \tag{3.44}$$

The mode-conditioned innovations $\nu_k^{j,a,b}$ can be defined as

$$\begin{aligned}
\nu_k^{j,0,0} &= \begin{bmatrix} 0_{n_{z1\times 1}} \\ \\ 0_{n_{z2\times 1}} \end{bmatrix}, \quad a = 0, b = 0 \\
\nu_k^{j,0,b} &= \begin{bmatrix} 0_{n_{z1\times 1}} \\ \\ \nu_k^{j,2(b)} \end{bmatrix}, \quad a = 0,\ b = 1, \cdots, \bar{m}_2 \\
\nu_k^{j,a,0} &= \begin{bmatrix} \nu_k^{j,1(a)} \\ \\ 0_{n_{z2\times 1}} \end{bmatrix}, \quad a = 1, \cdots, \bar{m}_1,\ b = 0 \\
\nu_k^{j,a,b} &= \begin{bmatrix} \nu_k^{j,1(a)} \\ \\ \nu_k^{j,2(b)} \end{bmatrix}, \quad a = 1, \cdots, \bar{m}_1,\ b = 1, \cdots, \bar{m}_2.
\end{aligned} \tag{3.45}$$

Exploiting the diffuse model for clutter in [12, 21], it turns out that (see **Appendix 1** for details)

$$\begin{aligned}
\beta_k^{j,0,0} &= C\frac{\left(1-P_{D_1}P_{G_1}\right)\left(1-P_{D_2}P_{G_2}\right)}{(V_k^1)^{\bar{m}_1}(V_k^2)^{\bar{m}_2}}, \quad a=0, b=0 \\
\beta_k^{j,0,b} &= C\frac{P_{D_2}\left(1-P_{D_1}P_{G_1}\right)\mathcal{N}\left[\nu_k^{j,2(b)};0,S_k^{j,2}\right]}{(V_k^2)^{\bar{m}_2-1}\bar{m}_2}, \quad a=0, \;\; b=1,\cdots,\bar{m}_2 \\
\beta_k^{j,a,0} &= C\frac{P_{D_1}\left(1-P_{D_2}P_{G_2}\right)\mathcal{N}\left[\nu_k^{j,1(a)};0,S_k^{j,1}\right]}{(V_k^1)^{\bar{m}_1-1}\bar{m}_1}, \quad a=1,\cdots,\bar{m}_1, \;\; b=0 \\
\beta_k^{j,a,b} &= C\frac{P_{D_1}P_{D_2}\mathcal{N}\left[\nu_k^{j,a,b};0,S_k^{j}\right]}{\bar{m}_1\bar{m}_2(V_k^1)^{\bar{m}_1-1}(V_k^2)^{\bar{m}_2-1}}, \quad a=1,\cdots,\bar{m}_1, \;\; b=1,\cdots,\bar{m}_2.
\end{aligned} \tag{3.46}$$

The likelihood function for each mode $j$ is

$$\Lambda_k^j := p\left(Y_k^1, Y_k^2 | M_k^j, Z^{k-1}\right) = \sum_{a=0}^{\bar{m}_1}\sum_{b=0}^{\bar{m}_2} p\left(Y_k^1, Y_k^2, \theta_k^{a,b} | M_k^j, Z^{k-1}\right) \tag{3.47}$$

where using the Bayes' formula, we obtain

$$p\left(Y_k^1, Y_k^2, \theta_k^{a,b} | M_k^j, Z^{k-1}\right) = p\left(Y_k^1, Y_k^2 | M_k^j, \theta_k^{a,b}, Z^{k-1}\right) P[\theta_k^{a,b}]$$

$$= \begin{cases}
\dfrac{\left(1-P_{D_1}P_{G_1}\right)\left(1-P_{D_2}P_{G_2}\right)}{\left[V_k^1\right]^{\bar{m}_1}\left[V_k^2\right]^{\bar{m}_2}}, & a=0,\; b=0 \\
\dfrac{\left(1-P_{D_1}P_{G_1}\right)\left(P_{D_2}P_{G_2}\right)/\bar{m}_2}{P_{G_2}\left[V_k^2\right]^{\bar{m}_2-1}} \times \mathcal{N}\left[\nu_k^{j,2(b)};0,S_k^{j,2}\right], & a=0,\; b=1,\cdots,\bar{m}_2 \\
\dfrac{\left(P_{D_1}P_{G_1}\right)\left(1-P_{D_2}P_{G_2}\right)/\bar{m}_1}{P_{G_1}\left[V_k^1\right]^{\bar{m}_1-1}} \times \mathcal{N}\left[\nu_k^{j,1(a)};0,S_k^{j,1}\right], & a=1,\cdots,\bar{m}_1,\; b=0 \\
\dfrac{\left(P_{D_1}P_{G_1}\right)\left(P_{D_2}P_{G_2}\right)/(\bar{m}_1\bar{m}_2)}{P_{G_1}\left[V_k^1\right]^{\bar{m}_1-1}P_{G_2}\left[V_k^2\right]^{\bar{m}_2-1}} \times \mathcal{N}\left[\nu_k^{j,a,b};0,S_k^{j}\right], & a=1,\cdots,\bar{m}_1,\; b=1,\cdots,\bar{m}_2.
\end{cases} \tag{3.48}$$

Using $\hat{x}^j_{k|k-1}$ (from (3.35)) and its covariance $P^j_{k|k-1}$ (from (3.36)), one computes the partial update $\hat{x}^j_{k|k}$ and its covariance $P^j_{k|k}$ according to the standard PDAF [21], except that the augmented state is conditioned on $\theta^{a,b}_k$ with data combination from sensors 1 and 2.

Define the combined mode-conditioned innovations

$$\nu^j_k := \sum_{\substack{a=0 \\ (a,b)\neq(0,0)}}^{\bar{m}_1} \sum_{b=0}^{\bar{m}_2} \beta^{j,a,b}_k \nu^{j,a,b}_k. \tag{3.49}$$

The partial update of the state estimate is given by

$$\hat{x}^{j,a,b}_{k|k} := E\left\{x_k | \theta^{a,b}_k, M^j_k, Z^{k-1}, Y^1_k, Y^2_k\right\} = \hat{x}^j_{k|k-1} + W^{j,a,b}_k \nu^{j,a,b}_k \tag{3.50}$$

where the mode-conditioned Kalman gains, $W^{j,a,b}_k$, are computed as

$$W^{j,a,b}_k = \begin{cases} W^{j,0,0}_k = 0, & \text{for} \quad a=0,\ b=0 \\ W^{j,a,0}_k = P^j_{k|k-1}\left[H^{j,1'}_k [S^{j,1}_k]^{-1} \ \ 0\right], & \text{for} \quad a\neq 0,\ b=0 \\ W^{j,0,b}_k = P^j_{k|k-1}\left[0 \ \ H^{j,2'}_k [S^{j,2}_k]^{-1}\right], & \text{for} \quad a=0,\ b\neq 0 \\ W^{j,a,b}_k = P^j_{k|k-1} H^{j'}_k [S^j_k]^{-1}, & \text{for} \quad a\neq 0,\ b\neq 0 \end{cases} \tag{3.51}$$

and $H^{j'}_k = \left[H^{j,1'}_k \ \ H^{j,2'}_k\right]$. Therefore, the mode-conditioned update of the state estimate is

$$\hat{x}^j_{k|k} := E\left\{x_k | M^j_k, Z^{k-1}, Y^1_k, Y^2_k\right\} = \sum_{a=0}^{\bar{m}_1} \sum_{b=0}^{\bar{m}_2} \beta^{j,a,b}_k \hat{x}^{j,a,b}_{k|k-1} \tag{3.52}$$

and the covariance of $\hat{x}^j_{k|k}$ is

$$P^j_{k|k} := P^j_{k|k-1} - \sum_{\substack{a=0 \\ (a,b)\neq(0,0)}}^{\bar{m}_1} \sum_{b=0}^{\bar{m}_2} \beta^{j,a,b}_k W^{j,a,b}_k S^{j,a,b}_k W^{j,a,b'}_k + \sum_{a=0}^{\bar{m}_1} \sum_{b=0}^{\bar{m}_2} \beta^{j,a,b}_k W^{j,a,b}_k \nu^{j,a,b}_k \nu^{j,a,b'}_k W^{j,a,b'}_k$$
$$- \left[\sum_{a=0}^{\bar{m}_1} \sum_{b=0}^{\bar{m}_2} \beta^{j,a,b}_k W^{j,a,b}_k \nu^{j,a,b}\right] \left[\sum_{a=0}^{\bar{m}_1} \sum_{b=0}^{\bar{m}_2} \beta^{j,a,b}_k W^{j,a,b}_k \nu^{j,a,b}\right]'. \tag{3.53}$$

**Step 5. Update of mode probabilities**($\forall j \in \mathcal{M}_n$) :

$$\mu^j_k := P\left[M^j_k | Y^k\right] = \frac{1}{C} \mu^{j-}_k \Lambda^j_k \tag{3.54}$$

where $C$ is a normalization constant such that $\sum_j \mu^j_k = 1$.

**Step 6. Combination of the mode-conditioned estimates**($\forall j \in \mathcal{M}_n$) :

The final state estimate update at time $k$ is given by

$$\hat{x}_{k|k} = \sum\nolimits_j \hat{x}^j_{k|k} \mu^j_k \tag{3.55}$$

and its covariance is given by

$$P_{k|k} = \sum\nolimits_j \left\{ P^j_{k|k} + \left[\hat{x}^j_{k|k} - \hat{x}_{k|k}\right] \left[\hat{x}^j_{k|k} - \hat{x}_{k|k}\right]' \right\} \mu^j_k. \tag{3.56}$$

### 3.5 Simulation Example

The following example of tracking a highly maneuvering target in clutter is considered.

**The True Trajectory**: The target starts at location [21689 10840 40] in Cartesian

coordinates in meters. The initial velocity (in m/s) is [-8.3 -399.9 0] and the target stays at constant altitude with a constant speed of 400 m/s. Its trajectory is:

- a straight line with constant velocity between 0 and 20s,
- a coordinated turn (0.15 rad/s) with constant acceleration of 60 m/s$^2$ between 20 and 35s,
- a straight line with constant velocity between 35 and 55s,
- a coordinated turn (0.1 rad/s) with constant acceleration of 40 m/s$^2$ between 55 and 70s,
- a straight line with constant velocity between 70 and 90s.

Fig. 3.2 shows the true trajectory of the target.

**The Target Motion Models**: The target motion models are patterned after [21]. In each mode the target dynamics are modelled in Cartesian coordinates as

$$x_k = Fx_{k-1} + Gv_{k-1}$$

where the state of the target is position, velocity, acceleration in each of the 3 Cartesian coordinates ($x, y$, and $z$). Thus $x_k$ is of dimension 9 ($n_x$=9). Three maneuver models are considered in the following discussion. The system matrices $F$, $G$, are defined as

$$F = \begin{bmatrix} F_b & 0 & 0 \\ 0 & F_b & 0 \\ 0 & 0 & F_b \end{bmatrix} \quad \text{and} \quad G = \begin{bmatrix} G_b & 0 & 0 \\ 0 & G_b & 0 \\ 0 & 0 & G_b \end{bmatrix}.$$

- **Model 1**. Nearly constant velocity model with zero mean perturbation in acceleration

$$F_b^1 = \begin{bmatrix} 1 & T & 0 \\ 0 & 1 & 0 \\ 0 & 0 & 0 \end{bmatrix} \quad \text{and} \quad G_b^1 = \begin{bmatrix} \frac{T^2}{2} \\ T \\ 0 \end{bmatrix},$$

where $T$ is the sampling period. The standard deviation of the process noise of $M^1$ is $5\text{m/s}^2$ (as in [21]).

- **Model 2**. Wiener process acceleration (nearly constant acceleration motion)

$$F_b^2 = \begin{bmatrix} 1 & T & \frac{T^2}{2} \\ 0 & 1 & T \\ 0 & 0 & 1 \end{bmatrix} \quad \text{and} \quad G_b^2 = \begin{bmatrix} \frac{T^2}{2} \\ T \\ 1 \end{bmatrix}$$

The standard deviation of the process noise of $M^2$ is $7.5\text{m/s}^2$ (as in [21]).

- **Model 3**. Wiener process acceleration (model with large acceleration increments, for the onset and termination of maneuvers), with $F_b^3 = F_b^2$ and $G_b^3 = G_b^2$. The standard deviation of the process noise of $M^3$ is $40\text{m/s}^2$ (as in [21]).

The initial model probabilities are $\mu_0^1 = 0.8$, $\mu_0^2 = 0.1$ and $\mu_0^3 = 0.1$. The mode switching probability matrix is given by (as in [21])

$$\begin{bmatrix} p_{11} & p_{12} & p_{13} \\ p_{21} & p_{22} & p_{23} \\ p_{31} & p_{32} & p_{33} \end{bmatrix} = \begin{bmatrix} 0.8 & 0.0 & 0.2 \\ 0.0 & 0.8 & 0.2 \\ 0.3 & 0.3 & 0.4 \end{bmatrix}.$$

**The Sensors**: Two sensors are used to obtain the measurements:

- ***Case 1***. Sensor 1 and Sensor 2 are located at $[x_1, y_1, z_1]$=[-4000 4000 0] m and $[x_2, y_2, z_2]$=[5000 0 0] m, respectively, and the central processor is collocated with sensor 1 platform.

- ***Case 2***. Sensor 1 and Sensor 2 are collocated at $[x_1, y_1, z_1]$=[-4000 4000 0] m together with the central processor.

The measurements from sensor $l$ for model $j$ are $z_k^l = h^l(x_k) + w_k^{j,l}$ for $l = 1$ and 2, reflecting range and azimuth angle for sensor 1 (radar) and azimuth and elevation angles for sensor 2 (infrared). The range, azimuth, and elevation angle transformations, respectively, are given by

$$r_l = \{(x - x_l)^2 + (y - y_l)^2 + (z - z_l)^2\}^{1/2} \tag{3.57}$$

$$a_l = \tan^{-1}[(y - y_l)/(x - x_l)] \tag{3.58}$$

$$e_l = \tan^{-1}[(z - z_l)/\{(x - x_l)^2 + (y - y_l)^2\}^{1/2}]. \tag{3.59}$$

The Jacobian matrices of $h^l(.)$ for sensors 1 and 2 are

$$H^{j,1} = \begin{bmatrix} \cos(e_1)\cos(a_1) & 0 & 0 & \cos(e_1)\sin(a_1) & 0 & 0 & \sin(e_1) & 0 & 0 \\ -\frac{\sin(a_1)}{r_1\cos(e_1)} & 0 & 0 & \frac{\cos(a_1)}{r_1\cos(e_1)} & 0 & 0 & 0 & 0 & 0 \end{bmatrix} \forall j \quad (3.60)$$

$$H^{j,2} = \begin{bmatrix} -\frac{\sin(a_2)}{r_2\cos(e_2)} & 0 & 0 & \frac{\cos(a_2)}{r_2\cos(e_2)} & 0 & 0 & 0 & 0 & 0 \\ -\frac{\sin(e_2)\cos(a_2)}{r_2} & 0 & 0 & -\frac{\sin(e_2)\sin(a_2)}{r_2} & 0 & 0 & \frac{\cos(e_2)}{r_2} & 0 & 0 \end{bmatrix} \forall j, \quad (3.61)$$

respectively. The measurement noise $w_k^{j,l}$ for sensor $l$ is assumed to be zero-mean white Gaussian with known covariances, $R^1$=diag$[q_r, q_{a1}]$=diag[400m$^2$,49 mrad$^2$] with $q_r$ and $q_{a1}$ denoting the variances for the radar range and azimuth measurement noises, respectively, and $R^2$ = diag$[q_{a2}, q_e]$ = diag[4mrad$^2$, 4mrad$^2$] with $q_{a2}$ and $q_e$ denoting the variances for the infrared sensor azimuth and elevation measurement noises, respectively. The sampling interval was $T$=1s and it was assumed that the probability of detection $P_D$=0.997 for both sensors.

**The Clutter**: For generating false measurements in simulations, the clutter was assumed to be Poisson distributed with expected number of $\lambda_1 = 50 \times 10^{-6}$/m mrad for sensor 1 and $\lambda_2 = 3.5 \times 10^{-4}$/m$^2$ mrad for sensor 2. These statistics were used for generating the clutter in all simulations. However, a nonparametric clutter model was used for implementing all the algorithms for target tracking.

**Other Parameters**: The gates for setting up the validation regions for both the sensors were based on the threshold $\gamma$=16 corresponding to a gate probability $P_G$=0.9997.

**Simulation Results**: Fig. 3.3 shows the RMSE (root mean-square error) in position for the proposed IMM/MSPDAF and the standard sequential IMM/MSPDAF [21] based on 200 Monte Carlo runs. It is seen that the proposed simultaneous measurement updating can significantly improve the accuracy of track estimation during the periods following the onset of the target maneuvers. The first maneuver starts at 20 sec and in Fig. 3.3 one can see a significant improvement from 22 sec through 26 sec. The second maneuver starts at 55 sec and in Fig. 3.3 one can see a significant improvement from 58 sec through 59 (in (a) or 60 in (b)) sec. That is, simultaneous measurement updating responds faster to maneuvers. Once the target is "settled" in a particular mode, there is insignificant differences between the two approaches. It is also seen that tracking with separated sensors can improve the accuracy of track estimation compared to using collocated sensors.

To assess the computational requirements of the two approaches, we computed the CPU time needed to execute 90 time steps in each run (averaged 100 Monte Carlo runs excluding data/clutter generation) in MATLAB 6.5 on a 2.8 GHz (Mobile) Pentium 4 operating under Windows XP (professional). The standard sequential IMM/MSPDAF needs 0.4862 secs (for all 90 time steps) compared to 0.5806 secs required by proposed IMM/MSPDAF. Thus there is, on the average, a 20.3% increase in computational cost.

## 3.6 Conclusions

We investigated an IMM/MSPDAF algorithm with simultaneous measurement update for tracking a highly maneuvering target in clutter. A past approach [45] using parallel sensor processing has ignored certain data association probabilities leading

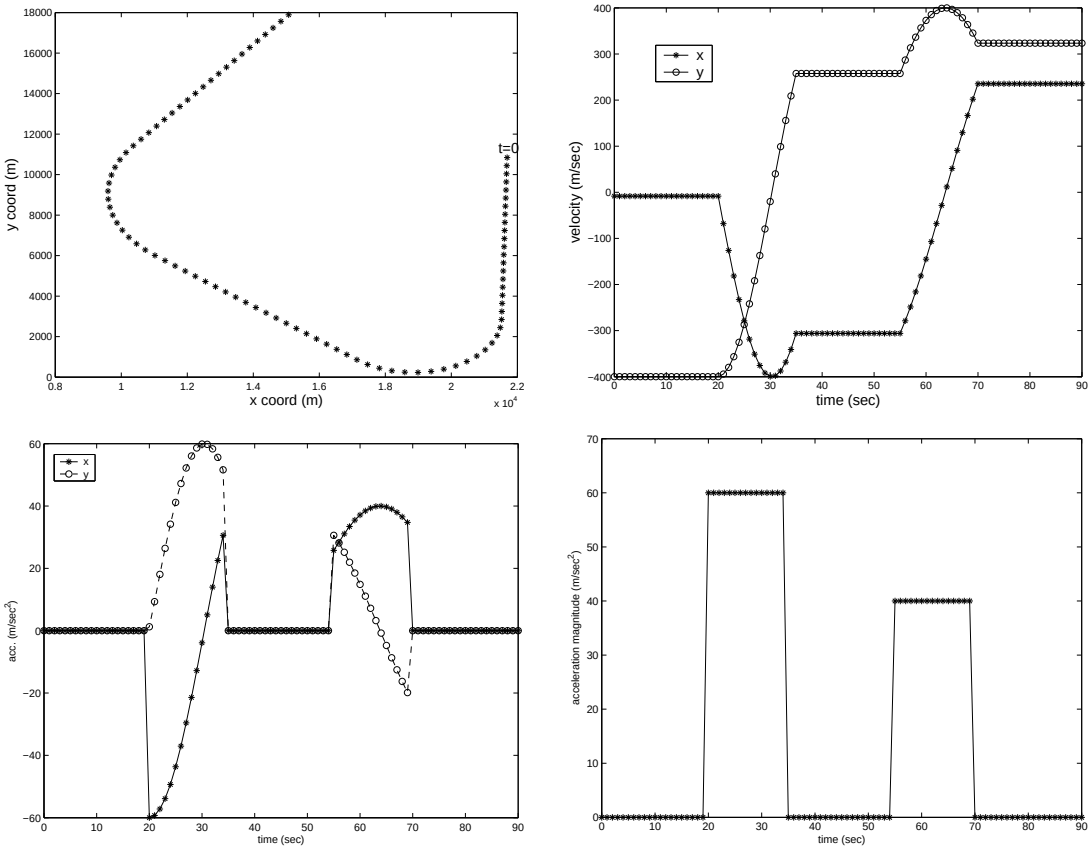


Figure 3.2: Trajectory of the maneuvering target (read left to right, top to bottom). (a) Position in $xy$ plane. (b) $x$ and $y$ velocities. (c) $x$ and $y$ accelerations. (d) magnitude of accelerations

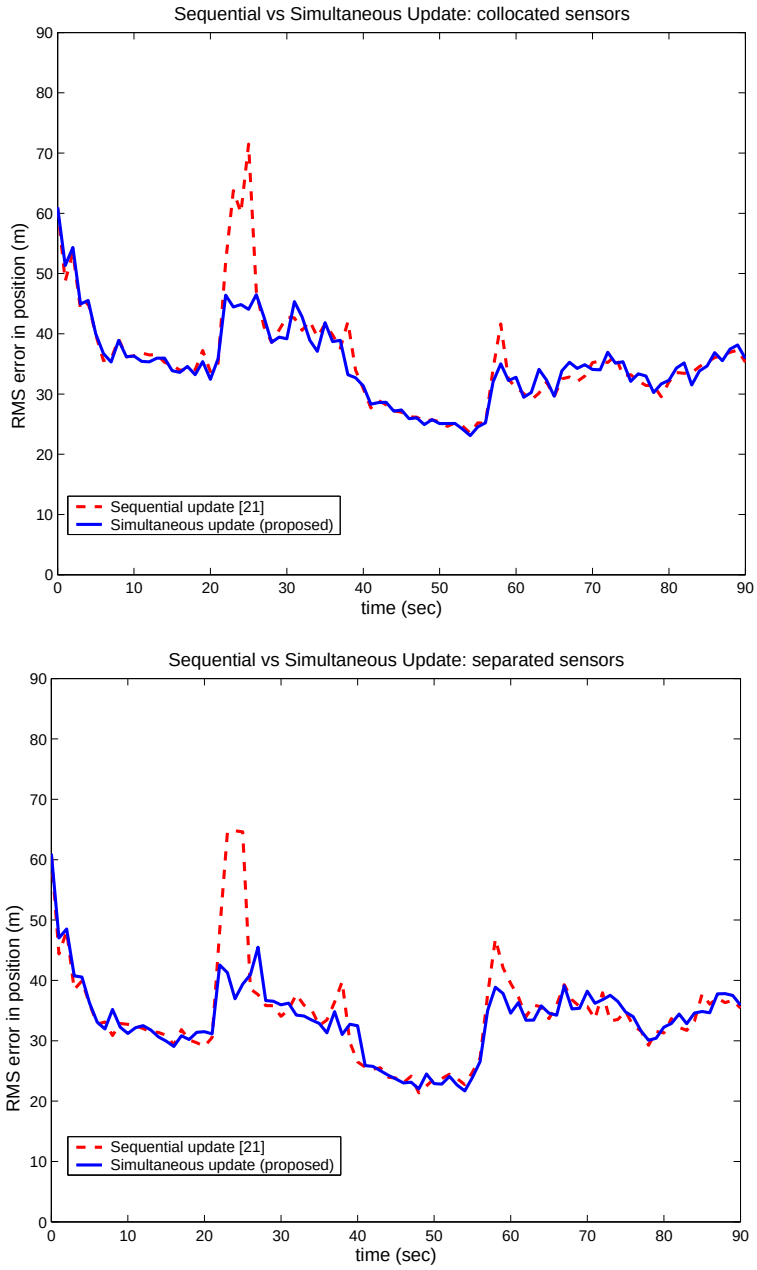


Figure 3.3: Performance of the simultaneous measurement updating IMM/MSPDAF in terms of the RMSE (root mean square error) in position (read top to bottom). (a) proposed IMM/MSPDAF vs standard sequential IMM/MSPDAF [21] with collocated sensors (Case 2). (b) proposed IMM/MSPDAF vs standard sequential IMM/MSPDAF [21] with separated sensors (Case 1).

to an inaccurate implementation. Another existing approach [46] applies only to non-maneuvering targets. Our proposed approach has extended the multisensor approach of [46] to maneuvering targets by employing a switching multiple model approach.

The proposed algorithm was illustrated via a simulation example where it outperformed a standard IMM/MSPDAF algorithm with sequential updating [21] during the periods following the onset of the target maneuvers. The simultaneous updating is expected to be more accurate [12] since it considers all association hypotheses coupled across multisensor while the sequential updating considers the separate hypothesis for each sensor. This improvement in accuracy is seen in our simulation example only during the periods following the onset of the target maneuvers. Once the target is settled in a particular mode, there is insignificant differences between the two approaches. The improvement in accuracy comes at the expense of a slight increase (20%) in the computational cost.

# Chapter 4

## Multisensor Tracking of a Maneuvering Target in Clutter with Asynchronous Measurements using Augmented State IMMPDA Filtering and Simultaneous Measurement Update

In this chapter, we discuss a suboptimal filtering algorithm for tracking a highly maneuvering target in a cluttered environment using multiple sensors dealing with possibly asynchronous (time delayed) measurements. The filtering algorithm is developed by applying the basic IMM approach, the PDA technique, and asynchronous measurement updating for state-augmented system estimation for the target. A state augmented approach is developed to estimate the time delay between local and remote sensors. A multisensor probabilistic data association filter is developed for parallel sensor processing for target tracking under clutter. The algorithm is illustrated via a highly maneuvering target tracking simulation example where two sensors, a radar and an infrared sensor, are used. Compared with an existing IMMPDA filtering algorithm with the assumption of synchronous (no delay) measurements sensor processing which is presented in Chapter 3, the proposed algorithm achieves considerable improvement (especially in the case of larger delays) in the accuracy of track estimation.

## 4.1 Introduction

We extend our simultaneous measurement update technique presented in Chapter 3 to asynchronous (delayed) measurements problem. In target tracking systems measurements are typically collected in "scans" or "frames" and then transmitted to a processing center [27, 35]. Asynchronous (delayed) measurements arise in a multisensor central tracking system due to communication network delays, varying preprocessing times at the sensor platforms and possibly lack of sampling time synchronization among sensor platforms (see Fig. 4.1).

One of the asynchronous measurement problems is that of out-of-sequence measurements (OOSM) where measurements at various sensors may arrive out-of-sequence (not in correct time order) at the central processor. OOSM has been considered using IMM [35, 36, 37]. In this chapter we do not consider OOSM (OOSM scenario is presented in Chapter 5.) but instead consider "in-sequence" measurements with a fixed-but-unknown relative time-delay among sensor measurements. Various sensor measurements are assumed to be at the same rate but not necessarily time synchronized. All measurements over one sampling interval (based on the local clock of the central processor) are collected at the central processor, attributed to one time instant and processed simultaneously. We exploit IMM and PDA techniques. It is assumed that a track has been formed (initiated) and the objective of this work is to investigate fixed-but-unknown relative time-delay (measurement timing mismatch) arising in a multisensor central tracking system.

In [26], fixed-lag smoothing techniques have been investigated using IMM algorithm combined with PDA filter in a multiple sensor scenario to propose a combined

IMM/MSPDAF (interacting multiple model multiple sensor probabilistic data association filter). We exploit the basic structure of [21] in combination with a state-augmented approach to deal with the fixed-but-unknown relative time-delay. In [21] and [45] it is assumed that the sensors are collocated and (time) synchronized with the sampling rate. In contrast, the sensor collocation and (time) synchronization are no longer assumed in this chapter. Also, we use simultaneous measurement updating of the state estimates. In this chapter, we also extend the multisensor approach of [46] to maneuvering targets (see Step 4 in Sec.4.4).

This chapter is organized as follows. Sec. 4.2 presents the problem formulation. Sec. 4.3 describes the state-augmented system approach. Sec. 4.4 describes the proposed augmented state IMM/MSPDAF (AS-IMM/MSPDAF) algorithm for asynchronous measurements. Simulation results using the proposed algorithm for a realistic problem are given in Sec. 4.5. Finally, Sec. 4.6 presents a discussion of the results and some conclusions.

## 4.2 Problem Formulation for Asynchronous measurements

The system dynamics and measurement equation which is synchronized with central processor are the same as in the problem formulation for the multiple model system in Chapter 3 (see (3.23)-(3.25)). Hence we do not reiterate them in this chapter. The basic scenario of multisensor target tracking system dealing with asynchronous measurements can be seen from Fig. 4.1. Assume that there is a fixed-but-unknown relative time delay $d_k$ between the remote sensor clock and the central processor clock at sample time $t_k$ as shown in Fig. 4.1. This time delay could be due to unsynchronized clocks at the two locations or due to inherent delay due to congestion, insufficient bandwidth

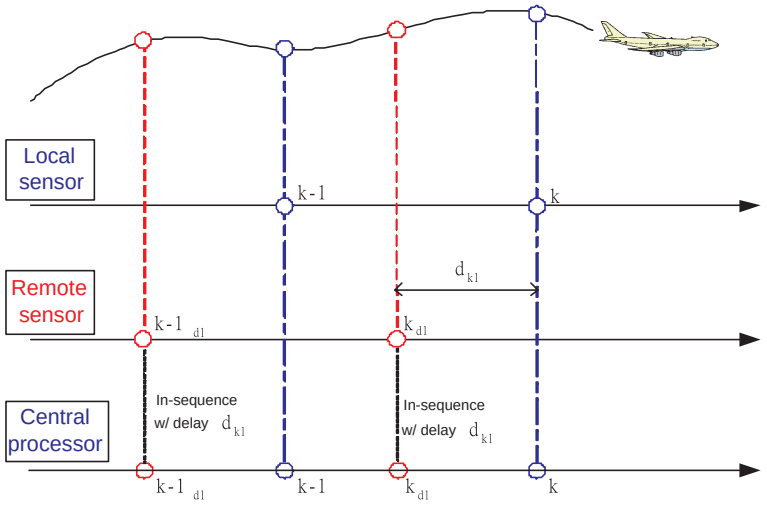


Figure 4.1: Target tracking with a fixed-but-unknown relative time delay $d_k$ between the remote sensor clock and the central processor clock at sample time $t_k$

etc. in the communication link between the remote sensor platform and the central processor. The measurements from sensor $l$ are sent to the central processor where all measurements collected between local sampling interval $(t_{k-1}, t_k]$ are attributed to time $t_k$. The state dynamics and measurements reported from the remote sensor platform at time $t_{k_{dl}}$ (henceforth will be denoted by $k_{dl}$) to the central processor at time $t_k$ can be modeled as (see Sec. 4.5 for some details)

$$x_{k_{dl}} = F^j_{k_{dl},k-1} x_{k-1} + G^j_{k_{dl},k-1} v^j_{k-1} \tag{4.1}$$

and

$$z^l_k = h^l(x_{k_{dl}}) + w^{j,l}_k \tag{4.2}$$

where $t_{k_{dl}} = t_k - d_{kl}$ and $d_{kl}$ is the time difference between the sampling time at the central processor and the measurement time at the local sensor (assume that $0 \leq d_{kl} < T$,

where $T$ is sampling time), $x_{k_{dl}}$ is the system state at $t_{k_{dl}}$ and of dimension $n_x$, $F^j_{k_{dl},k-1}$ and $G^j_{k_{dl},k-1}$ are the system matrices when model $j$ is in effect over the timing interval $(t_{k-1}, t_{k_{dl}}]$. See Sec. 4.5 for a concrete example of these models.

### 4.3 State-Augmented System

Define the augmented state $\bar{x}_k$ from $x_k$ as

$$\bar{x}_k = \begin{bmatrix} x_k \\ v^j_k \\ x_{k-1} \\ v^j_{k-1} \end{bmatrix} \tag{4.3}$$

where $x'_k$ denotes the transpose of $x_k$. Assume that there is a fixed-but-unknown delay, $d_{kl}$, between the central processor and the remote sensor $l$ platform. Using the above definitions (4.1, 4.3) and the measurement delay, $d_{kl}$ (see Fig. 4.1), the augmented state equation may be written more compactly as

$$\bar{x}_k = \bar{F}^j_{k,k-1}\bar{x}_{k-1} + \bar{G}^j_{k,k-1}v^j_k \tag{4.4}$$

and

$$d_{kl} = d_{(k-1)l} + v^{dl}_{k-1} \tag{4.5}$$

where $v^{dl}_{k-1}$ is a small processing noise assumed to be Gaussian noise with zero mean and (very) small but nonzero variance. Note that the process noise in (4.4) is $v^j_k$ (not at time $k-1$ but at time $k$). Above equations (4.4) and (4.5) can also be absorbed into another

augmented state $\tilde{x}_k$ as

$$\tilde{x}_k = \begin{bmatrix} \bar{x}_k \\ \\ d_{kl} \end{bmatrix} = \tilde{F}^j_{k,k-1}\tilde{x}_{k-1} + \tilde{G}^j_{k,k-1}\tilde{v}^j_k, \qquad \text{where} \quad \tilde{v}^j_k = \begin{bmatrix} v^j_k \\ \\ v^{dl}_{k-1} \end{bmatrix} \tag{4.6}$$

and $\tilde{F}_{k,k-1}$ and $\tilde{G}_{k,k-1}$ are defined in Sec. 4.5 (see (4.32)-(4.41)). Using the augmented state (4.6) the counterparts to ((3.24): measurements reported from local sensor) and ((4.2): measurements reported from remote sensor), respectively, are

$$z^l_k = h^l(\tilde{x}_k) + w^{j,l}_k = h^l([I, 0, 0, 0, 0]\tilde{x}_k) + w^{j,l}_k \tag{4.7}$$

and

$$z^l_k = h^l(\tilde{x}_k) + w^{j,l}_k = h^l([0, 0, F^j_{k_{dl},k-1}, G^j_{k_{dl},k-1}, 0]\tilde{x}_k) + w^{j,l}_k \tag{4.8}$$

for both measurements from local sensor and from remote sensor, respectively. To keep the notations and details to a bare minimum, we will consider the case of two sensors only and furthermore, we will assume that one of the sensors is either collocated with or is synchronized with the central processor, so that we will drop the subscript $l$ from $d_{kl}$. For more than two sensors, we need to augment $\tilde{x}_k$ with additional $d_k$'s (total $q-1$): in essence, these delays are relative to one of the sensors (reference sensor).

## 4.4 AS-IMM/MSPDAF Algorithm for Asynchronous Measurements

In this section, we now modify the augmented state IMM/MSPDA (AS-IMM/MSPDA) algorithms of [47] to apply to the multi-sensor asynchronous measurements system. We confine our attention to the case of 2 sensors; however, the algorithm can be easily

adapted to the case of arbitrary $q$ sensors. We will only briefly outline the basic steps in 'one cycle' (i.e., processing needed to update for a new set of measurements) of the proposed AS-IMM/MSPDA filter.

**Assumed available**: Given the state estimate $\hat{\tilde{x}}^j_{k-1|k-1} := E\{\tilde{x}_{k-1}|M^j_{k-1}, Z^{k-1}\}$, the associated covariance $\tilde{P}^j_{k-1|k-1}$, and the conditional mode probability $\mu^j_{k-1} := P[M^j_{k-1}|Z^{k-1}]$ at time $k-1$ for each mode $j \in \mathcal{M}_n$.

***Step 1. Interaction – mixing of the estimate from the previous time*** ($\forall j \in \mathcal{M}_n$) :

predicted mode probability:

$$\mu^{j-}_k := P[M^j_k|Z^{k-1}] = \sum_i p_{ij}\mu^i_{k-1} \tag{4.9}$$

mixing probability:

$$\mu^{i|j} := P[M^i_{k-1}|M^j_k, Z^{k-1}] = p_{ij}\mu^i_{k-1}/\mu^{j-}_k \tag{4.10}$$

mixed estimate:

$$\hat{\tilde{x}}^{0j}_{k-1|k-1} := E\{\tilde{x}_{k-1}|M^j_k, Z^{k-1}\} = \sum_i \hat{\tilde{x}}^i_{k-1|k-1}\mu^{i|j} \tag{4.11}$$

covariance of the mixed estimate:

$$\begin{aligned} \tilde{P}^{0j}_{k-1|k-1} &:= E\{[\tilde{x}_{k-1} - \hat{\tilde{x}}^{0j}_{k-1|k-1}][\tilde{x}_{k-1} - \hat{\tilde{x}}^{0j}_{k-1|k-1}]'|M^j_k, Z^{k-1}\} \\ &= \sum_i \{\tilde{P}^i_{k-1|k-1} + [\hat{\tilde{x}}^i_{k-1|k-1} - \hat{\tilde{x}}^{0j}_{k-1|k-1}][\hat{\tilde{x}}^i_{k-1|k-1} - \hat{\tilde{x}}^{0j}_{k-1|k-1}]'\}\mu^{i|j}. \end{aligned} \tag{4.12}$$

***Step 2. Predicted state and measurements for sensors 1 and 2 ($\forall j \in \mathcal{M}_n$)*** :

state prediction:

$$\hat{\tilde{x}}^j_{k|k-1} := E\{\tilde{x}_k | M^j_k, Z^{k-1}\} = \tilde{F}^j_{k-1} \hat{\tilde{x}}^{0j}_{k-1|k-1} \tag{4.13}$$

state prediction error covariance:

$$\begin{aligned} \tilde{P}^j_{k|k-1} &:= E\{[\tilde{x}_k - \hat{\tilde{x}}^j_{k|k-1}][\tilde{x}_k - \hat{\tilde{x}}^j_{k|k-1}]' | M^j_k, Z^{k-1}\} \\ &= \tilde{F}^j_{k-1} \tilde{P}^{0j}_{k-1|k-1} \tilde{F}^{j'}_{k-1} + \tilde{G}^j_{k-1} Q^j_{k-1} \tilde{G}^{j'}_{k-1} \end{aligned} \tag{4.14}$$

The mode-conditioned predicted measurement for sensor $l$ is

$$\hat{z}^{j,l}_k := h^l(\hat{\tilde{x}}^j_{k|k-1}). \tag{4.15}$$

Using the linearized version (4.15), the covariance of the mode-conditioned residual

$$\nu^{j,l(i)}_k := z^{l(i)}_k - \hat{z}^{j,l}_k \tag{4.16}$$

is given by (assume $q$=2, the case of 2 sensors)

$$S^{j,1}_k := E\{\nu^{j,1(i)}_k \nu^{j,1(i)'}_k | M^j_k, Z^{k-1}\} = \tilde{H}^{j,1}_k \tilde{P}^j_{k|k-1} \tilde{H}^{j,1'}_k + R^{j,1}_k, \tag{4.17}$$

$$S^{j,2}_k := E\{\nu^{j,2(i)}_k \nu^{j,2(i)'}_k | M^j_k, Z^{k-1}\} = \tilde{H}^{j,2}_k \tilde{P}^j_{k|k-1} \tilde{H}^{j,2'}_k + R^{j,2}_k \tag{4.18}$$

where $\tilde{H}_k^{j,l}$ is the first order derivative (Jacobian matrix) of $h^l(.)$ evaluated at the state prediction $\hat{\tilde{x}}_{k|k-1}^j$ (see (4.15)). Note that (4.17) and (4.18) assume that $z_k^{l(i)}$ originates from the target. The results (4.17) and (4.18) do not depend upon the actual measurements.

As mentioned earlier, since our approach to the problem deals not only with the asynchronous measurements but also with multiple simultaneous measurements [46, 48] arising from two separate sensors that are tracking a single target through a common surveillance region, a method for fusion of multiple measurements has to be devised. In order to do this, now the combined covariance $S_k^j$ of the mode-conditioned residual obtained from (4.17) and (4.18) also needs to be considered as follows

$$S_k^j := \begin{bmatrix} \tilde{H}_k^{j,1} \\ \\ \tilde{H}_k^{j,2} \end{bmatrix} \tilde{P}_{k|k-1}^j \begin{bmatrix} \tilde{H}_k^{j,1'} & \tilde{H}_k^{j,2'} \end{bmatrix} + \begin{bmatrix} R_k^{j,1} & 0 \\ \\ 0 & R_k^{j,2} \end{bmatrix}. \tag{4.19}$$

***Step 3. Measurement validation and state estimation for sensors 1 and 2*** $(\forall j \in \mathcal{M}_n)$ :

Since the measurement validation and state estimation process was well explained in steps 3 and 4 of Sec. 3.4 for a maneuvering target tracking scenario, we briefly describe the difference between standard simultaneous measurement update and state-augmented simultaneous measurement update in this step. Let

$$j_a := \arg \left\{ \max_{j \in \mathcal{M}_n} \left| S_k^{j,l} \right| \right\}.$$

Then measurement $z_k^{l(i)}$ ($i$=1,2,$\cdots$,$m_l$) is validated if and only if

$$[z_k^{l(i)} - \hat{z}_k^{j_a,l}]'[S_k^{j_a,l}]^{-1}[z_k^{l(i)} - \hat{z}_k^{j_a,l}] < \gamma \tag{4.20}$$

where $\gamma$ is an appropriate threshold. The volume of the validation region with the threshold $\gamma$ is

$$V_k^l := c_{n_{zl}}\gamma^{n_{zl}/2}|S_k^{j_a,l}|^{1/2}. \tag{4.21}$$

From among all the raw measurements from sensor $l$ at time $k$, i.e., $Z_k^l := \{z_k^{l(1)}, z_k^{l(2)}, \cdots, z_k^{l(m_l)}\}$, define the set of validated measurement for sensor $l$ at time $k$ as

$$Y_k^l := \{y_k^{l(1)}, y_k^{l(2)}, \cdots, y_k^{l(\bar{m}_l)}\} \tag{4.22}$$

where $\bar{m}_l$ is total number of validated measurement for sensor $l$ at time $k$ and

$$y_k^{l(i)} := z_k^{l(l_i)} \tag{4.23}$$

where $1 \leq l_1 < l_2 < \cdots < l_{\bar{m}_l} \leq m_l$ when $\bar{m}_l \neq 0$.

We define the association events (hypotheses) $\theta_k^{a,b}$ as in Eqn. (3.46). Therefore, there are a total of $\bar{m}_1\bar{m}_2+\bar{m}_1+\bar{m}_2+1$ possible association hypotheses, each of which has an association probability. The mode-conditioned association event probabilities $\beta_k^{j,a,b}$ can be defined and computed as in Eqns. (3.44)-(3.48).

Using $\hat{\tilde{x}}_{k|k-1}^j$ (from (4.13)) and its covariance $\tilde{P}_{k|k-1}^j$ (from (4.14)), one computes the partial update $\hat{\tilde{x}}_{k|k}^j$ and its covariance $\tilde{P}_{k|k}^j$ according to the standard PDAF [21], except that the augmented state is conditioned on $\theta_k^{a,b}$ with data fusion from sensors 1

and 2. Therefore, partial update of the state estimate

$$\hat{\tilde{x}}_{k|k}^{j,a,b} := E\left\{\tilde{x}_k|\theta_k^{a,b}, M_k^j, Z^{k-1}, Y_k^1, Y_k^2\right\} = \hat{\tilde{x}}_{k|k-1}^{j} + W_k^{j,a,b}\nu_k^{j,a,b} \tag{4.24}$$

where the combined mode-conditioned innovations $\nu_k^j$ and Kalman gains $W_k^{j,a,b}$, are computed as (3.49) and (3.51), respectively. Therefore, mode-conditioned update of the state estimate can be obtained as

$$\hat{\tilde{x}}_{k|k}^{j} := E\left\{\tilde{x}_k|M_k^j, Z^{k-1}, Y_k^1, Y_k^2\right\} = \sum_{i=0}^{\bar{m}_1}\sum_{b=0}^{\bar{m}_2}\beta_k^{j,a,b}\hat{\tilde{x}}_{k|k-1}^{j,a,b} \tag{4.25}$$

and covariance of $\hat{\tilde{x}}_{k|k}^{j}$ can be obtained as

$$\begin{aligned}\tilde{P}_{k|k}^{j} := \tilde{P}_{k|k-1}^{j} - \sum_{\substack{a=0\\(a,b)\neq(0,0)}}^{\bar{m}_1}\sum_{b=0}^{\bar{m}_2}\beta_k^{j,a,b}W_k^{j,a,b}S_k^{j,a,b}W_k^{j,a,b\prime} + \sum_{a=0}^{\bar{m}_1}\sum_{b=0}^{\bar{m}_2}\beta_k^{j,a,b}W_k^{j,a,b}\nu_k^{j,a,b}\nu_k^{j,a,b\prime}W_k^{j,a,b\prime}\\ - \left[\sum_{a=0}^{\bar{m}_1}\sum_{b=0}^{\bar{m}_2}\beta_k^{j,a,b}W_k^{j,a,b}\nu^{j,a,b}\right]\left[\sum_{a=0}^{\bar{m}_1}\sum_{b=0}^{\bar{m}_2}\beta_k^{j,a,b}W_k^{j,a,b}\nu^{j,a,b}\right]'.\end{aligned} \tag{4.26}$$

***Step 4. Update of mode probabilities*** $(\forall j \in \mathcal{M}_n)$ :

$$\mu_k^j := P\left[M_k^j|Z^k\right] = \frac{1}{C}\mu_k^{j-}\Lambda_k^j \tag{4.27}$$

where $C$ is a normalization constant such that $\sum_j \mu_k^j = 1$.

***Step 5 Combination of the mode-conditioned estimates*** $(\forall j \in \mathcal{M}_n)$ :

The final augmented state estimate update at time $k$ is given by

$$\hat{\tilde{x}}_{k|k} = \sum\nolimits_j \hat{\tilde{x}}_{k|k}^{j}\mu_k^j \tag{4.28}$$

and its covariance is given by

$$\tilde{P}_{k|k} = \sum\nolimits_j \left\{ \tilde{P}^j_{k|k} + \left[ \hat{\tilde{x}}^j_{k|k} - \hat{\tilde{x}}_{k|k} \right] \left[ \hat{\tilde{x}}^j_{k|k} - \hat{\tilde{x}}_{k|k} \right]' \right\} \mu^j_k. \tag{4.29}$$

From the final augmented state (see (4.28)), the state filtered vector $\hat{x}_{k|k}$ and the state smoothing vector $\hat{x}_{k-1|k}$ can be easily obtained.

## 4.5 Simulation Example

The following example of tracking a highly maneuvering target in clutter is considered. The target starts at location [21689 10840 40] in Cartesian coordinates in meters. The initial velocity (in m/s) is [-8.3 -399.9 0] and the target stays at constant altitude with a constant speed of 400 m/s. Its trajectory is a straight line with constant velocity between 0 and 20s, a coordinated turn (0.15 rad/s) with constant acceleration of 60 m/s$^2$ between 20 and 35s, a straight line with constant velocity between 35 and 55s, a coordinated turn (0.1 rad/s) with constant acceleration of 40 m/s$^2$ between 55 and 70s, and a straight line with constant velocity between 70 and 90s. The target motion models are patterned and modified after [21]. In each mode the target dynamics are modeled in Cartesian coordinates as

$$\tilde{x}_k = \tilde{F}^j_{k,k-1} \tilde{x}_{k-1} + \tilde{G}^j_{k,k-1} \tilde{v}^j_k \tag{4.30}$$

$$\tilde{x}_{k_{dl}} = \tilde{F}^j_{k_{dl},k-1} \tilde{x}_{k-1} + \tilde{G}^j_{k_{dl},k-1} \tilde{v}^j_k \tag{4.31}$$

where the augmented state of the target consists of position, velocity, acceleration, and the process noise in each of the three Cartesian coordinates ($x, y$, and $z$) at $t_k$ and $t_{k-1}$ as well as the delay time $d_k$ at $t_k$. Thus both $\tilde{x}_k$ and $\tilde{x}_{k_{dl}}$ are of dimension 25 ($n_x = 25$).

Three maneuver models are considered in the following discussion. The system matrices $\tilde{F}_{k,k-1}$, $\tilde{G}_{k,k-1}$, $\tilde{F}_{k_{dl},k-1}$ and $\tilde{G}_{k_{dl},k-1}$ are defined as

$$\tilde{F}^j_{k,k-1} = \begin{bmatrix} \bar{F}^j_{k,k-1} & 0 \\ 0 & I \end{bmatrix}, \qquad \tilde{G}^j_{k,k-1} = \begin{bmatrix} \bar{G}^j_{k,k-1} & 0 \\ 0 & I \end{bmatrix} \tag{4.32}$$

$$\tilde{F}^j_{k_{dl},k-1} = \begin{bmatrix} \bar{F}^j_{k_{dl},k-1} & 0 \\ 0 & I \end{bmatrix}, \qquad \tilde{G}^j_{k_{dl},k-1} = \begin{bmatrix} \bar{G}^j_{k_{dl},k-1} & 0 \\ 0 & I \end{bmatrix} \tag{4.33}$$

where

$$\bar{F}^j_{k,k-1} = \begin{bmatrix} \vec{F}^j_{k,k-1} & 0 \\ I & 0 \end{bmatrix}, \qquad \bar{G}^j_{k,k-1} = \begin{bmatrix} \vec{G}^j_{k,k-1} \\ 0 \end{bmatrix} \tag{4.34}$$

$$\bar{F}^j_{k_{dl},k-1} = \begin{bmatrix} \vec{F}^j_{k_{dl},k-1} & 0 \\ I & 0 \end{bmatrix}, \qquad \bar{G}^j_{k_{dl},k-1} = \begin{bmatrix} \vec{G}^j_{k_{dl},k-1} \\ 0 \end{bmatrix} \tag{4.35}$$

$$\vec{F}^j_{k,k-1} = \begin{bmatrix} F^j_{k,k-1} & G^j_{k,k-1} \\ 0 & 0 \end{bmatrix}, \qquad \vec{G}^j_{k,k-1} = \begin{bmatrix} 0 \\ I \end{bmatrix} \tag{4.36}$$

$$\vec{F}^j_{k_{dl},k-1} = \begin{bmatrix} F^j_{k_{dl},k-1} & G^j_{k_{dl},k-1} \\ 0 & 0 \end{bmatrix}, \qquad \vec{G}^j_{k_{dl},k-1} = \begin{bmatrix} 0 \\ I \end{bmatrix}, \tag{4.37}$$

$$F^j_{k,k-1} = \begin{bmatrix} F^j & 0 & 0 \\ 0 & F^j & 0 \\ 0 & 0 & F^j \end{bmatrix}, \qquad G^j_{k,k-1} = \begin{bmatrix} G^j & 0 & 0 \\ 0 & G^j & 0 \\ 0 & 0 & G^j \end{bmatrix}, \tag{4.38}$$

$$F^j_{k_{dl},k-1} = \begin{bmatrix} F^j_d & 0 & 0 \\ 0 & F^j_d & 0 \\ 0 & 0 & F^j_d \end{bmatrix}, \quad G^j_{k_{dl},k-1} = \begin{bmatrix} G^j_d & 0 & 0 \\ 0 & G^j_d & 0 \\ 0 & 0 & G^j_d \end{bmatrix}. \tag{4.39}$$

**Model 1**. Nearly constant velocity model with zero mean perturbation in acceleration

$$F^1 = \begin{bmatrix} 1 & T & 0 \\ 0 & 1 & 0 \\ 0 & 0 & 0 \end{bmatrix}, \quad G^1 = \begin{bmatrix} \frac{T^2}{2} \\ T \\ 0 \end{bmatrix}, \tag{4.40}$$

$$F^1_d = \begin{bmatrix} 1 & (T-d_k) & 0 \\ 0 & 1 & 0 \\ 0 & 0 & 0 \end{bmatrix}, \quad G^1_d = \begin{bmatrix} \frac{(T-d_k)^2}{2} \\ (T-d_k) \\ 0 \end{bmatrix}, \tag{4.41}$$

where $T$ is the sampling period. The standard deviation of the process noise of $M^1$ is 5 $\mathrm{m/s^2}$ (as in [21]).

**Model 2**. Wiener process acceleration (nearly constant acceleration motion)

$$F^2 = \begin{bmatrix} 1 & T & \frac{T^2}{2} \\ 0 & 1 & T \\ 0 & 0 & 1 \end{bmatrix}, \quad G^2 = \begin{bmatrix} \frac{T^2}{2} \\ T \\ 1 \end{bmatrix}, \tag{4.42}$$

$$F_d^2 = \begin{bmatrix} 1 & (T-d_k) & \frac{(T-d_k)^2}{2} \\ 0 & 1 & (T-d_k) \\ 0 & 0 & 1 \end{bmatrix}, \quad G_d^2 = \begin{bmatrix} \frac{(T-d_k)^2}{2} \\ (T-d_k) \\ 1 \end{bmatrix}. \tag{4.43}$$

The standard deviation of the process noise of $M^2$ is 7.5 m/s$^2$ (as in [21]).

**Model 3**. Wiener process acceleration (model with large acceleration increments, for the onset and termination of maneuvers), with $F^3 = F^2$, $G^3 = G^2$, $F_d^3 = F_d^2$ and $G_d^3 = G_d^2$. The standard deviation of the process noise of $M^3$ is 40 m/s$^2$ (as in [21]).

The initial model probabilities are $\mu_0^1 = 0.8$, $\mu_0^2 = 0.1$ and $\mu_0^3 = 0.1$. The mode switching probability matrix is given by (as in [21])

$$\begin{bmatrix} p_{11} & p_{12} & p_{13} \\ p_{21} & p_{22} & p_{23} \\ p_{31} & p_{32} & p_{33} \end{bmatrix} = \begin{bmatrix} 0.8 & 0.0 & 0.2 \\ 0.0 & 0.8 & 0.2 \\ 0.3 & 0.3 & 0.4 \end{bmatrix}. \tag{4.44}$$

**The Sensors**: Two sensors are used to obtain the measurements. Sensor 1 and Sensor 2 are located at $[x_1, y_1, z_1]$=[-4000 4000 0] m and $[x_2, y_2, z_2]$=[5000 0 0] m, respectively, and the central processor is collocated with sensor 1 platform (we assume that there is no time delay between sensor 1 and central processor and there is fixed-but-unknown time delay between sensor 2 and central processor). The measurements from sensor $l$ for model $j$ are $z_k^l = h^l(x_k) + w_k^{j,l}$ for $l = 1$ and 2, reflecting range and azimuth angle for sensor 1 (radar) and azimuth and elevation angles for sensor 2 (infrared). The range,

azimuth, and elevation angle transformations, respectively, are given by

$$r_l = \{(x-x_l)^2+(y-y_l)^2+(z-z_l)^2\}^{1/2} \tag{4.45}$$

$$a_l = \tan^{-1}[(y-y_l)/(x-x_l)] \tag{4.46}$$

$$e_l = \tan^{-1}[(z-z_l)/\{(x-x_l)^2+(y-y_l)^2\}^{1/2}]. \tag{4.47}$$

As we see from (3.23), (3.24), (4.1) and (4.2), the measurements obtained from sensors 1 and 2 can be expressed as

$$z_k^1 = h^1([I,0,0,0,0]\tilde{x}_k) + w_k^1 \tag{4.48}$$

$$z_k^2 = h^2([0,0,F_{k_d,k-1}^j, G_{k_d,k-1}^j, 0]\tilde{x}_k) + w_k^2. \tag{4.49}$$

The Jacobian matrices of $h$ for sensors 1 and 2 are

$$\tilde{H}^{j,1} = \begin{bmatrix} H^{j,1} & 0_{2\times 13} \end{bmatrix} \tag{4.50}$$

and

$$\tilde{H}^{j,2} = \begin{bmatrix} 0_{2\times 12} & H^{j,2}F_{k_d,k-1}^j & H^{j,2}G_{k_d,k-1}^j & H_d \end{bmatrix} \tag{4.51}$$

where

$$H^{j,1} = \begin{bmatrix} \cos e_1 \cos(a_1) & 0 & 0 & \cos(e_1)\sin(a_1) & 0 & 0 & \sin(e_1) & 0 & 0 \\ -\frac{\sin(a_1)}{r_1\cos(e_1)} & 0 & 0 & \frac{\cos(a_1)}{r_1\cos(e_1)} & 0 & 0 & 0 & 0 & 0 \end{bmatrix} \tag{4.52}$$

$$H^{j,2} = \begin{bmatrix} -\frac{\sin(a_2)}{r_2\cos(e_2)} & 0 & 0 & \frac{\cos(a_2)}{r_1\cos(e_2)} & 0 & 0 & 0 & 0 & 0 \\ -\frac{\sin(e_2)\cos(a_2)}{r_2} & 0 & 0 & -\frac{\sin(e_2)\sin(a_2)}{r_2} & 0 & 0 & \frac{cos(e_2)}{r_2} & 0 & 0 \end{bmatrix} \tag{4.53}$$

$$H_d = \begin{bmatrix} \frac{\cos(a_2)}{r_2\cos(e_2)} d\hat{f}_{k|k-1} - \frac{sin(a_2)}{r_2\cos(e_2)} d\hat{g}_{k|k-1} \\ \frac{\cos(e_2)}{r_2} d\hat{h}_{k|k-1} - \frac{\sin(e_2)}{r_2} d\hat{s}_{k|k-1} \end{bmatrix} \tag{4.54}$$

where

$$d\hat{f}_{k|k-1} = -[\hat{\hat{x}}^{(17)}_{k|k-1} + (T-\hat{d}_k)\hat{\hat{x}}^{(18)}_{k|k-1} + (T-\hat{d}_k)\hat{\hat{x}}^{(23)}_{k|k-1}] \tag{4.55}$$

$$d\hat{g}_{k|k-1} = -[\hat{\hat{x}}^{(14)}_{k|k-1} + (T-\hat{d}_k)\hat{\hat{x}}^{(15)}_{k|k-1} + (T-\hat{d}_k)\hat{\hat{x}}^{(22)}_{k|k-1}] \tag{4.56}$$

$$d\hat{h}_{k|k-1} = -[\hat{\hat{x}}^{(20)}_{k|k-1} + (T-\hat{d}_k)\hat{\hat{x}}^{(21)}_{k|k-1} + (T-\hat{d}_k)\hat{\hat{x}}^{(24)}_{k|k-1}] \tag{4.57}$$

$$d\hat{s}_{k|k-1} = 2(\hat{g}^2_{k|k-1} + \hat{f}^2_{k|k-1})^{-1/2}(\hat{g}_{k|k-1} + \hat{f}_{k|k-1})(d\hat{g}_{k|k-1} + d\hat{f}_{k|k-1}) \tag{4.58}$$

$$\hat{f}_{k|k-1} = \hat{\hat{x}}^{(16)}_{k|k-1} + (T-\hat{d}_k)\hat{\hat{x}}^{(17)}_{k|k-1} + \frac{(T-\hat{d}_k)^2}{2}\hat{\hat{x}}^{(18)}_{k|k-1} + \frac{(T-\hat{d}_k)^2}{2}\hat{\hat{x}}^{(23)}_{k|k-1} \tag{4.59}$$

$$\hat{g}_{k|k-1} = \hat{\hat{x}}^{(13)}_{k|k-1} + (T-\hat{d}_k)\hat{\hat{x}}^{(14)}_{k|k-1} + \frac{(T-\hat{d}_k)^2}{2}\hat{\hat{x}}^{(15)}_{k|k-1} + \frac{(T-\hat{d}_k)^2}{2}\hat{\hat{x}}^{(22)}_{k|k-1}. \tag{4.60}$$

The measurement noise $w^{j,l}_k$ for sensor $l$ is assumed to be zero-mean white Gaussian with known covariances, $R^1 = \text{diag}[q_r, q_{a1}] = \text{diag}[400\ \text{m}^2, 49\ \text{mrad}^2]$ with $q_r$ and $q_{a1}$ denoting the variances for the radar range and azimuth measurement noises, respectively, and $R^2 = \text{diag}[q_{a2}, q_e] = \text{diag}[4\ \text{mrad}^2, 4\ \text{mrad}^2]$ with $q_{a2}$ and $q_e$ denoting the variances for the infrared sensor azimuth and elevation measurement noises, respectively. The sampling

interval was $T$=1s and it was assumed that the probability of detection $P_d$=1 for both sensors.

**The Clutter**: For generating false measurements in simulations, the clutter was assumed to be Poisson distributed with expected number of $\lambda_1 = 13\times\ 10^{-6}$/m mrad for sensor 1 and $\lambda_2 = 7 \times 10^{-4}/\text{mrad}^2$ for sensor 2 [21, case 1]. These statistics were used for generating the clutter in all simulations. However, a nonparametric clutter model was used for implementing all the algorithms for target tracking.

**Other Parameters**: The gates for setting up the validation regions for both the sensors were based on the threshold $\gamma = 16$. With the measurement vector of dimension 2, this leads to a gate probability $P_G = 0.997$ (see [12, pages 95-96]).

**Simulation Results**: The results were obtained from 100 Monte Carlo runs. Fig. 4.2 shows the true trajectory of the target. Fig. 4.3 shows the delay estimates (given unknown but fixed timing mismatch between the two sensors) based on 100 Monte Carlo runs. Fig. 4.4 shows a comparison between the performances of the filtered state and the smoothed state (lag = 1) obtained from the state-augmented system (in position, velocity, and acceleration). It is seen from Fig. 4.4 that the smoothed state shows better accuracy than the filtered state as well described in [47]. Fig. 4.5 shows a comparison among the performances of the proposed augmented state IMM/MSPDAF (AS-IMM/MSPDAF) algorithm dealing with asynchronous measurements with unknown but fixed $d_k$, with known $d_k$, and the standard IMM/MSPDAF algorithm [38] with the assumption that $d_k$=0 always applies. Note that we apply "simultaneous measurement update" technique for all algorithms to get fair performance comparison. Table 4.1 shows the performance comparison between the proposed AS-IMM/MSPDAF algorithm dealing with asynchronous measurements with unknown but fixed $d_k$ and the standard

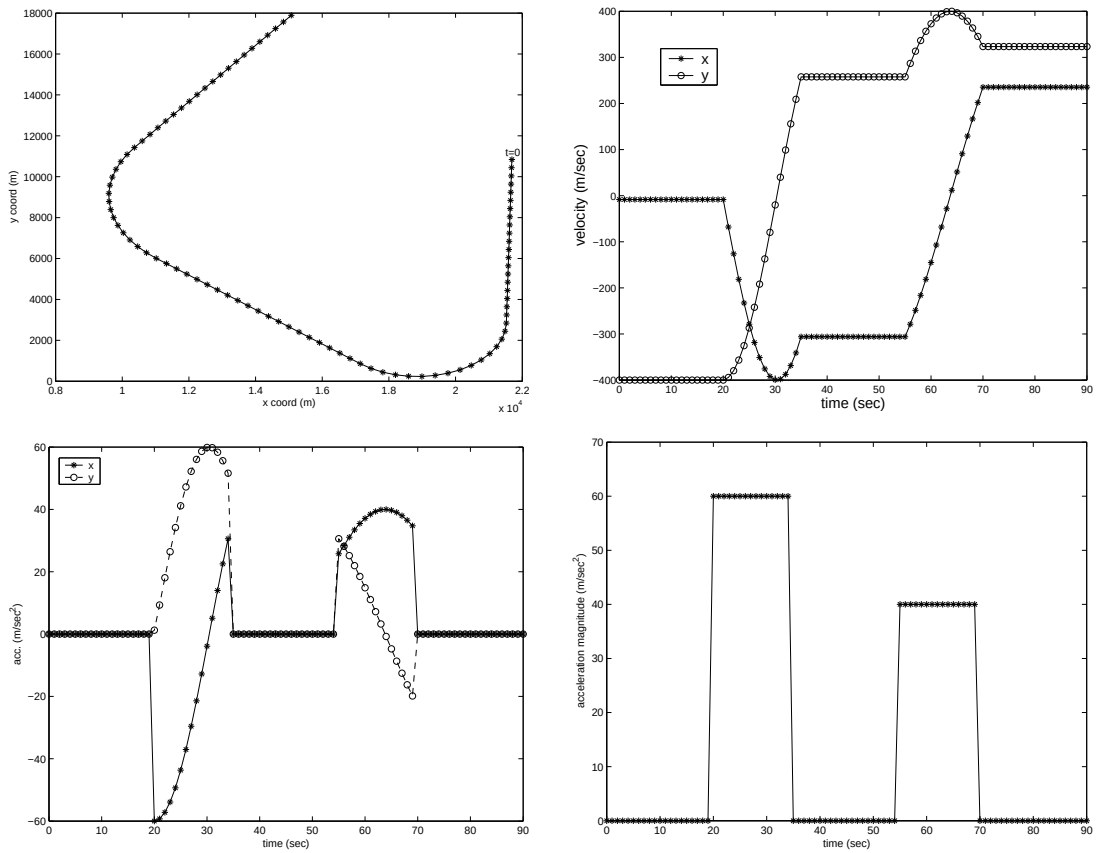


Figure 4.2: Trajectory of maneuvering target (read left to right, top to bottom). (a) Position in $xy$ plane. (b) $x$ and $y$ velocities. (c) $x$ and $y$ accelerations. (d) magnitude of accelerations

IMM/MSPDAF algorithm with the assumption that $d_k$=0. It is seen from Table 4.1 that the standard IMM/MSPDAF algorithm [38] suffered from track losses (from 2 to 86 out of 100 Monte Carlo runs) whereas the proposed AS-IMM/MSPDAF algorithm performed well in all 100 Monte Carlo runs. It is seen from Fig. 4.5 and Table 4.1 that when the unknown but fixed timing mismatch $d_k$ is more than one fifth of the sampling time, the performance improvement is significant compared with the standard IMM/MSPDAF algorithm [38] that ignores the time-delay $d_k$ (i.e., assumes it to be zero).

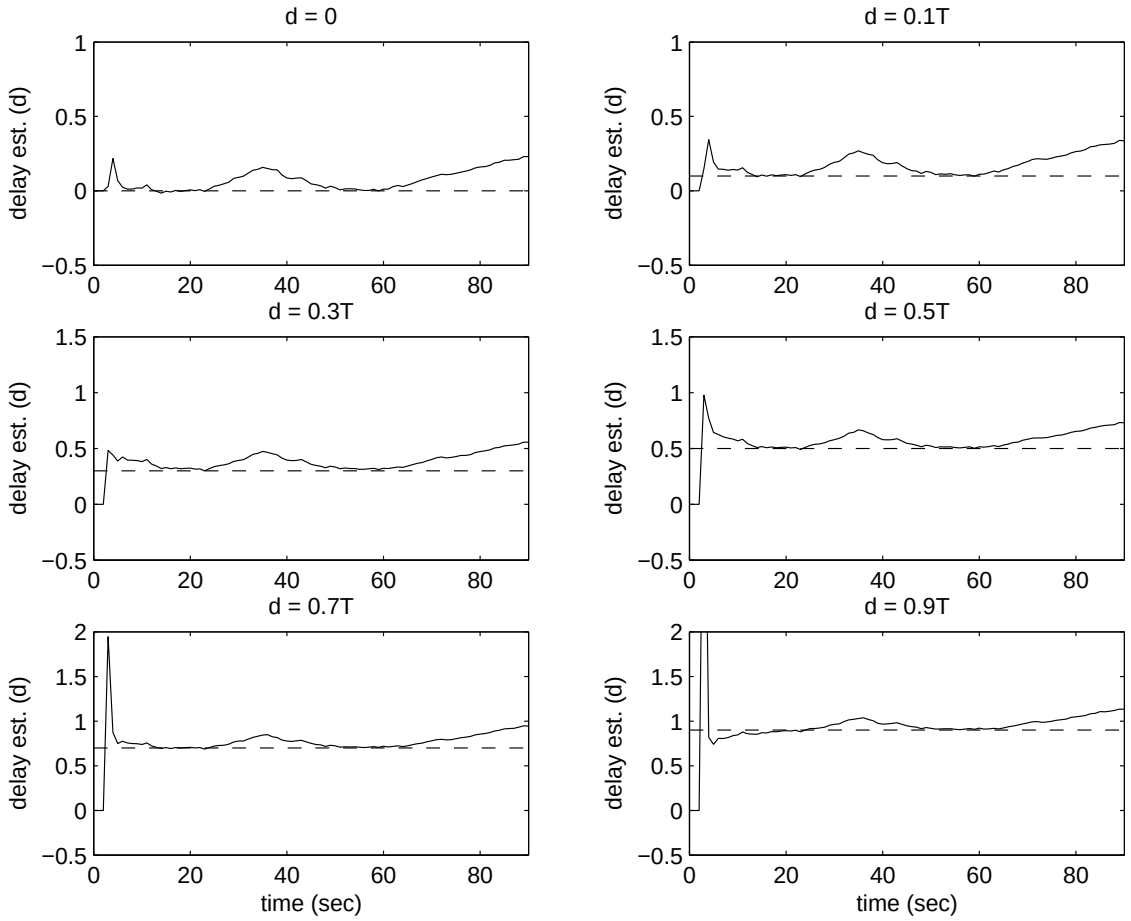


Figure 4.3: Estimation of delay (given unknown but fixed timing mismatch between two separated sensors) based on 100 Monte Carlo runs (read left to right, top to bottom). (a) d = 0. (b) d = $0.1T$. (c) d = $0.3T$. (d) d = $0.5T$. (e) d = $0.7T$. (f) d = $0.9T$. ($T$ = sampling rate). Solid: estimated delay $\hat{d}$; dashed: fixed delay $d$.

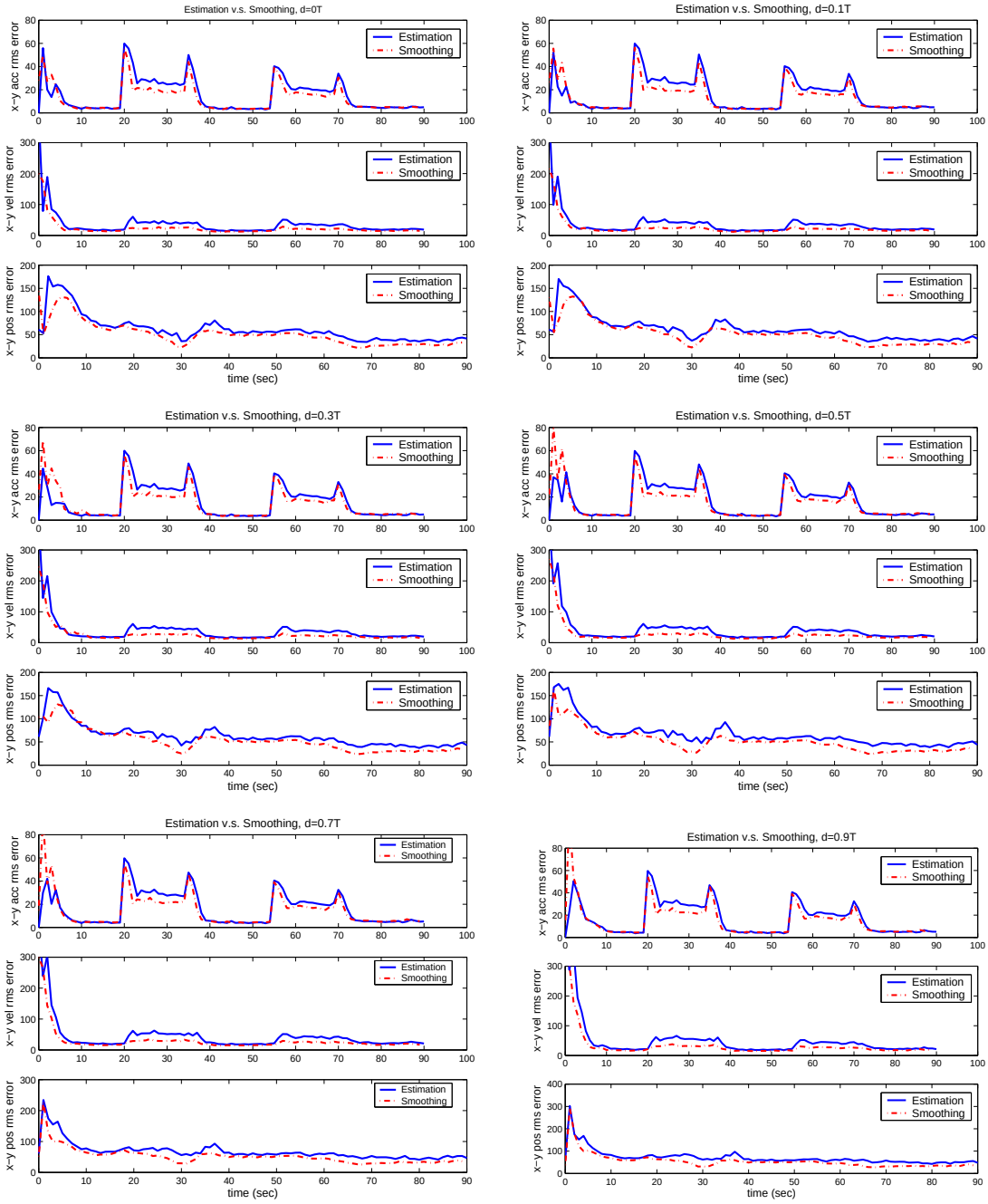


Figure 4.4: Comparison of filtered and smoothed (lag = 1) estimate for various delay values (acceleration, velocity, and position RMS errors (3 rows each), read left to right, top to bottom). (a) d = 0. (b) d = $0.1T$. (c) d = $0.3T$. (d) d = $0.5T$. (e) d = $0.7T$. (f) d = 0.9T. ($T$ = sampling rate). In the figure legends, estimation refers to filtering, and smoothing is with lag = 1. Solid: filtered estimate; dash-dot: smoothed estimate.

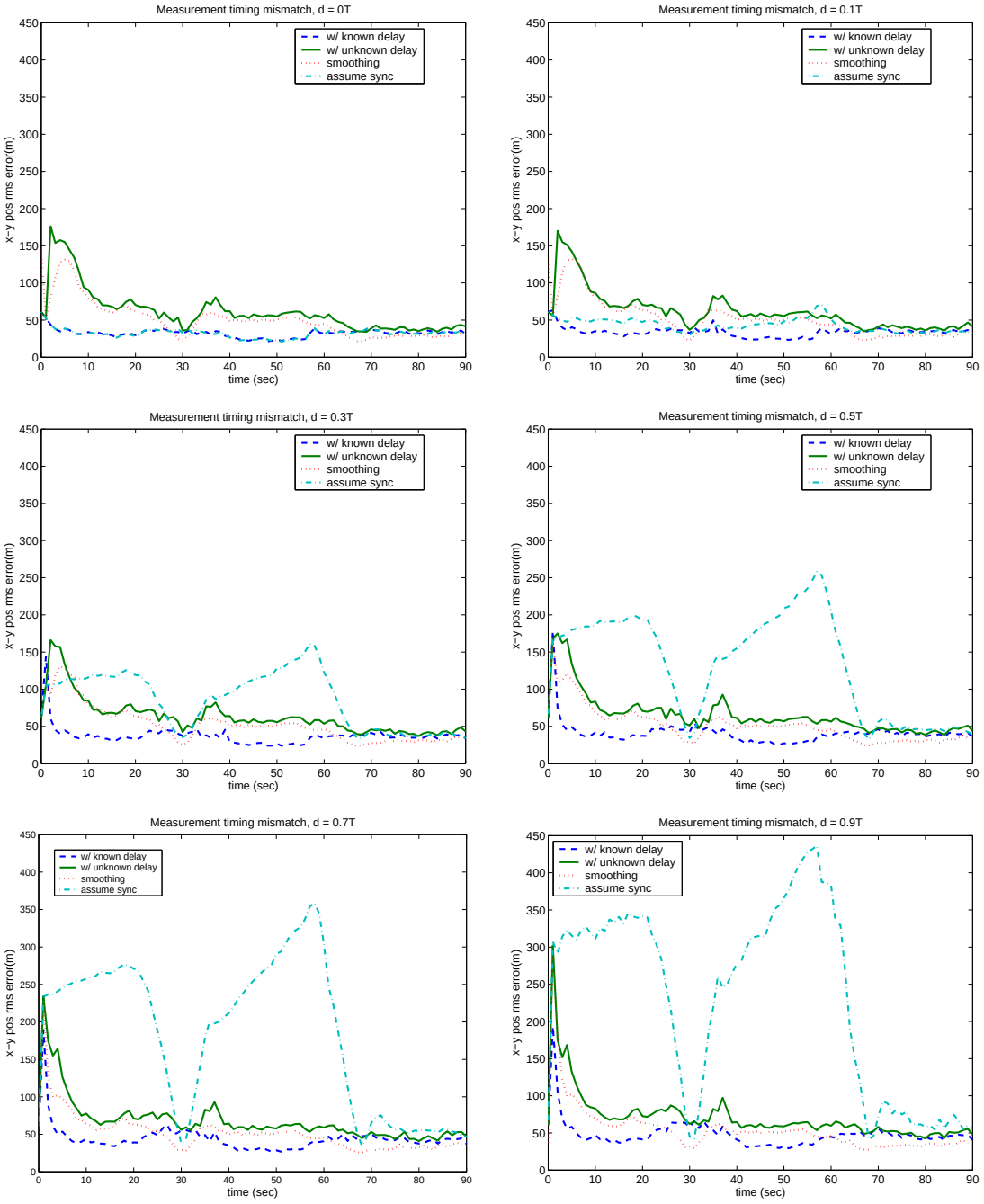


Figure 4.5: RMSE in position using IMM/MSPDAF for various delay values (read left to right, top to bottom). (a) d = 0. (b) d = $0.1T$. (c) d = $0.3T$. (d) d = $0.5T$. (e) d = $0.7T$. (f) d = $0.9T$. Unless otherwise stated, the results are for filtering. Solid: proposed AS-IMM/MSPDAF; dotted: proposed AS-IMM/MSPDAF (smoothing); dash-dot: standard IMM/MSPDAF [38]; dashed: proposed AS-IMM/MSPDAF with the knowledge of $d_k$.

| Unknown but fixed delay, $d_k$ | 0.0 | $0.1T$ | $0.3T$ | $0.5T$ | $0.7T$ | $0.9T$ |
|---|---|---|---|---|---|---|
| proposed AS-IMM/MSPDAF | **0** | **0** | **0** | **0** | **0** | **0** |
| standard IMM/MSPDAF [38] | **0** | **0** | **2** | **4** | **27** | **86** |

Table 4.1: Simulation Results: No. of lost tracks obtained from 100 Monte Carlo runs for fixed-but-unknown $d_k$

### 4.6 Conclusions

We investigated an augmented state IMM/MSPDAF algorithm with asynchronous measurement (there is unknown but fixed timing mismatch between sensor platforms) for tracking a highly maneuvering target in clutter. Simultaneous measurement update technique is applied for better data association. The proposed AS-IMM/MSPDAF algorithm was illustrated via a simulation example under various scenarios of known delay, estimated delay and ignoring delay, for various delay values.

Using the proposed AS-IMM/MSPDAF algorithm, the smoothed estimate $\hat{x}_{k-1|k}$ can be easily obtained from the augmented state estimate $\hat{\hat{x}}_{k|k}$ and the smoothed estimate always shows better performance (in terms of RMS error) than the filtered estimate $\hat{x}_{k-1|k-1}$. The performance comparison between the proposed algorithm dealing with unknown but fixed $d_k$ and the standard IMM/MSPDAF algorithm [38] that ignores $d_k$ shows that while the proposed AS-IMM/MSPDAF algorithm performed well in all 100 Monte Carlo runs, the standard IMM/MSPDAF algorithm [38] suffered from track losses.

# Chapter 5

# Multisensor Tracking of a Maneuvering Target in Clutter with Asynchronous and Possibly Out-of-Sequence Measurements using Augmented State IMMPDA Filtering and Simultaneous Measurement Update

In this chapter, a suboptimal filtering algorithm for tracking a highly maneuvering target in a cluttered environment using multiple sensors dealing with possibly out-of-sequence measurements (OOSM) and a fixed relative time-delay among sensor platforms is presented. The filtering algorithm is developed by applying the basic IMM approach, the PDA technique, and OOSM updating for the target. A state-augmented approach is developed to improve tracking performance with the possible presence of OOSM. A multisensor PDA filter is developed for parallel sensor processing for target tracking under clutter. The algorithm is illustrated via a highly maneuvering target tracking simulation example where two sensors, a radar and an infrared sensor, are used. Compared with an existing IMMPDA filtering algorithm with in-sequence only sensor processing, the proposed algorithm achieves considerable improvement in the accuracy of track estimation.

## 5.1 Introduction

In a multisensor central tracking system measurements are typically collected in "scans" or "frames" and then transmitted to a processing center [27]. The state equations are usually defined in continuous time and then discretized because the measurements

are obtained in discrete time - the sensor provides a "time stamp" with each measurement. In multisensor tracking systems that operate in a centralized manner [12, 44], i.e., the processing of the measurements from all sensors is done at a single center, there are usually different time delays in the arrival of the measurement data from the various sensors to the center. This can be easily seen to lead to situations where measurements from the same target arrive out of sequence. Such "out-of-sequence" measurement (OOSM) arrivals can occur even in the absence of scan/fram communication time delays, as discussed in [12]. In this system the processing of the measurement data from all the sensors is done at a single center, then there usually different time delays in the arrival of measurement data from different sensors to the central processor. This can possibly lead to situations where measurements from the same target arrive not in correct time order. This out-of-sequence measurements (OOSM) arrivals can occur due to communication network delays, varying preprocessing times at the sensor platforms and lack of sampling time synchronization among sensor platforms [35, 36]. The optimal solution for OOSM has been considered by Bar-Shalom in [35, 36, 37] for single measurement delay (1-step-lag case) and in [49] for multiple measurement delay (multistep-lag case). In this chapter we exploit IMM and PDA techniques. It is assumed that a track has been formed (initiated) and the objective of this work is to track a single maneuvering target in clutter arising in a multisensor central tracking system.

We exploit the basic structure of [21] in combination with a state-augmented approach to deal with OOSM. In [21, 45] it is assumed that the sensors are collocated and (time) synchronized with the sampling rate. In contrast, the sensor collocation and (time) synchronization are no longer assumed in this chapter. Also, unlike [21, 47, 25] which have used sequential updating of the state estimates with measurements, we use

parallel updating of the state estimates with measurements as mentioned in [38]. Ref. [50] extends the state-augmented approach of [38] to deal with asynchronous measurements for the maneuvering target tracking in clutter, however, it is limited to in-sequence measurements only. The state-augmented approach for target tracking in clutter with OOSM has been proposed in [51], however, it is limited to non-maneuvering target only. The maneuvering target tracking in clutter with OOSM problem using state-augmented approach combined with IMM and PDA has been proposed in [52]. In this dissertation, we extend the state-augmented approach of [52] to simultaneous measurement update, while allowing for lack of timing synchronization.

This chapter is organized as follows. Sec. 5.2 presents the modeling assumption. Sec. 5.3 presents the problem formulation. Sec. 5.4 describes the state-augmented system approach. Sec. 5.5 describes the proposed IMM/MSPDAF parallel detection fusion algorithm for OOSM. Simulation results using the proposed algorithm for a realistic problem are given in Sec. 5.6. Finally, Sec. 5.7 presents a discussion of the results and some conclusions.

## 5.2 Modeling Assumptions

In this chapter we consider *asynchronous measurements with possibly OOSM*. We extend our AS-IMM/MSPDAF algorithm discussed in Chapter 4 to deal with possibly out-of-sequence measurements (OOSM) in an asynchronous measurements scenario. Unlike AS-IMM/MSPDAF algorithm discussed in Chapter 4 which deals with fixed-but-unknown delay, we assume that there is a "fixed-and-known" relative time delay between the remote sensor clock and the central processor clock in this chapter. Our approach assumes as the following:

- Only two sensors were considered - more than two sensors also can be easily implemented by defining additional data association events (hypotheses).

- Various sensor measurements are assumed to be at the same sampling rate but not necessarily time synchronized.

- Measurement data over one sampling interval (based on the local clock of the central processor) are collected at the central processor, attributed to one time instant and processed simultaneously. (Central processor can distinguish OOSM out of measurement data by checking the "time stamp" of each measurement.)

- A sensor is called a local sensor when its platform is collocated with the central processor and there is no time delay between local sensor and central processor.

- A sensor is called a remote sensor when its platform is located at a distance from the central processor and there is possibly a "fixed-and-known" relative time delay between the remote sensor clock and the central processor clock at sample time $t_k$. (This time delay could be due to unsynchronized clocks at the two locations or due to inherent delay due to congestion, insufficient bandwidth, etc., in the communication link between the remote sensor platform and the central processor.).

- The measurement data arriving from remote sensor at any time $k$ has a probability $P_d$ of being delayed and delay is uniformly distributed with a maximum time delay less than or equal to $T$ ($T$ = sampling rate).

- Measurements arriving from remote sensor are either in-sequence but delayed or OOSM.

- OOSM can occur even in the absence of time-delayed scan/frame communication. (It includes the possibility that there is no measurement arrival from remote sensor to central processor.).

- The maximum time delay between the remote sensor clock and the central processor clock is $1T$.

## 5.3 Problem Formulation

We assume that the target dynamics can be modeled by one of $n$ hypothesized models. The model set is denoted as $\mathcal{M}_n := \{1, \cdots, n\}$ and there are total $q$ sensors. The event that model $j$ is in effect during the sampling period $(t_{k-1}, t_k]$ is denoted by $M_k^j$.

### 5.3.1 Target Dynamics

For the $j$th hypothesized model (mode), the state dynamics are modeled as

$$x_k = F_{k,k-1}^j x_{k-1} + G_{k,k-1}^j v_{k-1}^j \tag{5.1}$$

where $x_k$ is the system state at $t_k$ and of dimension $n_x$, $F_{k,k-1}^j$ and $G_{k,k-1}^j$ are the system matrices when model $j$ is in effect over the sampling period $(t_{k-1}, t_k]$. The process noise $v_{k-1}^j$ is a zero-mean white Gaussian process with covariance matrix $Q_{k-1}^j$. At the initial time $t_0$, the initial conditions for the system state of target under model $j$ is assumed to be Gaussian random variables with the known mean $\bar{x}_0^j$ and the known covariance $P_0^j$. The probability of model $j$ at $t_0$, $\mu_0^j = P[M_0^j]$, is also assumed to be known. The switching from model $M_{k-1}^i$ to model $M_k^j$ is governed by a finite-state stationary Markov

chain with known transition probabilities $p_{ij} = P[M_k^j | M_{k-1}^i]$. Henceforth, time $t_k$ will be denoted by $k$.

### 5.3.2 Measurements

We consider two sensor target tracking scenario. One of the sensor is the local sensor (say sensor 1) and the other is the remote sensor (say sensor 2). The measurements from each sensor are sent to the central processor where all measurements collected between local sampling interval $(t_{k-1}, t_k]$ are attributed to time $t_k$ (see Fig. 5.1). The measurements are modeled as follows.

**Measurements for local sensor (sensor 1)**

$$z_k^1 = h^1(x_k) + w_k^{j,1} \tag{5.2}$$

where $z_k^1$ is the (true) measurement vector (i.e., due to the target) at sensor 1 at $t_k$ and of dimension $n_{z1}$, $h^1$ is the nonlinear transformation of $x_k$ to $z_k^1$ for model $j$. A first-order linearized version of (5.2) is given by

$$z_k^1 = H_k^{j,1} x_k + w_k^{j,1} \tag{5.3}$$

where $H_k^{j,1}$ is the Jacobian matrix of $h^1$ evaluated at some value of the estimate of state $x_k$ (see Sec. 5.4). The measurement noise $w_k^{j,1}$ is a zero-mean white Gaussian process with covariance matrix $R_k^l$ and is mutually uncorrelated with the process noise $v_{k-1}^j$.

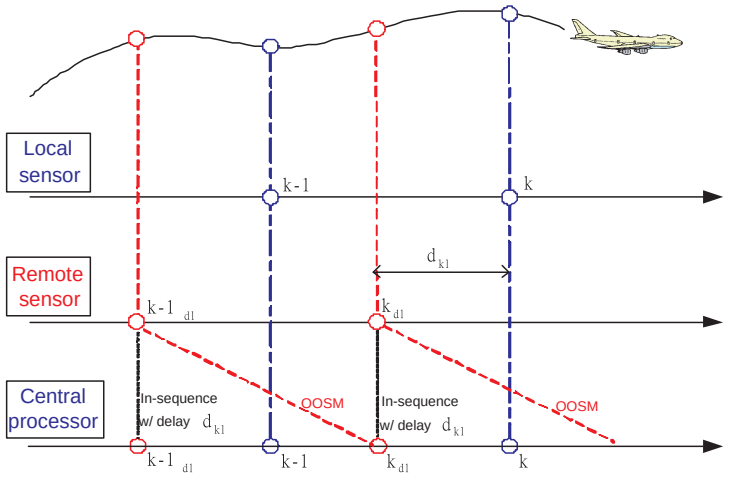


Figure 5.1: Asynchronous measurements: In-sequence but delayed measurements and out of sequence measurements (OOSM) in multisensor tracking system

**Measurements for remote sensor (sensor 2)**

We assume that there is a fixed-and-known relative time delay $d_{kl}$ at sample time $t_k$ between the remote sensor clock and the central processor (local sensor) clock at sample time $t_k$. Noting that the central processor can distinguish between OOSM and in-sequence-but-delayed measurements, the measurements arriving from remote sensor must be either in-sequence-but delayed measurements or OOSM. Therefore the measurements reported from the remote sensor platform at time $t_{k_{dl}}$ (henceforth will be denoted by $k_{dl}$) to the central processor at time $t_k$ can be modeled as (see Fig. 5.1)

$$\tilde{z}_k^2 = h^2(x_{k_{dl}}) + w_k^{j,2} \tag{5.4}$$

where (as in Sec. 4.2)

$$x_{k_{dl}} = F^{j}_{k_{dl},k-1} x_{k-1} + G^{j}_{k_{dl},k-1} v^{j}_{k-1}, \tag{5.5}$$

$\tilde{z}^2_k$ is the (true) measurement vector (i.e., due to the target) at sensor 2 (see (5.6)), $x_{k_{dl}}$ is the system state at $t_{k_{dl}}$ and of dimension $n_x$, $F^{j}_{k_{dl},k-1}$ and $G^{j}_{k_{dl},k-1}$ are the system matrices when model $j$ is in effect over the timing interval $(t_{k-1}, t_{k_{dl}}]$.

To process equation (5.4) for the delayed measurement from the remote sensor at the central processor, one has to consider all the possible data interpretations $\Psi$. Define a related set of mutually exclusive and exhaustive data interpretations $\Psi$ as follows:

- $\Psi_{11}$: Both in-sequence measurements and OOSM arrive from sensor 2 at the central processor at time $k$, and $\tilde{z}^2_k = \{z^2_k, z^2_{k-1}\}$,
- $\Psi_{10}$: Only in-sequence measurement arrives from sensor 2 at the central processor at time $k$, and $\tilde{z}^2_k = \{z^2_k\}$,
- $\Psi_{01}$: Only OOSM arrives from sensor 2 at the central processor at time $k$, and $\tilde{z}^2_k = \{z^2_{k-1}\}$,
- $\Psi_{00}$: No measurement arrives from sensor 2 at the central processor at time $k$ (due to absence of scan/frame), and $\tilde{z}^2_k =$ empty

where $z^2_k$ is the (true) measurement vector (i.e., due to the target) at sensor 2 at time $k_{dl}$, and $z^2_{k-1}$ is the (true) measurement vector at sensor 2 at time $k_{dl} - T$. Then (5.4)

can be rewritten as

$$\tilde{z}_k^2 = \begin{cases} \begin{bmatrix} z_k^2 \\ z_{k-1}^2 \end{bmatrix}, & \text{for } \Psi_{11} \\ z_k^2, & \text{for } \Psi_{10} \\ z_{k-1}^2, & \text{for } \Psi_{01} \\ \text{no measurement}, & \text{for } \Psi_{00}. \end{cases} \tag{5.6}$$

## 5.4 State-Augmented System

Define the augmented state $\tilde{x}_k$ from $x_k$ as

$$\tilde{x}_k' = [x_k', v_k', x_{k-1}', v_{k-1}', x_{k-2}', v_{k-2}'] \tag{5.7}$$

where $x_k'$ denotes the transpose of $x_k$. Assume that there is a fixed-and-known delay, $d_{kl}$, between the central processor and the remote sensor $l$ platform. Using the above definitions and (5.1), the augmented state equation may be written more compactly as

$$\tilde{x}_k = \tilde{F}_{k,k-1}^j \tilde{x}_{k-1} + \tilde{G}_{k,k-1}^j v_k^j, \tag{5.8}$$

$$\tilde{x}_{k_{dl}} = \tilde{F}_{k_{dl},k-1}^j \tilde{x}_{k-1} + \tilde{G}_{k_{dl},k-1}^j v_{k_{dl}}^j \tag{5.9}$$

where $\tilde{F}_{k,k-1}^j$, $\tilde{G}_{k,k-1}^j$, $\tilde{F}_{k_{dl},k-1}^j$, and $\tilde{G}_{k_{dl},k-1}^j$ are defined in Sec. 5.6 (see (5.53)-(5.60)). Note that the process noise in (5.8) is $v_k^j$ (at time $k$, not at time $k-1$). Using the augmented state (5.7) the counterparts to (5.2) and (5.4), respectively, are

$$z_k^1 = h^1(\tilde{x}_k) + w_k^{j,l} = h^1([I,0,0,0,0,0]\tilde{x}_k) + w_k^{j,l} \tag{5.10}$$

and

$$\tilde{z}_k^2 = \begin{cases} \begin{bmatrix} z_k^2 \\ z_{k-1}^2 \end{bmatrix} = h^2 \left( \begin{bmatrix} 0\ 0\ F_{dl}^j\, G_{dl}^j\ 0\ 0 \\ 0\ 0\ 0\ 0\ F_{dl}^j\, G_{dl}^j \end{bmatrix} \tilde{x}_k \right) + \begin{bmatrix} w_k^{j,2} \\ w_{k-1}^{j,2} \end{bmatrix}, & \text{for } \Psi_{11} \\ z_k^2 = h^2 \begin{bmatrix} 0\ 0\ F_{dl}^j\, G_{dl}^j\ 0\ 0 \end{bmatrix} \tilde{x}_k + w_k^{j,2}, & \text{for } \Psi_{10} \\ z_{k-1}^2 = h^2 \begin{bmatrix} 0\ 0\ 0\ 0\ F_{dl}^j\, G_{dl}^j \end{bmatrix} \tilde{x}_k + w_{k-1}^{j,2}, & \text{for } \Psi_{01} \\ \text{no measurement}, & \text{for } \Psi_{00}. \end{cases} \tag{5.11}$$

The following notations and definitions are used regarding the measurements at sensor $l$. Note that, in general, at any time some measurements may be due to clutter and some due to the target, i.e., there can be more than a single measurement at time $k$ at sensor $l$ ($l = 1, 2$). The measurement set (not yet validated) generated by sensor $l$ at time $k$ is denoted as

$$Z_k^l := \{z_k^{l(1)}, z_k^{l(2)}, \cdots, z_k^{l(m_l)}\} \tag{5.12}$$

where $m_l$ is the number of measurements generated by sensor $l$ at time $k$. Variable $z_k^{l(i)}$ ($i = 1,\cdots,m_l$) is the $i$th measurement within this set. The validated set of measurements of sensor $l$ at time $k$ will be denoted by $Y_k^l$, containing $\bar{m}_l$ ($\leq m_l$) measurement vectors. The cumulative set of validated measurements from sensor $l$ up to time $k$ is denoted as

$$Y^{k(l)} := \{Y_1^l, Y_2^l, \cdots, Y_k^l\}. \tag{5.13}$$

The cumulative set of validated measurements from all sensors up to time $k$ is denoted as

$$Z^k := \{Y^{k(1)}, Y^{k(2)}, \cdots, Y^{k(q)}\} \tag{5.14}$$

where $q$ is the number of sensors.

Our goal is to find the state estimate

$$\hat{\tilde{x}}_{k|k} := E\{\tilde{x}_k | Z^k\} \tag{5.15}$$

and the associated error covariance matrix

$$\tilde{P}_{k|k} := E\{[\tilde{x}_k - \hat{\tilde{x}}_{k|k}][\tilde{x}_k - \hat{\tilde{x}}_{k|k}]' | Z^k\} \tag{5.16}$$

where $x_k'$ denotes the transpose of $x_k$.

## 5.5 IMM/MSPDAF Algorithm for Asynchronous and Possibly Out-of-Sequence Measurements

We now modify the IMMPDA algorithms of [47] and [25] to apply to the multi-sensor asynchronous measurements system. We confine our attention to the case of 2 sensors; however, the algorithm can be adapted to the case of arbitrary $q$ sensors. We will only briefly outline the basic steps in 'one cycle' (i.e., processing needed to update for a new set of measurements) of the IMM/MSPDA filter.

*Assumed available*: Given the state estimate $\hat{\tilde{x}}^j_{k-1|k-1} := E\{\tilde{x}_{k-1} | M^j_{k-1}, Z^{k-1}\}$, the associated covariance $\tilde{P}^j_{k-1|k-1}$, and the conditional mode probability $\mu^j_{k-1} := P[M^j_{k-1} | Z^{k-1}]$ at time $k-1$ for each mode $j \in \mathcal{M}_n$.

***Step 1. Interaction – mixing of the estimate from the previous time*** ($\forall j \in \mathcal{M}_n$) :

predicted mode probability:

$$\mu_k^{j-} := P[M_k^j | Z^{k-1}] = \sum_i p_{ij} \mu_{k-1}^i. \tag{5.17}$$

mixing probability:

$$\mu^{i|j} := P[M_{k-1}^i | M_k^j, Z^{k-1}] = p_{ij} \mu_{k-1}^i / \mu_k^{j-}. \tag{5.18}$$

mixed estimate:

$$\hat{\tilde{x}}_{k-1|k-1}^{0j} := E\{\tilde{x}_{k-1} | M_k^j, Z^{k-1}\} = \sum_i \hat{\tilde{x}}_{k-1|k-1}^{i} \mu^{i|j}. \tag{5.19}$$

covariance of the mixed estimate:

$$\begin{aligned} \tilde{P}_{k-1|k-1}^{0j} &:= E\left\{[\tilde{x}_{k-1} - \hat{\tilde{x}}_{k-1|k-1}^{0j}][\tilde{x}_{k-1} - \hat{\tilde{x}}_{k-1|k-1}^{0j}]' | M_k^j, Z^{k-1}\right\} \\ &= \sum_i \left\{\tilde{P}_{k-1|k-1}^{i} + [\hat{\tilde{x}}_{k-1|k-1}^{i} - \hat{\tilde{x}}_{k-1|k-1}^{0j}][\hat{\tilde{x}}_{k-1|k-1}^{i} - \hat{\tilde{x}}_{k-1|k-1}^{0j}]'\right\} \mu^{i|j}. \end{aligned} \tag{5.20}$$

***Step 2. Predicted state and measurements for sensors 1 and 2*** ($\forall j \in \mathcal{M}_n$) :

state prediction:

$$\hat{\tilde{x}}_{k|k-1}^{j} := E\{\tilde{x}_k | M_k^j, Z^{k-1}\} = \tilde{F}_{k-1}^{j} \hat{\tilde{x}}_{k-1|k-1}^{0j}. \tag{5.21}$$

state prediction error covariance:

$$\tilde{P}_{k|k-1}^{j} := E\{[\tilde{x}_k - \hat{\tilde{x}}_{k|k-1}^{j}][\tilde{x}_k - \hat{\tilde{x}}_{k|k-1}^{j}]' | M_k^j, Z^{k-1}\}$$

$$= \quad \tilde{F}^j_{k-1}\tilde{P}^{0j}_{k-1|k-1}\tilde{F}^{j'}_{k-1} + \tilde{G}^j_{k-1}Q^j_{k-1}\tilde{G}^{j'}_{k-1}. \tag{5.22}$$

The mode-conditioned predicted measurements for sensors 1 and 2 are

$$\hat{z}^{j,1}_k \quad := \quad h^1(\hat{\hat{x}}^j_{k|k-1}), \tag{5.23}$$

$$\hat{\hat{z}}^{j,2}_k \quad := \quad h^2\left(\hat{\hat{x}}^j_{k|k-1}\right) = \begin{cases} \begin{bmatrix} \hat{z}^{j,2}_{k|k-1} \\ \hat{z}^{j,2}_{k-1|k-1} \end{bmatrix} & \text{for} \quad \Psi_{11} \\ \hat{z}^{j,2}_{k|k-1} & \text{for} \quad \Psi_{10} \\ \hat{z}^{j,2}_{k-1|k-1} & \text{for} \quad \Psi_{01} \\ \text{no measurement} & \text{for} \quad \Psi_{00}. \end{cases} \tag{5.24}$$

Using the linearized version (5.3) and (5.4), the covariance of the mode-conditioned residual

$$\nu^{j,1(i)}_k \quad := \quad z^{1(i)}_k - \hat{z}^{j,1}_k \tag{5.25}$$

$$\nu^{j,2(i,r)}_k \quad := \quad z^{2(i,r)}_k - \hat{\hat{z}}^{j,2}_k = \begin{cases} \begin{bmatrix} z^{2(i)}_k - \hat{z}^{j,2}_{k|k-1} \\ z^{2(r)}_{k-1} - \hat{z}^{j,2}_{k-1|k-1} \end{bmatrix} & \text{for} \quad \Psi_{11} \\ z^{2(i)}_k - \hat{z}^{j,2}_{k|k-1}, & \text{for} \quad \Psi_{10} \\ z^{2(r)}_{k-1} - \hat{z}^{j,2}_{k-1|k-1}, & \text{for} \quad \Psi_{01} \\ 0, & \text{for} \quad \Psi_{00} \end{cases} \tag{5.26}$$

are given by

$$S^{j,1}_k \quad := \quad E\{\nu^{j,1(i)}_k \nu^{j,1(i)'}_k | M^j_k, Z^{k-1}\} = \tilde{H}^{j,1}_k \tilde{P}^j_{k|k-1}\tilde{H}^{j,1'}_k + R^{j,1}_k \tag{5.27}$$

$$S_k^{j,2} := \begin{cases} \begin{bmatrix} \tilde{H}_k^{j,2} \\ \\ \tilde{H}_{k-1}^{j,2} \end{bmatrix} \tilde{P}_{k|k-1}^{j} \begin{bmatrix} \tilde{H}_k^{j,2'} & \tilde{H}_{k-1}^{j,2'} \end{bmatrix} + \begin{bmatrix} R_k^{j,2} & 0 \\ \\ 0 & R_{k-1}^{j,2} \end{bmatrix}, & \text{for } \Psi_{11} \\ \\ \tilde{H}_k^{j,2} \tilde{P}_{k|k-1}^{j} \tilde{H}_k^{j,2'} + R_k^{j,2}, & \text{for } \Psi_{10} \\ \\ \tilde{H}_{k-1}^{j,2} \tilde{P}_{k|k-1}^{j} \tilde{H}_{k-1}^{j,2'} + R_{k-1}^{j,2}, & \text{for } \Psi_{01} \end{cases} \tag{5.28}$$

where $\tilde{H}_k^{j,l}$ ($\tilde{H}_{k-1}^{j,l}$) is the first order derivative (Jacobian matrix) of $h^l(.)$ evaluated at the state prediction $\hat{\tilde{x}}_{k|k-1}^{j}$ ($\hat{\tilde{x}}_{k-1|k-1}^{j}$). Note that (5.27) and (5.28) assume that $z_k^{1(i)}$, $z_k^{2(i)}$, and $z_{k-1}^{2(r)}$ originate from the target. The results (5.27) and (5.28) do not depend upon the actual measurements.

As mentioned earlier, since our approach to the problem deals with the OOSM as well as multiple simultaneous measurements [46, 48] arising from two separate sensors that are tracking a single target through a common surveillance region, a method for fusion of multiple measurements has to be devised. In order to do this, now the combined covariance of the mode-conditioned residual obtained from (5.27) and (5.28) also needs to be considered as follows

$$S_k^j := E\left\{ \begin{bmatrix} \nu_k^{j,1(i)} \\ \\ \nu_k^{j,2(i,r)} \end{bmatrix} \begin{bmatrix} \nu_k^{j,1(i)'} & \nu_k^{j,2(i,r)'} \end{bmatrix} | M_k^j, Z^{k-1} \right\} \tag{5.29}$$

$$= \begin{cases} \begin{bmatrix} \tilde{H}_k^{j,1} \\ \tilde{H}_k^{j,2} \\ \tilde{H}_{k-1}^{j,2} \end{bmatrix} \tilde{P}_{k|k-1}^{j} \begin{bmatrix} \tilde{H}_k^{j,1'} & \tilde{H}_k^{j,2'} & \tilde{H}_{k-1}^{j,2'} \end{bmatrix} + \begin{bmatrix} R_k^{j,1} & 0 & 0 \\ 0 & R_k^{j,2} & 0 \\ 0 & 0 & R_{k-1}^{j,2} \end{bmatrix}, & \text{for } \Psi_{11} \\ \begin{bmatrix} \tilde{H}_k^{j,1} \\ \tilde{H}_k^{j,2} \end{bmatrix} \tilde{P}_{k|k-1}^{j} \begin{bmatrix} \tilde{H}_k^{j,1'} & \tilde{H}_k^{j,2'} \end{bmatrix} + \begin{bmatrix} R_k^{j,1} & 0 \\ 0 & R_k^{j,2} \end{bmatrix}, & \text{for } \Psi_{10} \\ \begin{bmatrix} \tilde{H}_k^{j,1} \\ \tilde{H}_{k-1}^{j,2} \end{bmatrix} \tilde{P}_{k|k-1}^{j} \begin{bmatrix} \tilde{H}_k^{j,1'} & \tilde{H}_{k-1}^{j,2'} \end{bmatrix} + \begin{bmatrix} R_k^{j,1} & 0 \\ 0 & R_{k-1}^{j,2} \end{bmatrix}, & \text{for } \Psi_{01} \\ \tilde{H}_k^{j,1} \tilde{P}_{k|k-1}^{j} \tilde{H}_k^{j,1'} + R_k^{j,1}, & \text{for } \Psi_{00}. \end{cases} \tag{5.30}$$

***Step 3. Measurement validation for sensors 1 and 2*** ($\forall j \in \mathcal{M}_n$) :

There is uncertainty regarding the measurements' origins. Therefore, we perform validation for each target separately. One sets up a validation gate for sensor $l$ centered at the mode-conditioned predicted measurement, $\hat{z}_k^{j,l}$. Let ($|A| = \det(A)$)

$$j_a := \arg\left\{ \max_{j \in \mathcal{M}_n} \left| S_k^{j,l} \right| \right\} \quad \text{and} \quad \bar{j}_a := \arg\left\{ \max_{j \in \mathcal{M}_n} \left| S_{k-1}^{j,2} \right| \right\}. \tag{5.31}$$

Then measurement $z_k^{l(i)}$ ($z_{k-1}^{2(r)}$) is validated if and only if

$$[z_k^{l(i)} - \hat{z}_k^{j_a,l}]' [S_k^{j_a,l}]^{-1} [z_k^{l(i)} - \hat{z}_k^{j_a,l}] < \gamma \quad \left( [z_k^{l(i)} - \hat{z}_{k-1}^{\bar{j}_a,2}]' [S_{k-1}^{\bar{j}_a,2}]^{-1} [z_k^{l(i)} - \hat{z}_{k-1}^{\bar{j}_a,2}] < \gamma \right) \tag{5.32}$$

where $\gamma$ is an appropriate threshold. The volume of the validation region with the threshold $\gamma$ is [12, Sec. 2.3.2]

$$V_k^l := c_{n_{zl}} \gamma^{n_{zl}/2} \left| S_k^{j_a,l} \right|^{1/2} \quad \left( V_{k-1}^2 := c_{n_{z2}} \gamma^{n_{z2}/2} \left| S_{k-1}^{\bar{j}_a,2} \right|^{1/2} \right). \tag{5.33}$$

After performing the validation for each target separately, we deal with all the validated data for measurement fusion.

***Step 4. State estimation with validated measurement from sensors 1 and 2*** $(\forall j \in \mathcal{M}_n)$ :

From among all the raw measurements from sensor $l$ at time $k$, i.e., $Z_k^l := \{z_k^{l(1)}, z_k^{l(2)}, \cdots, z_k^{l(m_l)}\}$, define the set of validated measurements for sensor $l$ at time $k$ as

$$Y_k^l := \{y_k^{l(1)}, y_k^{l(2)}, \cdots, y_k^{l(\bar{m}_l)}\} \tag{5.34}$$

where $\bar{m}_l$ is total number of validated measurements for sensor $l$ at time $k$ and

$$y_k^{l(i)} := z_k^{l(l_i)} \tag{5.35}$$

where $1 \leq l_1 < l_2 < \cdots < l_{\bar{m}_l} \leq m_l$ when $\bar{m}_l \neq 0$. From among all OOSM from sensor 2 measured at time $k-1$, i.e., $Z_{k-1}^2 := \{z_{k-1}^{2(1)}, z_{k-1}^{2(2)}, \cdots, z_{k-1}^{2(m_2^o)}\}$, define the set of validated measurements for sensor 2 at time $k-1$ as

$$Y_{k-1}^2 := \{y_{k-1}^{2(1)}, y_{k-1}^{2(2)}, \cdots, y_{k-1}^{2(\bar{m}_2^o)}\} \tag{5.36}$$

where $\bar{m}_2^o$ is total number of validated measurements for sensor 2 at time $k-1$. Hence any single measurement arriving at the central processor can be categorized into one of $Y_k^1$, $Y_k^2$ or $Y_{k-1}^2$. Define the association events (hypotheses) $\theta_k^{a,b,c}$ for all measurement data arriving at the central processor at time $k$ as follows

- $\theta_k^{0,0,0}$: none of the measurements in $Y_k^1$, $Y_k^2$ or $Y_{k-1}^2$ is target originated, $a = b = c = 0$,
- $\theta_k^{a,0,0}$: only $y_k^{1(a)}$ in $Y_k^1$ is a target measurement, all other measurements in $Y_k^1$, $Y_k^2$ or $Y_{k-1}^2$ are clutter, $a = 1, \cdots, \bar{m}_1$, $b = c = 0$,
- $\theta_k^{0,b,0}$: only $y_k^{2(b)}$ in $Y_k^2$ is a target measurement, all other measurements in $Y_k^1$, $Y_k^2$ or $Y_{k-1}^2$ are clutter, $a = c = 0$, $b = 1, \cdots, \bar{m}_2$,
- $\theta_k^{a,b,0}$: $y_k^{1(a)}$ and $y_k^{2(b)}$ in $Y_k^1$ and $Y_k^2$, respectively, are target measurements, all other measurements in $Y_k^1$, $Y_k^2$ or $Y_{k-1}^2$ are clutter, $a = 1, \cdots, \bar{m}_1$, $b = 1, \cdots, \bar{m}_2$, c=0,
- $\theta_k^{0,0,c}$: only $y_{k-1}^{2(c)}$ in $Y_{k-1}^2$ is a target measurement, all other measurements in $Y_k^1$, $Y_k^2$ or $Y_{k-1}^2$ are clutter, $a = b = 0$, $c = 1, \cdots, \bar{m}_2^o$,
- $\theta_k^{a,0,c}$: $y_k^{1(a)}$ and $y_{k-1}^{2(c)}$ in $Y_k^1$ and $Y_{k-1}^2$, respectively, are target measurements, all other measurements in $Y_k^1$, $Y_k^2$ or $Y_{k-1}^2$ are clutter, $a = 1, \cdots, \bar{m}_1$, b=0, $c = 1, \cdots, \bar{m}_2^o$,
- $\theta_k^{0,b,c}$: $y_k^{2(b)}$ and $y_{k-1}^{2(c)}$ in $Y_k^2$ and $Y_{k-1}^2$, respectively, are target measurements, all other measurements in $Y_k^1$, $Y_k^2$ or $Y_{k-1}^2$ are clutter, $a = 0, b = 1, \cdots, \bar{m}_2$ , $c = 1, \cdots, \bar{m}_2^o$,

- $\theta_k^{a,b,c}$: $y_k^{1(a)}$, $y_k^{2(b)}$ and $y_{k-1}^{2(c)}$ in $Y_k^1$, $Y_k^2$ and $Y_{k-1}^2$, respectively, are target measurements, all other measurements in $Y_k^1$, $Y_k^2$ or $Y_{k-1}^2$ are clutter, $a = 1, \cdots, \bar{m}_1$, $b = 1, \cdots, \bar{m}_2$, $c = 1, \cdots, \bar{m}_2^o$.

Therefore, there are a total of $\bar{m}_1\bar{m}_2\bar{m}_2^o+\bar{m}_1\bar{m}_2+\bar{m}_2\bar{m}_2^o+\bar{m}_1\bar{m}_2^o+\bar{m}_1+\bar{m}_2+\bar{m}_2^o+1$ possible association hypotheses, each of which has an association probability. Define the mode-conditioned association event probabilities as

$$\beta_k^{j,a,b,c} := P\{\theta_k^{a,b,c} | M_k^j, Y_k^1, Y_k^2, Y_{k-1}^2, Z^{k-1}\}. \tag{5.37}$$

Exploiting the diffuse model for clutter in [12, 21], it turns out that

$$\begin{aligned}
\beta_k^{j,0,0,0} &= C\frac{\left(1-P_{D_1}P_{G_1}\right)\left(1-P_{D_2}P_{G_2}\right)^2}{(V_k^1)^{\bar{m}_1}(V_k^2)^{\bar{m}_2}(V_{k-1}^2)^{\bar{m}_2^o}}, \quad a=b=c=0 \\
\beta_k^{j,a,0,0} &= C\frac{P_{D_1}\left(1-P_{D_2}P_{G_2}\right)^2\mathcal{N}\left[\nu_k^{j,1(a)};0,S_k^{j,1}\right]}{(V_k^1)^{\bar{m}_1-1}\bar{m}_1}, \quad a=1,\cdots,\bar{m}_1, \quad b=c=0 \\
\beta_k^{j,0,b,0} &= C\frac{P_{D_2}\left(1-P_{D_1}P_{G_1}\right)\left(1-P_{D_2}P_{G_2}\right)\mathcal{N}\left[\nu_k^{j,2(b)};0,S_k^{j,2}\right]}{(V_k^2)^{\bar{m}_2-1}\bar{m}_2}, \quad a=0, \quad b=1,\cdots,\bar{m}_2, \quad c=0 \\
\beta_k^{j,a,b,0} &= C\frac{P_{D_1}P_{D_2}\left(1-P_{D_2}P_{G_2}\right)\mathcal{N}\left[\tilde{\nu}_k^{j(a,b,0)};0,S_k^j\right]}{(V_k^1)^{\bar{m}_1-1}(V_k^2)^{\bar{m}_2-1}\bar{m}_1\bar{m}_2}, \quad a=1,\cdots,\bar{m}_1, \quad b=1,\cdots,\bar{m}_2, \quad c=0 \\
\beta_k^{j,0,0,c} &= C\frac{\left(1-P_{D_1}P_{G_1}\right)\left(1-P_{D_2}P_{G_2}\right)P_{D_2}\mathcal{N}\left[\nu_{k-1}^{j,2(c)};0,S_{k-1}^{j,2}\right]}{(V_{k-1}^2)^{\bar{m}_2^o-1}\bar{m}_2^o}, \quad a=b=0, \quad c=1,\cdots,\bar{m}_2^o \\
\beta_k^{j,a,0,c} &= C\frac{P_{D_1}P_{D_2}\left(1-P_{D_2}P_{G_2}\right)\mathcal{N}\left[\tilde{\nu}_k^{j(a,0,c)};0,\tilde{S}_k^{j,a,c}\right]}{(V_k^1)^{\bar{m}_1-1}(V_{k-1}^2)^{\bar{m}_2^o-1}\bar{m}_1}, \quad a=1,\cdots,\bar{m}_1, \quad b=0, \quad c=1,\cdots,\bar{m}_2^o \\
\beta_k^{j,0,b,c} &= C\frac{P_{D_2}^2\left(1-P_{D_1}P_{G_1}\right)\mathcal{N}\left[\tilde{\nu}_k^{j(0,b,c)};0,\tilde{S}_k^{j,b,c}\right]}{(V_k^2)^{\bar{m}_2-1}(V_{k-1}^2)^{\bar{m}_2^o-1}\bar{m}_2\bar{m}_2^o}, \quad a=0, \quad b=1,\cdots,\bar{m}_2, \quad c=1,\cdots,\bar{m}_2^o \\
\beta_k^{j,a,b,c} &= C\frac{P_{D_1}P_{D_2}^2\mathcal{N}\left[\tilde{\nu}_k^{j(a,b,c)};0,\tilde{S}_k^{j,a,b,c}\right]}{(V_k^1)^{\bar{m}_1-1}(V_k^2)^{\bar{m}_2-1}(V_{k-1}^2)^{\bar{m}_2^o-1}\bar{m}_1\bar{m}_2\bar{m}_2^o}, \quad a=1,\cdots,\bar{m}_1, \quad b=1,\cdots,\bar{m}_2, \quad c=1,\cdots,\bar{m}_2^o
\end{aligned} \tag{5.38}$$

where $P_{D_1}$ and $P_{D_2}$ are the detection probabilities that the sensors 1 and 2 detect the target, respectively, $P_{G_1}$ and $P_{G_2}$ are probabilities the target is in the validation region observed from sensors 1 and 2, respectively, $C$ is a normalization constant such that $\sum_{a=0}^{\bar{m}_1}\sum_{b=0}^{\bar{m}_2}\sum_{c=0}^{\bar{m}_2^1}\beta_k^{j,a,b,c}=1\ \forall j$. The mode-conditioned combined innovations $\tilde{\nu}_k^j$ can be defined as

$$\tilde{\nu}_k^{j(a,b,0)}=\begin{bmatrix}\nu_k^{j,1(a)}\\ \\ \nu_k^{j,2(b)}\end{bmatrix},\quad \tilde{\nu}_k^{j(a,0,c)}=\begin{bmatrix}\nu_k^{j,1(a)}\\ \\ \nu_{k-1}^{j,2(c)}\end{bmatrix},\quad \tilde{\nu}_k^{j(0,b,c)}=\begin{bmatrix}\nu_k^{j,2(b)}\\ \\ \nu_{k-1}^{j,2(c)}\end{bmatrix},$$
$$\tilde{\nu}_k^{j(a,b,c)}=\begin{bmatrix}\nu_k^{j,1(a)}\\ \\ \nu_k^{j,2(b)}\\ \\ \nu_{k-1}^{j,2(c)}\end{bmatrix}. \tag{5.39}$$

The likelihood function for each mode $j$ is

$$\begin{aligned}\Lambda_k^j &:= p\left[Y_k^1,Y_k^2,Y_{k-1}^2|M_k^j,Z^{k-1}\right]\\ &= \sum_{a=0}^{\bar{m}_1}\sum_{b=0}^{\bar{m}_2}\sum_{c=0}^{\bar{m}_2^1}p\left[Y_k^1,Y_k^2,Y_{k-1}^2,\theta_k^{a,b,c}|M_k^j,Z^{k-1}\right]\end{aligned} \tag{5.40}$$

where

$$p\left[Y_k^1,Y_k^2,Y_{k-1}^2,\theta_k^{a,b,c}|M_k^j,Z^{k-1}\right]=p\left[Y_k^1,Y_k^2,Y_{k-1}^2|M_k^j,\theta_k^{a,b,c},Z^{k-1}\right]P[\theta_k^{a,b,c}] \tag{5.41}$$

$$
= \begin{cases}
\frac{\left(1-P_{D_1}P_{G_1}\right)\left(1-P_{D_2}P_{G_2}\right)^2}{(V_k^1)^{\bar{m}_1}(V_k^2)^{\bar{m}_2}(V_{k-1}^2)^{\bar{m}_2^o}}, & a=b=c=0 \\
\frac{P_{D_1}\left(1-P_{D_2}P_{G_2}\right)^2\mathcal{N}\left[\nu_k^{j,1(a)};0,S_k^{j,1}\right]}{(V_k^1)^{\bar{m}_1-1}\bar{m}_1}, & a=1,\cdots,\bar{m}_1,\ \ b=c=0 \\
\frac{P_{D_2}\left(1-P_{D_1}P_{G_1}\right)\left(1-P_{D_2}P_{G_2}\right)\mathcal{N}\left[\nu_k^{j,2(b)};0,S_k^{j,2}\right]}{(V_k^2)^{\bar{m}_2-1}\bar{m}_2}, & a=0,\ \ b=1,\cdots,\bar{m}_2,\ \ c=0 \\
\frac{\mathcal{N}\left[\nu_k^{j(a,b,0)};0,S_k^{j,a,b}\right]P_{D_1}P_{D_2}\left(1-P_{D_2}P_{G_2}\right)}{\bar{m}_1\bar{m}_2(V_k^1)^{\bar{m}_1-1}(V_k^2)^{\bar{m}_2-1}}, & a=1,\cdots,\bar{m}_1,\ \ b=1,\cdots,\bar{m}_2,\ \ c=0 \\
\frac{\left(1-P_{D_1}P_{G_1}\right)\left(1-P_{D_2}P_{G_2}\right)P_{D_2}\mathcal{N}\left[\nu_{k-1}^{j,2(c)};0,S_{k-1}^{j,2}\right]}{(V_{k-1}^2)^{\bar{m}_2^o-1}\bar{m}_2^o}, & a=b=0,\ \ c=1,\cdots,\bar{m}_2^o \\
\frac{P_{D_1}P_{D_2}\left(1-P_{D_2}P_{G_2}\right)\mathcal{N}\left[\tilde{\nu}_k^{j(a,0,c)};0,\tilde{S}_k^{j,a,c}\right]}{(V_k^1)^{\bar{m}_1-1}(V_{k-1}^2)^{\bar{m}_2^o-1}\bar{m}_1}, & a=1,\cdots,\bar{m}_1,\ \ b=0,\ \ c=1,\cdots,\bar{m}_2^o \\
\frac{P_{D_2}^2\left(1-P_{D_1}P_{G_1}\right)\mathcal{N}\left[\tilde{\nu}_k^{j(0,b,c)};0,\tilde{S}_k^{j,b,c}\right]}{(V_k^2)^{\bar{m}_2-1}(V_{k-1}^2)^{\bar{m}_2^o-1}\bar{m}_2\bar{m}_2^o}, & a=0,\ \ b=1,\cdots,\bar{m}_2,\ \ c=1,\cdots,\bar{m}_2^o \\
\frac{P_{D_1}P_{D_2}^2\mathcal{N}\left[\tilde{\nu}_k^{j(a,b,c)};0,\tilde{S}_k^{j,a,b,c}\right]}{(V_k^1)^{\bar{m}_1-1}(V_k^2)^{\bar{m}_2-1}(V_{k-1}^2)^{\bar{m}_2^o-1}\bar{m}_1\bar{m}_2\bar{m}_2^o}, & a=1,\cdots,\bar{m}_1,\ \ b=1,\cdots,\bar{m}_2,\ \ c=1,\cdots,\bar{m}_2^o
\end{cases}
\tag{5.42}
$$

Using $\hat{\tilde{x}}_{k|k-1}^j$ (from (5.21)) and its covariance $\tilde{P}_{k|k-1}^j$ (from (5.22)), one computes the partial update $\hat{\tilde{x}}_{k|k}^j$ and its covariance $\tilde{P}_{k|k}^j$ according to the standard PDAF [21], except that the augmented state is conditioned on $\theta_k^{a,b,c}$ with data fusion from sensors 1 and 2. Define the combined mode-conditioned innovations

$$
\nu_k^j = \sum_{a=0}^{\bar{m}_1}\sum_{b=0}^{\bar{m}_2}\sum_{c=0}^{\bar{m}_2^1}\beta_k^{j,a,b,c}\nu_k^{j,a,b,c}. \tag{5.43}
$$

Therefore, partial update of the state estimate

$$
\hat{\tilde{x}}_{k|k}^{j,a,b,c} := E\left\{x_k|\theta_k^{a,b,c}, M_k^j, Z^{k-1}, Y_k^1, Y_k^2, Y_{k-1}^2\right\} = \hat{\tilde{x}}_{k|k-1}^j + W_k^{j,a,b,c}\nu_k^{j,a,b,c} \tag{5.44}
$$

where Kalman gains, $W_k^{j,a,b,c}$, are computed as

$$\begin{cases} W_k^{j,0,0,0} = 0, & \text{for} \quad a=b=c=0 \\ W_k^{j,a,0,0} = \tilde{P}_{k|k-1}^j \left[\tilde{H}_k^{j,1\prime}[S_k^{j,1}]^{-1} \;\; 0 \;\; 0\right], & \text{for} \quad a\neq 0,\ b=c=0 \\ W_k^{j,0,b,0} = \tilde{P}_{k|k-1}^j \left[0 \;\; \tilde{H}_k^{j,2\prime}[S_k^{j,2}]^{-1} \;\; 0\right], & \text{for} \quad a=0,\ b\neq 0,\ c=0 \\ W_k^{j,a,b,0} = \tilde{P}_{k|k-1}^j \left[[\tilde{H}_k^{j,1\prime} \;\; \tilde{H}_k^{j,2\prime}][S_k^j]^{-1} \;\; 0\right], & \text{for} \quad a\neq 0,\ b\neq 0,\ c=0 \\ W_k^{j,0,0,c} = \tilde{P}_{k|k-1}^j \left[0 \;\; 0 \;\; \tilde{H}_{k-1}^{j,2\prime}[S_{k-1}^{j,2}]^{-1}\right], & \text{for} \quad a=b=0,\ c\neq 0 \\ W_k^{j,a,0,c} = \tilde{P}_{k|k-1}^j \left[\tilde{H}_k^{j,1\prime}[S_k^{j,1}]^{-1} \;\; 0 \;\; \tilde{H}_{k-1}^{j,2\prime}[S_{k-1}^{j,2}]^{-1}\right], & \text{for} \quad a\neq 0,\ b=0,\ c\neq 0 \\ W_k^{j,0,b,c} = \tilde{P}_{k|k-1}^j \left[0 \;\; [\tilde{H}_k^{j,2\prime}\tilde{H}_{k-1}^{j,2\prime}][S_k^{j,2}]^{-1}\right], & \text{for} \quad a=0,\ b\neq 0,\ c\neq 0 \\ W_k^{j,a,b,c} = \tilde{P}_{k|k-1}^j \left[[\tilde{H}_k^{j,1\prime} \;\; \tilde{H}_k^{j,2\prime} \;\; \tilde{H}_{k-1}^{j,2\prime}][S_k^j]^{-1}\right], & \text{for} \quad a\neq 0,\ b\neq 0,\ c\neq 0. \end{cases} \tag{5.45}$$

Therefore, mode-conditioned update of the state estimate

$$\hat{\tilde{x}}_{k|k}^j := E\left\{x_k | M_k^j, Z^{k-1}, Y_k^1, Y_k^2, Y_{k-1}^2\right\} = \sum_{a=0}^{\bar{m}_1}\sum_{b=0}^{\bar{m}_2}\sum_{c=0}^{\bar{m}_2^1} \beta_k^{j,a,b,c}\hat{\tilde{x}}_{k|k-1}^{j,a,b,c} \tag{5.46}$$

and covariance of $\hat{\tilde{x}}_{k|k}^j$

$$\begin{aligned} \tilde{P}_{k|k}^j = \tilde{P}_{k|k-1}^j &- \sum_{\substack{a=0 \\ (a,b,c)\neq(0,0,0)}}^{\bar{m}_1}\sum_{b=0}^{\bar{m}_2}\sum_{c=0}^{\bar{m}_2^o} \beta_k^{j,a,b,c} W_k^{j,a,b,c} S_k^{j,a,b,c} W_k^{j,a,b,c\prime} \\ &+ \sum_{a=0}^{\bar{m}_1}\sum_{b=0}^{\bar{m}_2}\sum_{c=0}^{\bar{m}_2^1} \beta_k^{j,a,b,c} W_k^{j,a,b,c}\nu_k^{j,a,b,c}\nu_k^{j,a,b,c\prime} W_k^{j,a,b,c\prime} \\ &- \left[\sum_{a=0}^{\bar{m}_1}\sum_{b=0}^{\bar{m}_2}\sum_{c=0}^{\bar{m}_2^1} \beta_k^{j,a,b,c} W_k^{j,a,b,c}\nu^{j,a,b,c}\right]\left[\sum_{a=0}^{\bar{m}_1}\sum_{b=0}^{\bar{m}_2}\sum_{c=0}^{\bar{m}_2^1} \beta_k^{j,a,b,c} W_k^{j,a,b,c}\nu^{j,a,b,c}\right]'. \end{aligned} \tag{5.47}$$

***Step 5. Update of mode probabilities*** $(\forall j \in \mathcal{M}_n)$ :

$$\mu_k^j := P\left[M_k^j | Z^k\right] = \frac{1}{C}\mu_k^{j-}\Lambda_k^j \tag{5.48}$$

where $C$ is a normalization constant such that $\sum_j \mu_k^j = 1$.

***Step 6. Combination of the mode-conditioned estimates*** $(\forall j \in \mathcal{M}_n)$ :

The final augmented state estimate update at time $k$ is given by

$$\hat{\tilde{x}}_{k|k} = \sum\nolimits_j \hat{\tilde{x}}_{k|k}^j \mu_k^j \tag{5.49}$$

and its covariance is given by

$$\tilde{P}_{k|k} = \sum\nolimits_j \left\{ \tilde{P}_{k|k}^j + \left[\hat{\tilde{x}}_{k|k}^j - \hat{\tilde{x}}_{k|k}\right]\left[\hat{\tilde{x}}_{k|k}^j - \hat{\tilde{x}}_{k|k}\right]' \right\} \mu_k^j. \tag{5.50}$$

From the final augmented state (see (5.49)), the state filtered vector $\hat{x}_{k|k}$ and the state smoothing vector $\hat{x}_{k-1|k}$ can be easily obtained.

## 5.6 Simulation Example

The following example of tracking a highly maneuvering target in clutter is considered. The target starts at location [21689 10840 40] in Cartesian coordinates in meters. The initial velocity (in m/s) is [-8.3 -399.9 0] and the target stays at constant altitude with a constant speed of 400 m/s. Its trajectory is a straight line with constant velocity between 0 and 20s, a coordinated turn (0.15 rad/s) with constant acceleration of 60 $m/s^2$ between 20 and 35s, a straight line with constant velocity between 35 and 55s, a

coordinated turn (0.1 rad/s) with constant acceleration of 40 m/s$^2$ between 55 and 70s, and a straight line with constant velocity between 70 and 90s. The target motion models are patterned and modified after [21]. In each mode the target dynamics are modeled in Cartesian coordinates as

$$\tilde{x}_k = \tilde{F}^j_{k,k-1}\tilde{x}_{k-1} + \tilde{G}^j_{k,k-1}v^j_k, \tag{5.51}$$

$$\tilde{x}_{k_{dl}} = \tilde{F}^j_{k_{dl},k-1}\tilde{x}_{k-1} + \tilde{G}^j_{k_{dl},k-1}v^j_{k_{dl}} \tag{5.52}$$

where the augmented state of the target consists of position, velocity, acceleration, and the process noise in each of the three Cartesian coordinates ($x, y$, and $z$) at $t_k$, $t_{k-1}$ and $t_{k-2}$. Thus both $\tilde{x}_k$ and $\tilde{x}_{k_{dl}}$ are of dimension 36 ($n_x = 36$). Three maneuver models are considered in the following discussion. From (5.8) and (5.9), $\tilde{F}^j_{k,k-1}$, $\tilde{G}^j_{k,k-1}$, $\tilde{F}^j_{k_{dl},k-1}$ and $\tilde{G}^j_{k_{dl},k-1}$ are defined as

$$\tilde{F}^j_{k,k-1} = \begin{bmatrix} F^j_{k,k-1} & G^j_{k,k-1} & 0 & 0 & 0 & 0 \\ 0 & 0 & 0 & 0 & 0 & 0 \\ I & 0 & 0 & 0 & 0 & 0 \\ 0 & I & 0 & 0 & 0 & 0 \\ 0 & 0 & I & 0 & 0 & 0 \\ 0 & 0 & 0 & I & 0 & 0 \end{bmatrix}, \quad \tilde{G}^j_{k,k-1} = \begin{bmatrix} 0 \\ I \\ 0 \\ 0 \\ 0 \\ 0 \end{bmatrix} \tag{5.53}$$

$$\tilde{F}^j_{k_{dl},k-1} = \begin{bmatrix} F^j_{k_{dl},k-1} & G^j_{k_{dl},k-1} & 0 & 0 & 0 & 0 \\ 0 & 0 & 0 & 0 & 0 & 0 \\ I & 0 & 0 & 0 & 0 & 0 \\ 0 & I & 0 & 0 & 0 & 0 \\ 0 & 0 & I & 0 & 0 & 0 \\ 0 & 0 & 0 & I & 0 & 0 \end{bmatrix}, \quad \tilde{G}^j_{k_{dl},k-1} = \begin{bmatrix} 0 \\ I \\ 0 \\ 0 \\ 0 \\ 0 \end{bmatrix} \tag{5.54}$$

where the system matrices $F_{k,k-1}$, $G_{k,k-1}$, $F_{k_{dl},k-1}$ and $G_{k_{dl},k-1}$ are defined as

$$F^j_{k,k-1} = \begin{bmatrix} F^j & 0 & 0 \\ 0 & F^j & 0 \\ 0 & 0 & F^j \end{bmatrix}, \quad G^j_{k,k-1} = \begin{bmatrix} G^j & 0 & 0 \\ 0 & G^j & 0 \\ 0 & 0 & G^j \end{bmatrix}, \tag{5.55}$$

$$F^j_{k_{dl},k-1} = \begin{bmatrix} F^j_d & 0 & 0 \\ 0 & F^j_d & 0 \\ 0 & 0 & F^j_d \end{bmatrix}, \quad G^j_{k_{dl},k-1} = \begin{bmatrix} G^j_d & 0 & 0 \\ 0 & G^j_d & 0 \\ 0 & 0 & G^j_d \end{bmatrix}. \tag{5.56}$$

**Model 1**. Nearly constant velocity model with zero mean perturbation in acceleration

$$F^1 = \begin{bmatrix} 1 & T & 0 \\ 0 & 1 & 0 \\ 0 & 0 & 0 \end{bmatrix}, \quad G^1 = \begin{bmatrix} \frac{T^2}{2} \\ T \\ 0 \end{bmatrix}, \tag{5.57}$$

$$F_d^1 = \begin{bmatrix} 1 & (T - d_{kl}) & 0 \\ 0 & 1 & 0 \\ 0 & 0 & 0 \end{bmatrix}, \quad G_d^1 = \begin{bmatrix} \frac{(T-d_{kl})^2}{2} \\ (T - d_{kl}) \\ 0 \end{bmatrix}, \tag{5.58}$$

where $T$ is the sampling period. The standard deviation of the process noise of $M^1$ is 5 $\mathrm{m/s^2}$ (as in [21]).

**Model 2**. Wiener process acceleration (nearly constant acceleration motion)

$$F^2 = \begin{bmatrix} 1 & T & \frac{T^2}{2} \\ 0 & 1 & T \\ 0 & 0 & 1 \end{bmatrix}, \quad G^2 = \begin{bmatrix} \frac{T^2}{2} \\ T \\ 1 \end{bmatrix}, \tag{5.59}$$

$$F_d^2 = \begin{bmatrix} 1 & (T - d_{kl}) & \frac{(T-d_{kl})^2}{2} \\ 0 & 1 & (T - d_{kl}) \\ 0 & 0 & 1 \end{bmatrix}, \quad G_d^2 = \begin{bmatrix} \frac{(T-d_{kl})^2}{2} \\ (T - d_{kl}) \\ 1 \end{bmatrix}. \tag{5.60}$$

The standard deviation of the process noise of $M^2$ is 7.5 $\mathrm{m/s^2}$ (as in [21]).

**Model 3**. Wiener process acceleration (model with large acceleration increments, for the onset and termination of maneuvers), with $F^3 = F^2$, $G^3 = G^2$, $F_d^3 = F_d^2$ and $G_d^3 = G_d^2$. The standard deviation of the process noise of $M^3$ is 40 $\mathrm{m/s^2}$ (as in [21]).

The initial model probabilities are $\mu_0^1 = 0.8$, $\mu_0^2 = 0.1$ and $\mu_0^3 = 0.1$. The mode switching probability matrix is given by (as in [21])

$$\begin{bmatrix} p_{11} & p_{12} & p_{13} \\ p_{21} & p_{22} & p_{23} \\ p_{31} & p_{32} & p_{33} \end{bmatrix} = \begin{bmatrix} 0.8 & 0.0 & 0.2 \\ 0.0 & 0.8 & 0.2 \\ 0.3 & 0.3 & 0.4 \end{bmatrix}. \tag{5.61}$$

**The Sensors**: Two sensors are used to obtain the measurements. Sensor 1 and Sensor 2 are located at $[x_1, y_1, z_1]$=[-4000 4000 0] m and $[x_2, y_2, z_2]$=[5000 0 0] m, respectively, and the central processor is collocated with sensor 1 platform (we assume that there is no time delay between sensor 1 and central processor and, on the other hand, there is fixed-and-known time delay between sensor 2 and central processor). The measurements from sensor $l$ for model $j$ are $z_k^l = h^l(x_k) + w_k^{j,l}$ for $l = 1$ and 2, reflecting range and azimuth angle for sensor 1 (infrared) and azimuth and elevation angles for sensor 2 (radar) . The range, azimuth, and elevation angle transformations, respectively, are given by

$$r_l = \left[(x - x_l)^2 + (y - y_l)^2 + (z - z_l)^2\right]^{1/2} \tag{5.62}$$

$$a_l = \tan^{-1}[(y - y_l)/(x - x_l)] \tag{5.63}$$

$$e_l = \tan^{-1}\left\{(z - z_l)/[(x - x_l)^2 + (y - y_l)^2]^{1/2}\right\}. \tag{5.64}$$

The measurements obtained from sensors 1 and 2 can be expressed as we see from (5.1), (5.2), (5.4) and (5.11). The measurement noise $w_k^{j,l}$ for sensor $l$ is assumed to be zero-mean white Gaussian with known covariances, $R^1 = \text{diag}[q_{a1}, q_e] = \text{diag}[4\text{mrad}^2, 4\text{mrad}^2]$

with $q_{a1}$ and $q_e$ denoting the variances for the infrared sensor azimuth and elevation measurement noises, and $R^2 = \text{diag}[q_r, q_{a2}] = \text{diag}[400\text{m}^2, 49\text{mrad}^2]$ with $q_r$ and $q_{a2}$ denoting the variances for the radar range and azimuth measurement noises, respectively. The sampling interval was $T$=1s and it was assumed that the probability of detection $P_D$=1 for both sensors. The time difference between the sampling time at the central processor (local sensor) and the measurement time at the remote sensor $d_{kl}$ is fixed-and-known to be $0.5T$. The data at any time $k$ has a probability $P_d = 0.4$ ($P_d = 0.25$ also applied for comparison) of being delayed where the delay is uniformly distributed with a maximum time delay less than or equal to $T$ where $T$ is sampling rate.

**The Clutter**: For generating false measurements in simulations, the clutter was assumed to be Poisson distributed with expected number of $\lambda_1 = 2 \times 10^{-4}/$ mrad$^2$ for sensor 1 (infrared) and $\lambda_2 = 20 \times 10^{-6}$/m-mrad for sensor 2 (radar) [21, case 1]. These statistics were used for generating the clutter in all simulations. However, a nonparametric clutter model was used for implementing all the algorithms for target tracking.

**Other Parameters**: The gates for setting up the validation regions for both the sensors were based on the threshold $\gamma$=16. With the measurement vector of dimension 2, this leads to a gate probability $P_G$=0.9997 (see [12, pages 95-96]).

**Simulation Results**: The results were obtained from 100 Monte Carlo runs. Fig. 5.2 shows the true trajectory of the target. Fig. 5.3 (a) and (b) show RMS error comparison in position among proposed AS-IMM/MSPDAF algorithm dealing with OOSM, standard AS-IMM/MSPDAF algorithm [50] with OOSM discarding, and AS-IMM/MSPDAF algorithm applied to the hypothetical case of $P_d = 0$. The first maneuver starts at 20 sec and in Fig. 5.3 (b) one can see a significant improvement from 25 sec through 36 sec. The

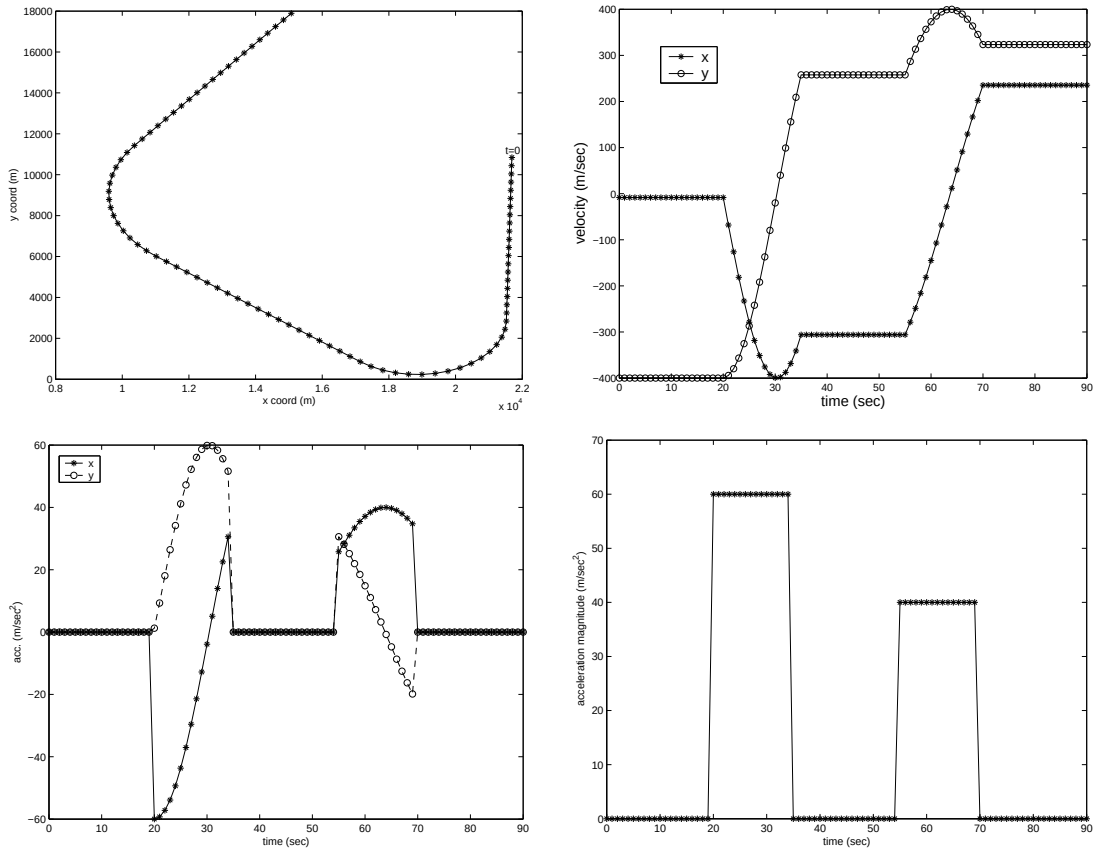


Figure 5.2: Trajectory of maneuvering target (read left to right, top to bottom). (a) Position in $xy$ plane. (b) $x$ and $y$ velocities. (c) $x$ and $y$ accelerations. (d) magnitude of accelerations.

second maneuver starts at 55 sec and in Fig. 5.3 (b) one can see a significant improvement from 60 sec through 68 sec. That is, the proposed AS-IMM/MSPDAF algorithm responds faster to maneuvers. Once the target is "settled" in a particular mode, there is insignificant differences between the two approaches. It is seen from Fig. 5.3 (a) and (b) that the higher delay probability $P_d$, the more significant performance improvement can be obtained compared with the standard AS-IMM/MSPDAF algorithm [50] that ignores and discards possibly existing OOSM.

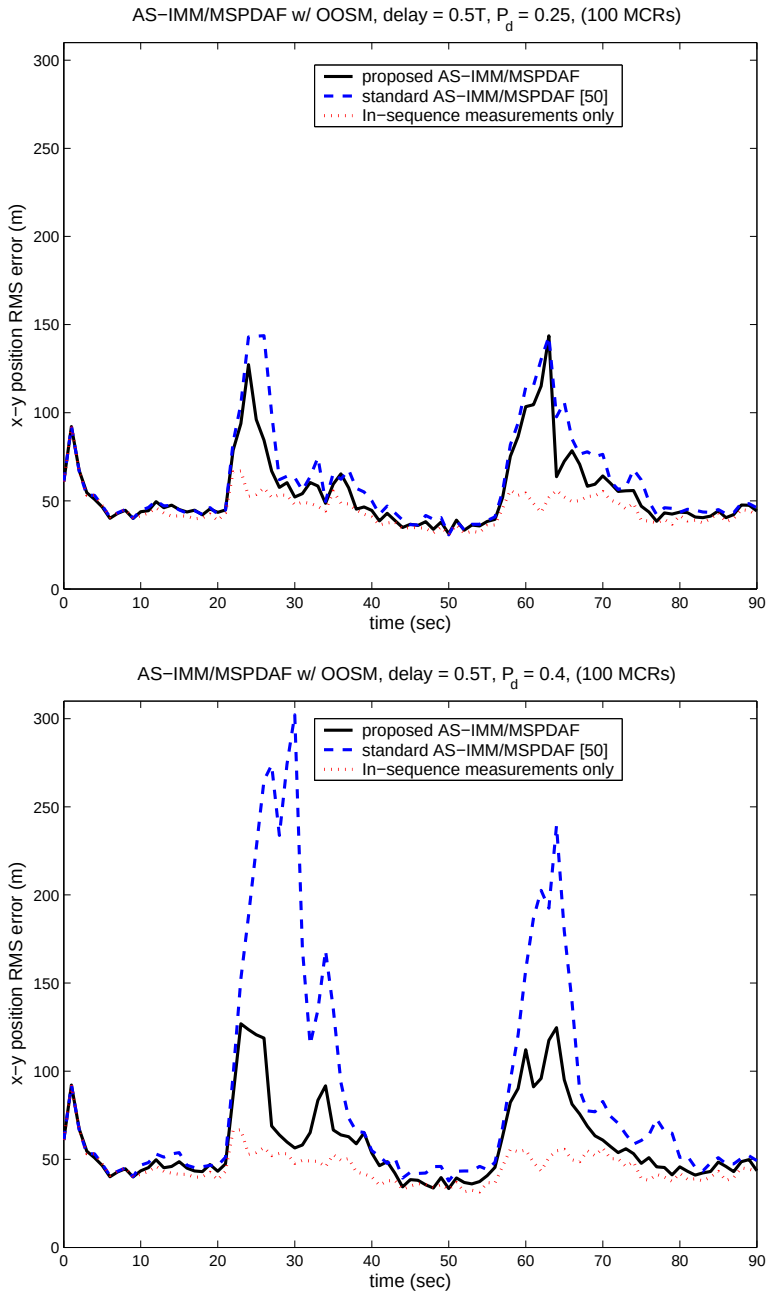


Figure 5.3: AS-IMM/MSPDA comparison (RMSE in position, read top to bottom) for various probabilities of delayed measurement, $P_d = 0.25$ and 0.4: (a) $P_d$=0.25. (b) $P_d$=0.4. Solid: proposed AS-IMM/MSPDAF algorithm dealing with OOSM; dashed: AS-IMM/MSPDAF algorithm [50] with OOSM discarding; dotted: AS-IMM/MSPDAF algorithm applied to the hypothetical case of $P_d = 0$.

## 5.7 Conclusions

We investigated an augmented state IMM/MSPDAF algorithm with asynchronous measurement (there is fixed-and-known timing mismatch between sensor platforms with possible OOSM) for tracking a highly maneuvering target in clutter. Simultaneous measurement update technique is applied for better data association and is expected to be more accurate [12] since it considers all association hypotheses coupled across multisensor while in the sequential updating considers the separate hypothesis for each sensor. Our proposed approach has extended the multisensor approach of Chapter 4 (or see [50]) to OOSM by employing additional data association. The proposed algorithm was illustrated via a simulation example where it outperformed a standard AS-IMM/MSPDAF algorithm with OOSM discarding [50] especially during the periods following the onset of the target maneuvers. This improvement in accuracy is seen in our simulation example only during the periods following the onset of the target maneuvers. Once the target is settled in a particular mode, there is insignificant differences between the two approaches. As one can easily notice, the higher delay probability $P_d$ (with more OOSM appearances), the more significant performance improvement can be obtained compared with the standard AS-IMM/MSPDAF algorithm [50] that ignores and discards possibly existing OOSM.

# Chapter 6

# Tracking of Multiple Maneuvering Targets in Clutter with Possibly Merged Measurements using IMM and JPDAM Coupled Filtering

In this chapter, we present a suboptimal filtering algorithm for tracking multiple highly maneuvering targets in a cluttered environment using multiple sensors. We concentrate on two targets which temporarily move in close formation, giving rise to a single detection due to the resolution limitations of the sensor. The filtering algorithm is developed by applying the basic IMM approach and the joint probabilistic data association with merged measurements (JPDAM) technique and coupled target state estimation to a Markovian switching system. The algorithm is illustrated via a simulation example involving tracking of two highly maneuvering, at times closely spaced, targets with possibly unresolved measurements. Compared with an existing IMM/JPDA filtering algorithm developed without allowing for merged measurements, the proposed algorithm achieves significant improvement in the accuracy of track estimation during target merging period.

## 6.1 Introduction

In this chapter, we consider the problem of tracking multiple maneuvering targets which temporarily operate in close formation in clutter. This class of problem has received considerable attention in the literature [5, 12, 21, 22, 44, 45]. The switching multiple model approach has been found to be quite effective in modeling highly maneuvering targets [12, 14, 21, 29, 30, 33, 45]. In this approach various "modes" of target motion are represented by distinct kinematic models, and in a Bayesian framework, the

target maneuvers are modeled by switching among these models controlled by a Markov chain. In the presence of clutter, the measurements at the sensors may not all have originated from the target-of-interest. In this case one has to solve the problem of data association. An effective approach in a Bayesian framework is that of probabilistic data association (PDA) [12, 22, 33] for a single target in clutter and that of joint probabilistic data association (JPDA) [10, 12, 22, 27, 33] for multiple targets in clutter.

Typically it is assumed that the number of targets is known and for each target, a tracks have been formed (initiated), so that the objective is that of track maintenance. In [21] such a problem has been considered using multiple sensors, PDA, and switching multiple models. The optimal solution (in the minimum mean-square error sense) to target state estimation given sensor measurements and absence of clutter, requires exponentially increasing (with time) computational complexity; therefore, one has to resort to suboptimal approximations. For the switching multiple model approach, the interacting multiple model (IMM) algorithm of [30] has been found to offer a good compromise between the computational and storage requirements and estimation accuracy [29]. In the presence of clutter, one has to account for measurements of uncertain origin (target or clutter?). Here too, in a Bayesian framework, one has to resort to approximations to reduce the computational complexity, resulting in the PDA filter [5, 12, 21, 22, 45]. In [21] the IMM algorithm has been combined with a PDA filter in a multiple sensor scenario to propose a combined IMM/MSPDAF (interacting multiple model/ multisensor probabilistic data association filter) algorithm. In [10, 22] multiple targets in clutter (but without using switching multiple models) have been considered using JPDA filter which, unlike the PDA filter, accounts for the interference from other targets. Various

versions of IMM/JPDA (interacting multiple model/ joint probabilistic data association) filters for multiple target tracking using switching multiple models may be found in [12, 23, 24, 25, 26]. While [24, 26] present uncoupled filters (i.e., assume that different target states are mutually independent conditioned on the past measurements), [12, 23, 25] present coupled filters (i.e., assume that there exists "share" measurements, yielding cross-covariances which reflect the correlation between the targets' state estimation errors). [23] presents an "exact" JPDA coupled filter for non-switching models using the framework of a linear descriptor system. For switching models, [24] presents IMM/JPDA uncoupled filter approximations. In [25], an IMM/JPDA coupled filtering algorithm has been presented where a simulation example resulted in fewer target swapping compared with uncoupled IMM/JPDA.

When two targets are "closely" spaced, they may give rise to a single detection due to the resolution limitations of the sensor. For instance, in radar ranging, returns from multiple targets could fall in the same range cell, resulting in one unresolved detection only [11, 28]. Standard tracking algorithms that ignore such a phenomenon can lead to poor performance in multiple target tracking [11, 28]. Despite its importance, prior work on tracking with unresolved measurements in general and modeling of resolution capability of a sensor in particular, is sparse. Prior work includes [11] and [28] and references therein. In [11] the resolution phenomena related to tracking have been treated on the basis of a grid of resolution cells "frozen" ([28]) in space. In [28] the resolution capability of a sensor is described in terms of a conditional probability of the event that two targets are unresolved, conditioned on the relative distance between the two targets in terms of the measured variables (range, azimuth, etc.). A simple Gaussian shape is assumed which captures the sensor behavior in a mathematically trackable way.

While [11] considers JPDA for data association, [28] exploits multiple hypothesis tracking (MHT). Under the Bayesian framework, there are two basic methods of measurement-to-track association in multiple target environments [12]: JPDA and multiple hypothesis tracking (MHT). The MHT filter associates feasible measurements to track and form multiple hypotheses for track extension. It is measurement-oriented approach whereas JPDA is a target-oriented approach. Moreover, MHT is a multiscan approach utilizing several scans of measurements to make data association decisions. MHT makes hard decisions where highly improbable hypotheses are pruned to reduce the computational burden. The JPDA filter is a single scan approach which does not make hard decisions; rather it updates a track with a weighed sum of the measurements which could have (reasonably) originated from the target in track.

In this chapter we propose to use sensor resolution modeling of [28] in conjunction with JPDA coupled filtering and interacting multiple model (IMM) approach (see e.g. [25] for tracking with resolved measurements). As noted in [27], IMMPDA filter is in general superior to IMM/MHT filter when the associated computational cost and performance are considered. Therefore, our emphasis will be on IMM/JPDA techniques. Neither [11] nor [28] consider multiple switching kinematic models for maneuvering targets; rather they are limited to single (nonswitching) kinematic models per target to achieve much enhanced performance.

This chapter is organized as follows. The problem formulation is presented in Sec. 6.2. The modeling scheme for the merged measurements is focused in Sec. 6.3. Sec. 6.4 describes the proposed IMM/JPDAM algorithm with coupled filtering. Simulation results using the proposed algorithm for a realistic problem are given in Sec. 6.5. Finally, Sec. 6.6 presents a discussion of the results and some conclusions.

## 6.2 Problem Formulation

Assume that there are a total of two targets with the target set denoted as $\mathcal{T}_2$. Assume that the target dynamics can be modeled by one of $n$ hypothesized models. The model set is denoted as $\mathcal{M}_n := \{1, \cdots, n\}$ and there are total $q$ sensors from which $q \times 2$, or less (if probability of target detection is less than one) or more (due to clutter), measurement vectors are generated at a time. For target $r$ ($r \in \mathcal{T}_2$), the event that model $j$ is in effect during the sampling period $(t_{k-1}, t_k]$ will be denoted by $M_k^j(r)$. Although two targets share a common model set, they may be in a different motion status from time to time.

### 6.2.1 Target Dynamics

For the $j$-th hypothesized model (mode), the state dynamics of target $r$ ($r \in \mathcal{T}_2$), are modeled as

$$x_k(r) = F_{k-1}^j(r)x_{k-1}(r) + G_{k-1}^j(r)v_{k-1}^j(r) \tag{6.1}$$

where $x_k(r)$ is the system state of target $r$ at $t_k$ and of dimension $n_x$ (assuming all targets share a common state space), $F_{k-1}^j(r)$ and $G_{k-1}^j(r)$ are the system matrices when model $j$ is in effect over the sampling period $(t_{k-1}, t_k]$ for target $r$. The process noise $v_{k-1}^j(r)$ is a zero-mean white Gaussian process with covariance matrix $Q_{k-1}^j$ (same for all targets). At the initial time $t_0$, the initial conditions for the system state of target $r$ under each model $j$ are assumed to be Gaussian random variables with the known mean $\bar{x}_0^j(r)$ and the known covariance $P_0^j(r)$. The probability of model $j$ at $t_0$, $\mu_0^j(r) = P[M_0^j(r)]$, is also assumed to be known. The switching from model $M_{k-1}^i(r)$ to model $M_k^j(r)$ is governed

by a finite-state stationary Markov chain (same for all targets) with known transition probabilities $p_{ij} = P[M_k^j(r)|M_{k-1}^i(r)]$. Henceforth, time $t_k$ will be denoted by $k$.

In coupled state estimation the states of two targets are estimated jointly [12]. To this end define the "global coupled" state

$$x_k := \text{col}\{x_k(1), x_k(2)\} \tag{6.2}$$

and the corresponding matrices/vectors $J := \text{col}\{j_1, j_2\}$ where $j_r \in \mathcal{M}_n$ is model $j$ for target $r$,

$$F_k^J := \text{block} - \text{diag}\{F_k^{j_1}(1), F_k^{j_2}(2)\} \tag{6.3}$$

$$G_k^J := \text{block} - \text{diag}\{G_k^{j_1}(1), G_k^{j_2}(2)\} \tag{6.4}$$

$$v_k^J := \text{col}\{v_k^{j_1}(1), v_k^{j_2}(2)\}. \tag{6.5}$$

Then we have the state equation for two targets as

$$x_k = F_{k-1}^J x_{k-1} + G_{k-1}^J v_{k-1}^J \tag{6.6}$$

where

$$E\{v_k^J v_k^{J'}\} = Q_k^J := \text{block} - \text{diag}\{Q_k^{j_1}, Q_k^{j_2}\}. \tag{6.7}$$

Define the global mode

$$M_k^J := \{M_k^{j_1}(1), M_k^{j_2}(2)\}. \tag{6.8}$$

The two targets are assumed to evolve independently of each other. Therefore, the transition probability for the global modes are given by

$$p_{IJ} := P[M_k^{j_1}(1), M_k^{j_2}(2) | M_{k-1}^{i_1}(1), M_{k-1}^{i_2}(2)] = \prod_{r=1}^{2} p_{i_r j_r}. \tag{6.9}$$

Similarly we have

$$\mu_0^J := P[M_0^{j_1}(1), M_0^{j_2}(2)] = \prod_{r=1}^{2} \mu_0^{j_r}(r). \tag{6.10}$$

### 6.2.2 Measurements

For the $j$-th hypothesized model (mode), measurements of target $r$ ($r \in \mathcal{T}_2$), are modeled, when resolved, as

$$z_k^l(r) = h^l(x_k(r)) + w_k^{j,l}(r) \quad \text{for} \;\; l = 1, \cdots, q \tag{6.11}$$

where $z_k^l(r)$ is the (true) measurement vector (i.e., due to target $r$) from sensor $l$ at $t_k$ and of dimension $n_{zl}$, and $h^l$ is the nonlinear transformation of $x_k(r)$ to $z_k^l(r)$ ($l = 1, \cdots, q$). The measurement noise $w_k^{j,l}(r)$ is a zero-mean white Gaussian process with covariance matrix $R_k^l$ (same for all targets) and is mutually uncorrelated with the process noise $v_{k-1}^j(r)$. Similarly define the global measurement vector at sensor $l$ as

$$z_k^l := \text{col}\{z_k^l(1), z_k^l(2)\} \tag{6.12}$$

and related vectors

$$h^l(x_k) = \text{col}\{h^l(x_k(1)), h^l(x_k(2))\}, \tag{6.13}$$

$$w_k^{J,l} := \text{col}\{w_k^{j_1,l}(1), w_k^{j_2,l}(2)\} \tag{6.14}$$

where

$$E\{w_k^{J,l} w_k^{J,l'}\} = R_k^l := \text{block} - \text{diag}\{R_k^l, R_k^l\}. \tag{6.15}$$

Then the measurement equation for two targets at sensor $l$ (assuming no clutter and perfect detections) is given by

$$z_k^l = h^l(x_k) + w_k^{J,l} \quad \text{for} \;\; l = 1, \cdots, q. \tag{6.16}$$

Regarding the measurements at sensor $l$, we follow the notations and definitions used in [26]. Note that, in general, at any time $k$, some measurements may be due to clutter and some due to the target(s). The measurement set (not yet validated) generated by sensor $l$ at time $k$ is denoted as $Z_k^l := \{z_k^{l(1)}, z_k^{l(2)}, \cdots, z_k^{l(m_l)}\}$ where $m_l$ is the number of measurements generated by sensor $l$ at time $k$. Variable $z_k^{l(i)}$ $(i = 1, \cdots, m_l)$ is the $i$th measurement within the set. The validated set of measurements of sensor $l$ at time $k$ will be denoted by $Y_k^l := \{y_k^{l(1)}, y_k^{l(2)}, \cdots, y_k^{l(\bar{m}_l)}\}$ where $\bar{m}_l$ is total number of validated measurement for sensor $l$ at time $k$. And $y_k^{l(i)} := z_k^{l(l_i)}$ where $1 \leq l_1 < l_2 < \cdots < l_{\bar{m}_l} \leq m_l$ when $\bar{m}_l \neq 0$. The cumulative set of validated measurements from sensor $l$ up to time $k$ is denoted as $Y^{k(l)} := \{Y_1^l, Y_2^l, \cdots, Y_k^l\}$. The cumulative set of validated measurements from all sensors up to time $k$ is denoted as $Z^k := \{Y^{k(1)}, Y^{k(2)}, \cdots, Y^{k(q)}\}$ where $q$ is the number of sensors.

Assuming that there are possibly unresolved measurements from two targets (i.e., measurement association with two targets simultaneously), any measurement therefore is either associated with a target, two targets, or caused by clutter. Our goal is to find

the state estimate

$$\hat{x}_{k|k} := E\{x_k|Z^k\} \tag{6.17}$$

and the associated error covariance matrix

$$P_{k|k} := E\{[x_k - \hat{x}_{k|k}][x_k - \hat{x}_{k|k}]'|Z^k\} \tag{6.18}$$

where $x'_k$ denotes the transpose of $x_k$. Included in the above formulation is state estimates of individual targets.

## 6.3 Modeling for the Merged Measurements

### 6.3.1 Modeling Assumptions

In an earlier work Trunk [55, 56] assumed that the (one-dimensional) location of an unresolved detection has a pdf (probability density function) given by the convolution of *a*) a uniform density between the predicted target positions, and *b*) the Gaussian density of the measurement error. Later Chang and Bar-Shalom [11] presented an unresolved measurement modeling approach based on the following assumptions: *c*) merging of two measurements occurs if the noisy measurements (rather than the predicted measurement) fall in the same resolution cell, *d*) the elements of each (multidimensional) measurement are uncorrelated, and *e*) the relative strengths of the signal should be taken into account (the merged measurement will be closer to the stronger signal). In [28] Koch and Keuk assumed that, in case of a resolution conflict, *f*) the detection probabilities for resolved targets $P_D$ and the detection probabilities for unresolved targets $P_D^a$ may be

different and $g$) the detection process and the production of measurements are statistically independent. Based upon earlier research the present approach assumes as the following:

- Only two targets were considered - more than two targets also can be easily implemented by defining additional association events (hypotheses).
- The merged measurements arise when two targets are so close that the noisy measurements (rather than the predicted measurement) fall in the same resolution cell due to a lack of resolution of each sensors.
- The relative strengths $\beta_k$ (see (6.20)) of the signal is a small measurement noise assumed to be Gaussian with 0.5 mean and (very) small variance ($0 < \beta_k < 1$), however, for our simulation example, we set $\beta_k$=0.5 for all $k$.
- False detections (clutter) not related to the targets are equally distributed in the validation region and their number is assumed to be Poisson distributed.
- The detection probabilities for resolved targets $P_D$ and unresolved targets $P_D^a$ are the same.

### 6.3.2 Measurement Model

Due to a lack of resolution at the sensor a detection may correspond to both targets. Let $s_k^l(r)$ denote the signal power from target $r$ at sensor $l$ at time $k$. For unresolved targets at time $k$, the measurement equation for two targets at sensor $l$ (assuming no clutter and perfect detections with merged measurements of targets $r_1$ and $r_2$, ($r_1, r_2 \in$

$\mathcal{T}_2$)), are modeled as (we follow [11])

$$\begin{aligned} z_k^{l,a} &= \beta_k z_k^l(1) + (1-\beta_k) z_k^l(2) \\ &= h^{l,a}(x_k) + w_k^{l,a} \quad \text{for } \ l = 1, \cdots, q \end{aligned} \tag{6.19}$$

where

$$\beta_k = \frac{s_k^l(1)}{s_k^l(1) + s_k^l(2)}, \quad 0 < \beta_k < 1, \tag{6.20}$$

$$h^{l,a}(x_k) = \beta_k h^l(x_k(1)) + (1-\beta_k) h^l(x_k(2)), \tag{6.21}$$

$$w_k^{l,a} = \beta_k w_k^l(1) + (1-\beta_k) w_k^l(2), \tag{6.22}$$

$$E\{w_k^{l,a} w_k^{l,a'}\} = R_k^{l,a}. \tag{6.23}$$

Define the measurement distance between two targets

$$\begin{aligned} z_k^{l,d} &= z_k^l(1) - z_k^l(2) \\ &= h^{l,d}(x_k) + w_k^{l,d} \quad \text{for } \ l = 1, \cdots, q \end{aligned} \tag{6.24}$$

where

$$h^{l,d}(x_k) = h^l(x_k(1)) - h^l(x_k(2)), \tag{6.25}$$

$$w_k^{l,d} = w_k^l(1) - w_k^l(2), \tag{6.26}$$

$$E\{w_k^{l,d} w_k^{l,d'}\} = R_k^{l,d}. \tag{6.27}$$

Note that the corresponding error covariance $R_k^{l,d}$ in (6.27) does not depend on the time $k$ or mode $J$ but depend only on the sensor resolution. Henceforth, the error covariance $R_k^{l,d}$ will be denoted by $R^{l,d}$.

### 6.3.3 Sensor Resolution Model

Let $\mathcal{A}$ denote the event that both targets are unresolved. For sensor $l$, a related conditional probability of unresolved targets $P_k^{l,a}$ can be introduced as (we follow [28])

$$\begin{aligned} P_k^{l,a} &:= P(\mathcal{A}|x_k) = \exp\left\{-\frac{1}{2}\left[h^l(x_k(1)) - h^l(x_k(2))\right]^T R^{l,d^{-1}}\left[h^l(x_k(1)) - h^l(x_k(2))\right]\right\} \\ &= \left|2\pi R^{l,d}\right|^{1/2}\mathcal{N}\left(0; h^{l,d}(x_k), R^{l,d}\right). \end{aligned} \tag{6.28}$$

The positive definite $n_{zl} \times n_{zl}$ matrix $R^{l,d}$ is determined by corresponding sensor resolution (measurement accuracy). Using the Gaussian-like structure of $P_k^{l,a}$, the mathematics involved can be simplified [28]. In the simulation examples presented later, we illustrate our model by a 2-D radar measuring range and azimuth as well as an infrared measuring azimuth and elevation angle. In this case, the range resolution is essentially determined by the length of the emitted pulse, the angular resolution is limited by the beam width. Following [28] we assume that the different measurement resolutions are independent of each other so that $R^{l,d}$ is diagonal.

As an example, in 2-D radar case, following [28] we assume that the different measurement resolution is statistically independent from each other. The conditional probability of merged measurement detected from unresolved target $P_k^{l,a}$ will depend on their relative measurement distance $z_k^{l,d}$ but the exact (ideal) analytical description will be very difficult. However, the above algorithm intuitively captures the underlying reality

as follows: $P_k^{l,a}$ will be one as $z_k^{l,d} \to 0$ and will remain large for small $z_k^{l,d}$'s. On the other hand, for large $z_k^{l,d}$'s, $P_k^{l,a}$ will be zero and the transient region will be narrow. Hence $P_k^{l,a}$ can be modeled as a Gaussian-like function of $z_k^{l,d}$ introducing a width to approximately describe the resolution capability of the sensor. According to the above discussion we assume [28]

$$P_k^{l,a} = P(\mathcal{A}|z_k^{l_1,d}, z_k^{l_2,d}) = \exp\left[-\frac{1}{2}\left\{\left(\frac{z_k^{l_1,d}}{\alpha^{l_1}}\right)^2 + \left(\frac{z_k^{l_2,d}}{\alpha^{l_2}}\right)^2\right\}\right] \tag{6.29}$$

where $z_k^{l_i,d} := z_k^{l(i)}(1) - z_k^{l(i)}(2)$ ($i$=1,2) is the distance between possibly unresolved targets in terms of $i$-th measurement vector (such as range or azimuth in 2-D radar) and $\alpha^{l_i}$ (not function of time $k$) is the corresponding resolution of sensor $l$. Eqn. (6.29) reflects the fact that the resolution capability of a sensor does not only depend upon the sensor features but also on the signal processing applied and the random target fluctuations [28].

### 6.4 IMM/JPDAM Coupled Filtering Algorithm

We now modify the IMM/JPDA coupled filtering algorithm of [25] to apply to the coupled system (6.1)-(6.10); it will be called IMM/JPDAMCF (CF stands for coupled filter). The approach of [25], in turn, is based on the approaches of [12], [21], and [26]. We confine our attention to the case of 2 sensors. As the IMM/JPDACF algorithm is well-explained in [25] and [12, Sec. 6.2], and, for the possibly unresolved measurements, the JPDAM algorithm is well-explained in [12, Sec. 6.4], the MHT algorithm is well-explained in [28], we will only briefly outline the basic steps in 'one cycle' (i.e., processing needed to update for a new set of measurements) of the IMM/JPDAM coupled filter.

**Assumed available**: Given the state estimate $\hat{x}^J_{k-1|k-1} := E\{x_{k-1}|M^J_{k-1}, Z^{k-1}\}$, the associated covariance $P^J_{k-1|k-1}$, and the conditional mode probability $\mu^J_{k-1} := P[M^J_{k-1}|Z^{k-1}]$ at time $k-1$ for each mode $J \in \bar{\mathcal{M}}_n := \mathcal{M}_n \times \mathcal{M}_n$.

***Step 1. Interaction - mixing of the estimate from the previous time*** ($\forall J \in \bar{\mathcal{M}}_n$):

predicted mode probability:

$$\mu^{J-}_k := P[M^J_k|Z^{k-1}] = \sum_I p_{IJ}\mu^I_{k-1}. \tag{6.30}$$

mixing probability:

$$\mu^{I|J} := P[M^I_{k-1}|M^J_k, Z^{k-1}] = p_{IJ}\mu^I_{k-1}/\mu^{J-}_k. \tag{6.31}$$

mixed estimate:

$$\hat{x}^{0J}_{k-1|k-1} := E\left\{x_{k-1}|M^J_k, Z^{k-1}\right\} = \sum_I \hat{x}^I_{k-1|k-1}\mu^{I|J}. \tag{6.32}$$

covariance of the mixed estimate:

$$\begin{aligned} P^{0J}_{k-1|k-1} &:= E\left\{[x_{k-1} - \hat{x}^{0J}_{k-1|k-1}][x_{k-1} - \hat{x}^{0J}_{k-1|k-1}]'|M^J_k, Z^{k-1}\right\} \\ &= \sum_I \left\{P^I_{k-1|k-1} + [\hat{x}^I_{k-1|k-1} - \hat{x}^{0J}_{k-1|k-1}][\hat{x}^I_{k-1|k-1} - \hat{x}^{0J}_{k-1|k-1}]'\right\}\mu^{I|J}. \end{aligned} \tag{6.33}$$

***Step 2. Predicted state and measurements for sensor 1*** ($\forall J \in \bar{\mathcal{M}}_n$):

state prediction:

$$\hat{x}^J_{k|k-1} := E\left\{x_k|M^J_k, Z^{k-1}\right\} := F^J_{k-1}\hat{x}^{0J}_{k-1|k-1}. \tag{6.34}$$

state prediction error covariance:

$$\begin{aligned} P^J_{k|k-1} &:= E\left\{[x_k - \hat{x}^J_{k|k-1}][x_k - \hat{x}^J_{k|k-1}]'|M^J_k, Z^{k-1}\right\} \\ &= F^J_{k-1}P^{0J}_{k-1|k-1}F^{J'}_{k-1} + G^J_{k-1}Q^J_{k-1}G^{J'}_{k-1}. \end{aligned} \tag{6.35}$$

***For two resolved targets***: Using (6.11) and (6.34), the global mode-conditioned predicted measurement for sensor 1 is

$$\hat{z}^{J,1}_k := h^1(\hat{x}^J_{k|k-1}). \tag{6.36}$$

Using the linearized (6.16), the covariance of the mode-conditioned residual

$$\nu^{J,1(I)}_k := z^{1(I)}_k - \hat{z}^{J,1}_k, \quad \text{where } z^{1(I)}_k := \text{col}\{z^{1(i_1)}_k, z^{1(i_2)}_k\} \tag{6.37}$$

is given by

$$S^{J,1}_k := E\left\{\nu^{J,1(I)}_k \nu^{J,1(I)'}_k|M^J_k, Z^{k-1}\right\} = H^{J,1}_k P^J_{k|k-1}H^{J,1'}_k + R^1_k \tag{6.38}$$

$$S^{j_1,1}_k := E\left\{\nu^{j_1,1(I)}_k \nu^{j_1,1(I)'}_k|M^J_k, Z^{k-1}\right\} = H^{j_1,1}_k P^J_{k|k-1}H^{j_1,1'}_k + R^1_k \tag{6.39}$$

$$S^{j_2,1}_k := E\left\{\nu^{j_2,1(I)}_k \nu^{j_2,1(I)'}_k|M^J_k, Z^{k-1}\right\} = H^{j_2,1}_k P^J_{k|k-1}H^{j_2,1'}_k + R^1_k. \tag{6.40}$$

$H_k^{J,1} := \text{block} - \text{diag}\{H_k^{j_1,1}, H_k^{j_2,1}\}$ is the first order derivative (Jacobian matrix) of $h^1(.)$ evaluated at the state prediction $\hat{x}_{k|k-1}^J$.

***For unresolved targets***: Using (6.19),(6.24), and (6.34), the global mode-conditioned predicted measurement for sensor 1 is

$$\hat{z}_k^{J,1,a} := h^{1,a}(\hat{x}_{k|k-1}^J). \tag{6.41}$$

Introduce a pseudo-measurement (as in [28])

$$\hat{z}_k^{J,1,d} := h^{1,d}(\hat{x}_{k|k-1}^J). \tag{6.42}$$

Using the linearization around $\hat{x}_{k|k-1}^J$, the covariance of the mode-conditioned residual ($\hat{z}_k^{J,1,d}$ set to zero [28])

$$\nu_k^{J,1,a} := \begin{bmatrix} z_k^{1,a} \\ 0 \end{bmatrix} - \begin{bmatrix} \hat{z}_k^{J,1,a} \\ \hat{z}_k^{J,1,d} \end{bmatrix} \tag{6.43}$$

is given by

$$\begin{aligned} S_k^{J,1,a} &:= E\left\{\nu_k^{J,1,a}\nu_k^{J,1,a'}|M_k^J, Z^{k-1}\right\} \\ &= \begin{bmatrix} H_k^{J,1,a} \\ H_k^{J,1,d} \end{bmatrix} P_{k|k-1}^J \begin{bmatrix} H_k^{J,1,a'} & H_k^{J,1,d'} \end{bmatrix} + \begin{bmatrix} R_k^{1,a} & 0 \\ 0 & R^{1,d} \end{bmatrix} \end{aligned} \tag{6.44}$$

where $H_k^{J,1,a} = [\beta_k H^{j_1,1} \quad (1-\beta_k)H^{j_2,1}]$ and $H_k^{J,1,d} = [H_k^{j_1,1} \quad -H_k^{j_2,1}]$. In (6.43) the measurement residual $\nu_k^{J,1,a}$ is the formulation of both, the mean position and the distance of the targets. Therefore, an assumed resolution conflict results in a fictitious measurement

of $z_k^{1,d}$ with value 0 and error covariance $R^{1,d}$ [28].

***Step 3. Measurement validation for sensor 1 ($\forall J \in \bar{\mathcal{M}}_n$)***:

There is uncertainty regarding the measurements' origins. Therefore, first perform measurement validation for each target $r$ ($r \in \mathcal{T}_2$) separately. For target $r$, the validation region is taken to be the same for all models, i.e., as the largest of them.

***For two resolved targets***: Let $S_k^{j_r,1}(r)$ denote the $n_{z1} \times n_{z1}$ submatrix of $S_k^{J,1}$ including the rows and columns of the letter numbered as $(r-1)n_{z1}+m, m = 1, 2$. That is, $S_k^{j_r,1}(r)$ based on the information relevant to target $r$ only. Let $\hat{z}_k^{j_r,1}(r)$ denote the $n_{z1} \times 1$ subcolumn of $\hat{z}_k^{J,1}$ including the rows of the letter numbered as $(r-1)n_{z1}+m, m = 1, 2$. That is, $\hat{z}_k^{j_r,1}(r)$ is the mode-conditioned predicted measurement of target $r$ for sensor 1. Let ($|A| = \det(A)$)

$$\bar{j}_r := \arg \left\{ \max_{j_r \in \mathcal{M}_n} \left| S_k^{j_r,1}(r) \right| \right\}. \tag{6.45}$$

Then measurement $z_k^{1(i)}$ ($i$=1,2,$\cdots$,$m_l$) is validated if and only if

$$[z_k^{1(i)} - \hat{z}_k^{\bar{j}_r,1}(r)]'[S_k^{\bar{j}_r,1}(r)]^{-1}[z_k^{1(i)} - \hat{z}_k^{\bar{j}_r,1}(r)] < \gamma \tag{6.46}$$

where $\gamma$ is an appropriate threshold. The volume of the validation region with the threshold $\gamma$ is [12, Sec. 2.3.2]

$$V_k^1(r) := c_{n_{z1}} \gamma^{n_{z1}/2} |S_k^{\bar{j}_r,1}(r)|^{1/2}. \tag{6.47}$$

After performing the validation for each target separately, the volume of validation region for the whole target set is approximated by $V_k^1 = \sum_{r=1}^{2} V_k^1(r)$.

***For unresolved targets***: For unresolved targets at time $k$, $S_k^{J,1,a}$ is a $n_{z1} \times n_{z1}$ matrix

and is based on the information relevant to the merged targets. Let $\hat{z}_k^{J,1,a}$ denote the $n_{z1} \times 1$ column matrix. That is, $\hat{z}_k^{J,1,a}$ is the mode-conditioned predicted measurement of the merged targets for sensor 1. Let

$$\bar{J}_a := \arg \left\{ \max_{j \in \mathcal{M}_n} \left| S_k^{J,1,a} \right| \right\}. \tag{6.48}$$

Then measurement for unresolved targets $z_k^{1(i)}$ ($i$=1,2,$\cdots$,$m_l$) is validated if and only if

$$[z_k^{1(i)} - \hat{z}_k^{\bar{J}_a,1,a}]' [S_k^{\bar{J}_a,1,a}]^{-1} [z_k^{1(i)} - \hat{z}_k^{\bar{J}_a,1,a}] < \gamma \tag{6.49}$$

where $\gamma$ is an appropriate threshold. The volume of the validation region with the threshold $\gamma$ is

$$V_k^1(a) := c_{n_{z1}} \gamma^{n_{z1}/2} |S_k^{\bar{J}_a,1,a}|^{1/2}. \tag{6.50}$$

After performing the validation for each target separately, the volume of validation region for the whole target set is $V_k^1 = V_k^1(a)$.

***Step 4. State estimation with validated measurement from sensor 1 ($\forall J \in \bar{\mathcal{M}}_n$)***:

From among all the raw measurements from sensor 1 at time $k$, i.e.,

$$Z_k^1 := \{z_k^{1(1)}, z_k^{1(2)}, \cdots, z_k^{1(m_1)}\}, \tag{6.51}$$

define the set of validated measurement for sensor $l$ at time $k$ as

$$Y_k^1 := \{y_k^{1(1)}, y_k^{1(2)}, \cdots, y_k^{1(\bar{m}_1)}\} \tag{6.52}$$

where $\bar{m}_1$ is total number of validated measurement for sensor 1 at time $k$. And

$$y_k^{1(i)} := z_k^{1(l_i)} \tag{6.53}$$

where $1 \leq l_1 < l_2 < \cdots < l_{\bar{m}_l} \leq m_1$ when $\bar{m}_1 \neq 0$. We now consider joint probabilistic data association across targets with possibly unresolved measurements following [12],[25].

A marginal association event $\theta_{ir}$ is said to be effective at time $k$ when the validated measurement $y_k^{1(i)}$ is associated with (i.e., originated from) target $r$ ($r = 0, 1, 2$ where $r = 0$ means that the measurement is caused by clutter). Assuming that two targets can be possibly unresolved and detected as a single target, a joint association event $\Theta$ is effective when a set of marginal events $\{\theta_{ir}\}$ holds true simultaneously. That is, $\Theta = \bigcap_{i=1}^{\bar{m}_1} \theta_{ir_i}$ where $r_i$ is the index of the target to which measurement $y_k^{1(i)}$ is associated in the event under consideration. Define the validation matrix (as in [12])

$$\Omega = [\omega_{ir}] \quad i = 1, \cdots, \bar{m}_1, \quad \text{for} \;\; r = 0, 1, 2 \tag{6.54}$$

where $\omega_{ir} = 1$ if the measurement $i$ lies in the validation gate of target $r$, else it is zero. A joint association event $\Theta$ is represented by the event matrix

$$\hat{\Omega}(\Theta) = [\hat{\omega}_{ir}(\Theta)] \quad i = 1, \cdots, \bar{m}_1, \quad \text{for} \;\; r = 0, 1, 2 \tag{6.55}$$

where $\hat{\omega}_{ir}(\Theta) = 1$ if $\theta_{ir} \subset \Theta$, and $\hat{\omega}_{ir}(\Theta) = 0$ otherwise. A feasible association event is one ($\Sigma_{r=0}^{2} \hat{\omega}_{ir}(\Theta) = 1$) when a measurement originated from only one source (i.e., from a target or clutter) or two ($\Sigma_{r=0}^{2} \hat{\omega}_{ir}(\Theta) = 2$) when a measurement originated from two sources (i.e., from two targets). The detection indicator where at most one measurement

can be originated from a target

$$\delta_r(\Theta) = \Sigma_{i=1}^{\bar{m}_1} \hat{\omega}_{ir}(\Theta) \leq 1 \quad \text{for} \;\; r = 1, 2. \tag{6.56}$$

The feasible association joint events $\Theta$ are mutually exclusive and exhaustive.

Following the definitions in [12], define the binary measurement association indicator

$$\tau_i(\Theta) = \Sigma_{r=1}^{2} \hat{\omega}_{ir}(\Theta) \leq 2 \quad \text{for} \;\; i = 1, \cdots, \bar{m}_1 \tag{6.57}$$

to indicate whether the validated measurement $y_k^{1(i)}$ is associated with target(s) in event $\Theta$. Further, the number of false (unassociated) measurements in event $\Theta$ is

$$\phi(\Theta) = \Sigma_{i=1}^{\bar{m}_1} [1 - \min(1, \tau_i(\Theta))]. \tag{6.58}$$

A resolution indicator, $\rho(\Theta)$, is defined to be one when $\tau_i(\Theta) \leq 1$ and zero otherwise. We will limit our discussion to nonparametric JPDA [12].

The likelihood function for the global mode $J$ can be evaluated as

$$\Lambda_k^{J,1} := p\left(Y_k^1 | M_k^J, Z^{k-1}\right) = \sum_{\Theta} p\left(Y_k^1 | \Theta, M_k^J, Z^{k-1}\right) P[\Theta | M_k^J, Z^{k-1}] \tag{6.59}$$

where the conditioning on $\bar{m}_1$ is implicit in the event $\Theta$. The second term (apriori joint association probabilities) in the last line of (6.59), *when targets are merged*, can be evaluated as [28]

$$P[\Theta | M_k^J, Z^{k-1}] \;\; = \;\; \int P[\Theta | x_k, M_k^J, Z^{k-1}] p(x_k | M_k^J, Z^{k-1}) dx_k$$

$$= \int D(\Theta) P[\mathcal{A}|x_k] p(x_k|M_k^J, Z^{k-1}) dx_k \tag{6.60}$$
$$= D(\Theta) \int P[\mathcal{A}|x_k] \mathcal{N}\left(x_k; \hat{x}_{k|k-1}^J, P_{k|k-1}^J\right) dx_k$$

where

$$D(\Theta) = \frac{\phi(\Theta)!\epsilon}{\bar{m}_1!} \prod_{r=1}^{2} (P_D)^{\delta_r(\Theta)} (1 - P_D)^{1-\delta_r(\Theta)}, \tag{6.61}$$

$P_D$ is the detection probability at sensor 1 (assumed to be the same for all targets) and $\epsilon > 0$ is a "diffuse" prior (for nonparametric modeling of clutter) whose exact value is irrelevant. Define

$$P_k^{J,1,a} = \int P(\mathcal{A}|x_k) \mathcal{N}\left(x_k; \hat{x}_{k|k-1}^J, P_{k|k-1}^J\right) dx_k \tag{6.62}$$

$$= \left|2\pi R^{1,d}\right|^{1/2} \mathcal{N}\left(0; \left[H_k^{j_1,1} - H_k^{j_2,1}\right] \hat{x}_{k|k-1}^J, \left[\begin{array}{cc} H_k^{j_1,1} & -H_k^{j_2,1} \end{array}\right] P_{k|k-1}^{J,1} \left[\begin{array}{c} H_k^{j_1,1'} \\ -H_k^{j_2,1'} \end{array}\right] + R^{1,d}\right).$$

The last line of (6.62) can be obtained by substituting (6.34) into the first line of (6.62). For details, see [28] and **Appendix B**. Then we have

$$P[\Theta|M_k^J, Z^{k-1}] = \begin{cases} D(\Theta)(1 - P_k^{J,1,a}) & \text{for resolved target(s)} \\ D(\Theta) P_k^{J,1,a} & \text{for merged targets.} \end{cases} \tag{6.63}$$

Unlike [26], we do not assume that the states of the targets (including the modes) conditioned on the past observations are mutually independent. Then we have

$$p\left(Y_k^1|\Theta, M_k^J, Z^{k-1}\right) = V_1^{-\phi(\Theta)} p\left(\tilde{Y}_k^1(\Theta)|M_k^J, Z^{k-1}\right) \tag{6.64}$$

where $\tilde{Y}_k^1(\Theta) \subset Y_k^1$ is a subset of the validated measurements $Y_k^1$, consisting of the measurements associated with the targets as specified by $\Theta$. The number of measurements in $\tilde{Y}_k^1(\Theta)$ is equal $\bar{m}_1 - \phi(\Theta)$ where $\phi(\Theta)$ is the number of false alarms.

Define a $\bar{m}_1 \times [\bar{m}_1 - \phi(\Theta)]$ matrix $\underline{\hat{\Omega}}(\Theta)$ as a submatrix of $\hat{\Omega}(\Theta)$ obtained by deleting the first column and all null columns of $\hat{\Omega}(\Theta)$. Then for a given $\Theta$, we have a measurement vector $\tilde{Y}_k^1(\Theta)$ of dimension $(\Sigma_{i=1}^{\bar{m}_1} \min[1, \tau_i(\Theta)])n_{z1}$ given by

$$\tilde{Y}_k^1(\Theta) = (I_{n_{z1}} \otimes \underline{\hat{\Omega}}'(\Theta))\text{col}\{y_k^{1(i)}, i = 1, 2, \cdots, \bar{m}_1\} \tag{6.65}$$

where we stack up all target-associate validated measurements in $\Theta$ in ascending order of targets, $I_n$ is the $n \times n$ identity matrix, and the symbol $\otimes$ denotes the Kronecker product. Define a $[(\bar{m}_1 - \phi(\Theta))z_{z1}] \times [2n_x]$ matrix $H_k^{J,1}(\Theta)$ as a submatrix of $H_k^{J,1}$ obtained by deleting all $i$-th block rows of $H_k^{J,1}$ for which $\delta_i(\Theta) = 0$. That is, we have modified $H_k^{J,1}$ to keep only the block elements associated with target-associated measurements in $\Theta$.

To further simplify the equation for $\tilde{Y}_k^1(\Theta)$, one has to consider all the possible joint association events $\Theta$. Define a related set of mutually exclusive and exhaustive data interpretations $\Psi$ as follows (here we follow [28])

- $\Psi_{11}$: Both targets were resolved and detected ($\phi(\Theta) = \bar{m}_1 - 2$),
- $\Psi_{10}$: Both targets were resolved and only target 1 was detected ($\phi(\Theta) = \bar{m}_1 - 1, \delta_1(\Theta) = 1, \delta_2(\Theta) = 0$),
- $\Psi_{01}$: Both targets were resolved and only target 2 was detected ($\phi(\Theta) = \bar{m}_1 - 1, \delta_1(\Theta) = 0, \delta_2(\Theta) = 1$),

- $\Psi_1$: Both targets were detected but merged as a single measurement ($\phi(\Theta) = \bar{m}_1 - 1, \delta_1(\Theta) = 1, \delta_2(\Theta) = 1$),

- $\Psi_0$: No target was detected ($\phi(\Theta) = \bar{m}_1$).

It then follows that the linearized measurement equation for $\tilde{Y}_k^1(\Theta)$ is given by

$$\tilde{Y}_k^1(\Theta) = \begin{cases} H_k^{J,1}(\Theta)x_k + w_k^{J,1}, & \text{for } \Theta \in \Psi_{11} \\ H_k^{j_1,1}(\Theta)x_k + w_k^{j_1,1}(1), & \text{for } \Theta \in \Psi_{10} \\ H_k^{j_2,1}(\Theta)x_k + w_k^{j_2,1}(2), & \text{for } \Theta \in \Psi_{01} \\ \begin{bmatrix} H_k^{J,1,a}(\Theta) \\ H_k^{J,1,d}(\Theta) \end{bmatrix} x_k + \begin{bmatrix} w_k^{J,1,a} \\ w_k^{J,1,d} \end{bmatrix}, & \text{for } \Theta \in \Psi_1. \end{cases} \tag{6.66}$$

Conditioned on the joint association event $\Theta$ and mode $J$, the "coupled" innovation is given by

$$\nu_k^{J,1}(\Theta) = \begin{cases} \tilde{Y}_k^1(\Theta) - \hat{z}_k^{J,1}(\Theta), & \text{for } \Theta \in \Psi_{11} \\ \tilde{Y}_k^1(\Theta) - \hat{z}_k^{j_1,1}(\Theta), & \text{for } \Theta \in \Psi_{10} \\ \tilde{Y}_k^1(\Theta) - \hat{z}_k^{j_2,1}(\Theta), & \text{for } \Theta \in \Psi_{01} \\ \tilde{Y}_k^1(\Theta) - \begin{bmatrix} \hat{z}_k^{J,1,a}(\Theta) \\ \hat{z}_k^{J,1,d}(\Theta) \end{bmatrix}, & \text{for } \Theta \in \Psi_1, \\ 0, & \text{for } \Theta \in \Psi_0 \end{cases} \tag{6.67}$$

where $\hat{z}_k^{J,1}(\Theta)$ ($\hat{z}_k^{J,1,a}(\Theta)$, $\hat{z}_k^{J,1,d}(\Theta)$) are subvector(s) of $\hat{z}_k^{J,1}$ ($\hat{z}_k^{J,1,a}$, $\hat{z}_k^{J,1,d}$) obtained by deleting all $i$-th block rows ($n_{z1} \times 1$) of $\hat{z}_k^{J,1}$ ($\hat{z}_k^{J,1,a}$, $\hat{z}_k^{J,1,d}$) for which $\delta_i(\Theta) = 0$. The covariance of mode-conditioned residual conditioned on the joint association event $\Theta$ is

given by

$$S_k^{J,1}(\Theta) = H_k^{J,1}(\Theta) P_{k|k-1}^J H_k^{J,1\prime}(\Theta) + R_k^{J,1}, \quad \text{for} \ \ \Theta \in \Psi_{11}$$

$$S_k^{j_1,1}(\Theta) = H_k^{j_1,1}(\Theta) P_{k|k-1}^{j_1}(1) H_k^{j_1,1\prime}(\Theta) + R_k^{j_1,1}, \quad \text{for} \ \ \Theta \in \Psi_{10}$$

$$S_k^{j_2,1}(\Theta) = H_k^{j_2,1}(\Theta) P_{k|k-1}^{j_2}(2) H_k^{j_2,1\prime}(\Theta) + R_k^{j_2,1}, \quad \text{for} \ \ \Theta \in \Psi_{01}$$

$$S_k^{J,1,a}(\Theta) = \begin{bmatrix} H_k^{J,1,a}(\Theta) \\ H_k^{J,1,d}(\Theta) \end{bmatrix} P_{k|k-1}^J \begin{bmatrix} H_k^{J,1,a\prime}(\Theta) & H_k^{J,1,d\prime}(\Theta) \end{bmatrix} + \begin{bmatrix} R_k^{J,1,a} & 0 \\ 0 & R^{1,d} \end{bmatrix}, \quad \text{for} \ \ \Theta \in \Psi_1, \tag{6.68}$$

where $P_{k|k-1}^{j_1}(1)$ and $P_{k|k-1}^{j_2}(2)$ are diagonal submatrices of $P_{k|k-1}^J$.

There are a total of $(\bar{m}_1 + 1) \times (\bar{m}_1 + 1)$ possible association hypotheses, each of which has an association probability. Then we have

$$p\left(Y_k^1 | \Theta, M_k^J, Z^{k-1}\right) \begin{cases} V_1^{2-\bar{m}_1} p(\tilde{Y}_k^1(\Theta) | M_k^J, Z^{k-1}), & \text{for} \ \ \Theta \in \Psi_{11} \\ V_1^{1-\bar{m}_1} p(\tilde{Y}_k^1(\Theta) | M_k^J, Z^{k-1}), & \text{for} \ \ \Theta \in \Psi_{10} \\ V_1^{1-\bar{m}_1} p(\tilde{Y}_k^1(\Theta) | M_k^J, Z^{k-1}), & \text{for} \ \ \Theta \in \Psi_{01} \\ V_1^{1-\bar{m}_1} p(\tilde{Y}_k^1(\Theta) | M_k^J, Z^{k-1}), & \text{for} \ \ \Theta \in \Psi_1 \\ V_1^{-\bar{m}_1}, & \text{for} \ \ \Theta \in \Psi_0 \end{cases} \tag{6.69}$$

where the conditional pdf (probability density function) of the validated measurements $\tilde{Y}_k^1(\Theta)$ given their origins (specified by $\Theta$) and the global mode $J$, is given by

$$p\left(\tilde{Y}_k^1(\Theta)|M_k^J, Z^{k-1}\right) = \begin{cases} \mathcal{N}\left(\tilde{Y}_k^1(\Theta); \hat{z}_k^{J,1}(\Theta), S_k^{J,1}(\Theta)\right), & \text{for } \Theta \in \Psi_{11} \\ \mathcal{N}\left(\tilde{Y}_k^1(\Theta); \hat{z}_k^{j_1,1}(\Theta), S_k^{j_1,1}(\Theta)\right), & \text{for } \Theta \in \Psi_{10} \\ \mathcal{N}\left(\tilde{Y}_k^1(\Theta); \hat{z}_k^{j_2,1}(\Theta), S_k^{j_2,1}(\Theta)\right), & \text{for } \Theta \in \Psi_{01} \\ \mathcal{N}\left(\tilde{Y}_k^1(\Theta); \begin{bmatrix} \hat{z}_k^{J,1,a}(\Theta) \\ \hat{z}_k^{J,1,d}(\Theta) \end{bmatrix}, S_k^{J,1,a}(\Theta)\right), & \text{for } \Theta \in \Psi_1 \end{cases} \tag{6.70}$$

The probability of the joint association event $\Theta$ given that global mode $J$ is effective from time $k$-1 through $k$ is

$$\begin{aligned} \beta_k^{J,1}(\Theta) &:= P[\Theta|M_k^J, Z^{k-1}, Y_k^1] \\ &= \frac{1}{c} p(Y_k^1|\Theta, M_k^J, Z^{k-1}) P[\Theta|M_k^J, Z^{k-1}] \end{aligned} \tag{6.71}$$

where the first term can be calculated from (6.64)-(6.68), the second term from (6.61)-(6.63), and $c$ is a normalization constant such that

$$\Sigma_\Theta P[\Theta|M_k^J, Z^{k-1}, Y_k^1] = 1. \tag{6.72}$$

Using $\hat{x}_{k|k-1}^J$ (from 6.34) and its covariance $P_{k|k-1}^J$ (from 6.35), one computes the partial update $\hat{x}_{k|k}^J$ and its covariance $P_{k|k}^J$ following the standard PDAF [12], except that the global state is conditioned on $\Theta$, not the marginal events $\theta_{ir}$; details follow.

Kalman gain:

$$W_k^{J,1}(\Theta) = \begin{cases} P_{k|k-1}^J H_k^{J,1}(\Theta)' \left[S_k^{J,1}(\Theta)\right]^{-1}, & \text{for } \Theta \in \Psi_{11} \\ P_{k|k-1}^{j_1} H_k^{j_1,1}(\Theta)' \left[S_k^{j_1,1}(\Theta)\right]^{-1}, & \text{for } \Theta \in \Psi_{10} \\ P_{k|k-1}^{j_2} H_k^{j_2,1}(\Theta)' \left[S_k^{j_2,1}(\Theta)\right]^{-1}, & \text{for } \Theta \in \Psi_{01} \\ P_{k|k-1}^J \begin{bmatrix} H_k^{J,1,a}(\Theta) \\ H_k^{J,1,d}(\Theta) \end{bmatrix}' \left[S_k^{J,1,a}(\Theta)\right]^{-1}, & \text{for } \Theta \in \Psi_1 \end{cases} \tag{6.73}$$

Partial update of the state estimate:

$$\begin{aligned} \hat{x}_{k|k}^{J,1}(\Theta) &:= E\left\{x_k | \Theta, M_k^J, Z^{k-1}, Y_k^1\right\} \\ &= \begin{cases} \hat{x}_{k|k-1}^J + W_k^{J,1}(\Theta)\nu_k^{J,1}(\Theta), & \text{for } \Theta \in \Psi_{11} \\ \hat{x}_{k|k-1}^J + \begin{bmatrix} W_k^{J,1}(\Theta)\nu_k^{J,1}(\Theta) \\ 0_{n_x \times 1} \end{bmatrix}, & \text{for } \Theta \in \Psi_{10} \\ \hat{x}_{k|k-1}^J + \begin{bmatrix} 0_{n_x \times 1} \\ W_k^{J,1}(\Theta)\nu_k^{J,1}(\Theta) \end{bmatrix}, & \text{for } \Theta \in \Psi_{01} \\ \hat{x}_{k|k-1}^J + W_k^{J,1}(\Theta)\nu_k^{J,1}(\Theta), & \text{for } \Theta \in \Psi_1 \\ \hat{x}_{k|k-1}^J, & \text{for } \Theta \in \Psi_0. \end{cases} \end{aligned} \tag{6.74}$$

Mode-conditioned update of the state estimate:

$$\hat{x}_{k|k}^{J,1} := E\left\{x_k | M_k^J, Z^{k-1}, Y_k^1\right\} = \sum_{\Theta} \beta_k^{J,1}(\Theta)\hat{x}_{k|k}^{J,1}(\Theta) \tag{6.75}$$

Covariance of $\hat{x}^{J,1}_{k|k}(\Theta)$:

$$P^{J,1}_{k|k}(\Theta) = \begin{cases} P^J_{k|k-1} - W^{J,1}_k(\Theta) S^{J,1}_k(\Theta) W^{J,1}_k(\Theta)', & \text{for } \Theta \in \Psi_{11} \\ P^J_{k|k-1} - \begin{bmatrix} W^{J,1}_k(\Theta) S^{j_1,1}_k(\Theta) W^{J,1}_k(\Theta)' & 0_{n_x \times n_x} \\ 0_{n_x \times n_x} & 0_{n_x \times n_x} \end{bmatrix}, & \text{for } \Theta \in \Psi_{10} \\ P^J_{k|k-1} - \begin{bmatrix} 0_{n_x \times n_x} & 0_{n_x \times n_x} \\ 0_{n_x \times n_x} & W^{J,1}_k(\Theta) S^{j_2,1}_k(\Theta) W^{J,1}_k(\Theta)' \end{bmatrix}, & \text{for } \Theta \in \Psi_{01} \\ P^J_{k|k-1} - W^{J,1}_k(\Theta) S^{J,1,a}_k(\Theta) W^{J,1}_k(\Theta)', & \text{for } \Theta \in \Psi_1 \\ P^J_{k|k-1}, & \text{for } \Theta \in \Psi_0. \end{cases} \tag{6.76}$$

Covariance of $\hat{x}^J_{k|k}$: $P^{J,1}_{k|k} := E\left\{(x_k - \hat{x}^{J,1}_{k|k})(x_k - \hat{x}^{J,1}_{k|k})' | Y^1_k, Z^{k-1}, M^J_k\right\}$

$$\begin{aligned} &= P^J_{k|k-1} - \sum_{\Theta \in \Psi_{10}} \beta^{J,1}_k(\Theta) W^{J_1}_k(\Theta) S^{J_1,1}_k(\Theta) W^{J_1}_k(\Theta)' - \sum_{\Theta \in \Psi_{01}} \beta^{J,1}_k(\Theta) W^{J_2}_k(\Theta) S^{J_2,1}_k(\Theta) W^{J_2}_k(\Theta)' \\ &\quad - \sum_{\Theta \in \Psi_{11},\Psi_1} \beta^{J,1}_k(\Theta) W^{J,1}_k(\Theta) S^{J,1}_k(\Theta) W^{J,1}_k(\Theta)' + \sum_{\Theta \in \Psi_{11},\Psi_1} \beta^{J,1}_k(\Theta) W^{J,1}_k(\Theta) \nu^{J,1}_k(\Theta) \nu^{J,1}_k(\Theta)' W^{J,1}_k(\Theta)' \\ &\quad + \sum_{\Theta \in \Psi_{10}} \beta^{J,1}_k(\Theta) W^{J_1}_k(\Theta) \nu^{J_1,1}_k(\Theta) \nu^{J_1,1}_k(\Theta)' W^{J_1}_k(\Theta)' \\ &\quad + \sum_{\Theta \in \Psi_{01}} \beta^{J,1}_k(\Theta) W^{J_2}_k(\Theta) \nu^{J_2,1}_k(\Theta) \nu^{J_2,1}_k(\Theta)' W^{J_2}_k(\Theta)' \\ &\quad - \left[\sum_{\Theta \in \Psi_{10}} \beta^{J,1}_k(\Theta) W^{J_1}_k(\Theta) \nu^{J_1,1}_k(\Theta)'\right] \left[\sum_{\Theta \in \Psi_{10}} \beta^{J,1}_k(\Theta) W^{J_1}_k(\Theta) \nu^{J_1,1}_k(\Theta)'\right]' \\ &\quad - \left[\sum_{\Theta \in \Psi_{01}} \beta^{J,1}_k(\Theta) W^{J_2}_k(\Theta) \nu^{J_2,1}_k(\Theta)'\right] \left[\sum_{\Theta \in \Psi_{01}} \beta^{J,1}_k(\Theta) W^{J_2}_k(\Theta) \nu^{J_2,1}_k(\Theta)'\right]' \\ &\quad - \left[\sum_{\Theta \in \Psi_{11},\Psi_1} \beta^{J,1}_k(\Theta) W^{J,1}_k(\Theta) \nu^{J,1}_k(\Theta)'\right] \left[\sum_{\Theta \in \Psi_{11},\Psi_1} \beta^{J,1}_k(\Theta) W^{J,1}_k(\Theta) \nu^{J,1}_k(\Theta)'\right]' \end{aligned} \tag{6.77}$$

where

$$W_k^{J_1}(\Theta) = \begin{bmatrix} W_k^{J,1}(\Theta) & 0_{n_x \times n_{z_l}} \\ 0_{n_x \times n_{z_l}} & 0_{n_x \times n_{z_l}} \end{bmatrix}, \quad W_k^{J_2}(\Theta) = \begin{bmatrix} 0_{n_x \times n_{z_l}} & 0_{n_x \times n_{z_l}} \\ 0_{n_x \times n_{z_l}} & W_k^{J,1}(\Theta) \end{bmatrix},$$

$$S_k^{J_1}(\Theta) = \begin{bmatrix} S_k^{j_1}(\Theta) & 0_{n_{z_l} \times n_{z_l}} \\ 0_{n_{z_l} \times n_{z_l}} & 0_{n_{z_l} \times n_{z_l}} \end{bmatrix}, \quad S_k^{J_2}(\Theta) = \begin{bmatrix} 0_{n_{z_l} \times n_{z_l}} & 0_{n_{z_l} \times n_{z_l}} \\ 0_{n_{z_l} \times n_{z_l}} & S_k^{j_2,1}(\Theta) \end{bmatrix}, \tag{6.78}$$

$$\nu_k^{J_1}(\Theta) = \begin{bmatrix} \nu_k^{J,1}(\Theta) \\ 0_{n_{z_l} \times 1} \end{bmatrix}, \quad \nu_k^{J_2}(\Theta) = \begin{bmatrix} 0_{n_{z_l} \times 1} \\ \nu_k^{J,1}(\Theta) \end{bmatrix}.$$

Eqn. (6.77) follows in a manner similar to eqn. (3.4.2-10) in [12]. For details, see [12].

***Step 5. The mode-conditioned predicted measurements for sensor 2*** ($\forall J \in \bar{\mathcal{M}}_n$):

***For two resolved targets***: The "predicted" measurement for sensor 2 is given by

$$\hat{z}_k^{J,2} := h^2(\hat{x}_{k|k}^{J,1}). \tag{6.79}$$

The covariance of the global mode-conditioned residual $\nu_k^{J,2(I)} := z_k^{2(I)} - \hat{z}_k^{J,2}$, where $z_k^{2(I)} := \text{col}\{z_k^{2(i_1)}, z_k^{2(i_2)}\}$, is given by

$$S_k^{J,2} := E\{\nu_k^{J,2(I)} \nu_k^{J,2(I)'} | M_k^J, Z^{k-1}, Y_k^1\} := H_k^{J,2} P_{k|k}^{J,1} H_k^{J,2'} + R_k^2. \tag{6.80}$$

where $H_k^{J,2} := \text{block} - \text{diag}\{H_k^{j_1,2}, H_k^{j_2,2}\}$ is the first order derivative (Jacobian matrix) of $h^2(.)$ evaluated at the state prediction $\hat{x}_{k|k}^{J,1}$.

***For unresolved targets***: The "predicted" measurement for sensor 2 is given by

$$\hat{z}_k^{J,2,a} := h^{2,a}(\hat{x}_{k|k}^{J,1}). \tag{6.81}$$

Define

$$\hat{z}_k^{J,2,d} := h^{2,d}(\hat{x}_{k|k}^{J,1}). \tag{6.82}$$

Using the linearized (6.19) and (6.24), the covariance of the mode-conditioned residual

$$\nu_k^{J,2,a} := \begin{bmatrix} z_k^{J,2,a} \\ 0 \end{bmatrix} - \begin{bmatrix} \hat{z}_k^{J,2,a} \\ \hat{z}_k^{J,2,d} \end{bmatrix} \tag{6.83}$$

is given by

$$\begin{aligned} S_k^{J,2,a} &:= E\left\{ \nu_k^{J,2,a} \nu_k^{J,2,a'} | M_k^J, Z^{k-1}, Y_k^1 \right\} \\ &= \begin{bmatrix} H_k^{J,2,a} \\ H_k^{J,2,d} \end{bmatrix} P_{k|k}^{J,1} \begin{bmatrix} H_k^{J,2,a'} & H_k^{J,2,d'} \end{bmatrix} + \begin{bmatrix} R_k^{2,a} & 0 \\ 0 & R^{2,d} \end{bmatrix} \end{aligned} \tag{6.84}$$

where $H_k^{J,2,a} = [\beta_k H^{j_1,2} \;\; (1-\beta_k) H^{j_2,2}]$ ($H_k^{J,2,d} = [H^{j_1,2} \;\; -H^{j_2,2}]$) is the first order derivative (Jacobian matrix) of $h^{2,a}(.)$ ($h^{2,d}(.)$) evaluated at the state prediction $\hat{x}_{k|k}^{J,1}$.

***Step 6. Measurement validation measurements for sensor 2 ($\forall J \in \bar{\mathcal{M}}_n$)***:

This is similar to Step 3 where we replace $S_k^{J,1}$ with $S_k^{J,2}$, $z_k^{1(i)}$ with $z_k^{2(i)}$, $m_1$ with $m_2$, $V_k^1(r)$ with $V_k^2(r)$, and $V_k^1$ with $V_k^2$. Details are similar to that in Step 3, hence omitted.

***Step 7. Update with validated measurements for sensor 2 ($\forall J \in \bar{\mathcal{M}}_n$)***:

This is similar to Step 4. Using the validated measurements obtained from Step 6 and starting from $\hat{x}^{J,1}_{k|k}$ and $P^{J,1}_{k|k}$, one computes the final updates $\hat{x}^{J}_{k|k}$ and $P^{J}_{k|k}$, and the likelihood

$$\begin{aligned}\Lambda^{J,2}_k &:= p\left[Y^2_k, |M^J_k, Z^{k-1}, Y^1_k\right] \\ &= \sum_{\Theta} p\left[Y^2_k|\Theta, M^J_k, Z^{k-1}, Y^1_k\right] P\{\Theta|M^J_k, Z^{k-1}, Y^1_k\}. \end{aligned} \tag{6.85}$$

Details are similar to that in Step 4, hence omitted.

***Step 8. Update of mode probabilities*** ($\forall j \in \mathcal{M}_n$, $\forall r \in \mathcal{T}_2$):

$$\mu^J_k := P[M^J_k|Z^k] = \frac{1}{c}\mu^{J-}_k \Lambda^{J,1}_k \Lambda^{J,2}_k \tag{6.86}$$

where $c$ is a normalization constant such that $\Sigma_J \mu^J_k = 1$. For individual targets we have

$$\mu^{j_1}_k(1) := P[M^{j_1}_k(1)|Z^k] = \sum_{j_2=1}^{n} \mu^{j_1,j_2}_k, \quad \mu^{j_2}_k(2) = \sum_{j_1=1}^{n} \mu^{j_1,j_2}_k \tag{6.87}$$

with $J = (j_1, j_2)$ in (6.86).

***Step 9. Combination of the mode-conditioned estimates*** ($\forall r \in \mathcal{T}_2$):

The final global state estimate update at time $k$ is given by

$$\hat{x}_{k|k} = \sum\nolimits_J \hat{x}^J_{k|k} \mu^J_k \tag{6.88}$$

and its covariance is given by

$$P_{k|k} = \sum\nolimits_J \left\{ P^J_{k|k} + \left[\hat{x}^J_{k|k} - \hat{x}_{k|k}\right]\left[\hat{x}^J_{k|k} - \hat{x}_{k|k}\right]' \right\} \mu^J_k. \tag{6.89}$$

The state estimate $\hat{x}_{k|k}(r)$ for target $r$ is the $n_x$-subvector of $\hat{x}_{k|k}$ consisting of elements $(r-1)n_x + m$, $m = 1, 2$.

***Remark 1.*** In the above algorithm we used sequential updating of the state estimates with measurements (one sensor at a time - see Steps 4 and 7) as in [21] and [26]. This approach is suboptimal but leads to computational savings as one does not have to simultaneously associate measurements across sensors (as in [46], [48], [53]). In Step 4 we are interested in $E\{x_k|M_k^J, Z_k^{k-1}, Y_k^1\}$ which is decomposed as in (6.79) conditioned on $\Theta$'s; Measurements $Y_k^2$ are not considered in this step. If one were to seek $E\{x_k|M_k^J, Z_k^{k-1}, Y_k^1, Y_k^2\}$, then we would have to follow the approach of [46]-[53] by picking all possible association events across sensors also.

***Remark 2.*** Compared to the uncoupled filtering of [26] where the equations are formulated conditioned on marginal association events $\theta_{ir}$, here we have conditioning on joint association events $\Theta$ for couples filtering. Eqn. (6.70) does not decompose into the product of marginal probabilities as in [26].

***Remark 3.*** Partition the set of all $\Theta$s into disjoint sets $\bar{\Theta}_i$s such that $\bar{\Theta}_i := \{\Theta|\delta_r(\Theta) = \delta_r(\tilde{\Theta})\ \forall r,\ \tilde{\Theta} \in \bar{\Theta}_i\}$ where $i = 1, 2, \cdots, K$. For instance, for $N$=2, we have $K$=5 with $\bar{\Theta}_1$=all $\Theta$s in which there are two validated measurements associated with two targets, $\bar{\Theta}_2$=all $\Theta$s in which one validated measurements associated with target 1 and none with target 2, $\bar{\Theta}_3$=all $\Theta$s in which one validated measurements associated with target 2 and none with target 1, $\bar{\Theta}_4$=all $\Theta$s in which one validated unresolved measurement associated with two targets, $\bar{\Theta}_5$=all $\Theta$s in which none of the validated measurements are associated with any target. It is then easily seen that $W_k^{J,1}(\Theta)$, $H_k^{J,1}(\Theta)$, $S_k^{J,1}(\Theta)$ and $\beta_k^{J,1}(\Theta)$ in Step 4, all are invariant for $\Theta \in \bar{\Theta}_i$. This fact can be used to simplify computations in (6.77). Similar comments apply to Step 7.

***Remark 4.*** If one substitutes (6.65) into (6.66), then one obtains a linear descriptor system type of equation such as (12) in [23]. Therefore, the standard state-space system framework used in this dissertation and the linear descriptor system framework used in [23] are equivalent (except that [23] uses non-switching models whereas we use Markovian switching models).

## 6.5 Simulation Example

The following example of tracking two highly maneuvering targets in clutter is patterned after [25].

***The True Trajectory***: We consider the same scenario as that in [25] except for a linear shift in the x and y-directions in the trajectory of target 1 to achieve merged target with a long-term duration. Target 1 starts at location [21689+$d_x$ 10840+$d_y$ 40] with $d_x$=-3040m and $d_y$=5500m in Cartesian coordinates in meters. The initial velocity (in m/s) is [-8.3 -399.9 0] and the target stays at constant altitude with a constant speed of 400 m/s. Its trajectory is:

- a straight line with constant velocity between 0 and 27s,
- a coordinated turn (0.15 rad/s) with constant acceleration of 60 m/$s^2$ between 27 and 42s,
- a straight line with constant velocity between 42 and 47s,
- a coordinated turn (0.1 rad/s) with constant acceleration of 40 m/$s^2$ between 47 and 65s,
- a straight line with constant velocity between 65 and 87s.

Target 2 starts at location [30000 -3040 40] in Cartesian coordinates in meters. The initial velocity (in m/s) is [-382 157 0] and the target stays at constant altitude with a constant speed of 413 m/s. Its trajectory is:

- a straight line with constant velocity between 0 and 44s,
- a coordinated turn (0.075 rad/s) with constant acceleration of 30 m/$s^2$ between 44 and 59s,
- a straight line with constant velocity between 59 and 87s.

***The Target Motion Models***: These are exactly as in [25]. In each mode the target dynamics are modelled in Cartesian coordinates as $x_k(r) = F(r)x_{k-1}(r) + G(r)v_{k-1}(r)$ where the state of the target is position, velocity, and acceleration in each of the 3 Cartesian coordinates ($x, y$, and $z$). Model 1 for Nearly constant velocity model with zero mean perturbation in acceleration; Model 2 for Wiener process acceleration (nearly constant acceleration motion); Model 3 for Wiener process acceleration (model with large acceleration increments, for the onset and termination of maneuvers). The details regarding these models have been described in previous chapters and identical. The initial model probabilities for two targets are identical: $\mu_0^1 = 0.8$, $\mu_0^2 = 0.1$ and $\mu_0^3 = 0.1$. The mode switching probability matrix for two targets is also identical and is as in previous chapters.

***The Sensors***: Two sensors (we assume collocation, and time synchronization of observations, etc.) are used to obtain the measurements. The measurements from sensor $l$ for model $j$ are $z_k^l = h^l(x_k) + w_k^l$, $l = 1, 2$, reflecting range and azimuth angle for sensor 1 (radar) and azimuth and elevation angles for sensor 2 (infrared). The range, azimuth, and elevation angle transformations would be given by $r = (x^2 + y^2 + z^2)^{1/2}$, $a = \tan^{-1}[y/x]$,

$e = \tan^{-1}[z/(x^2+y^2)^{1/2}]$, respectively. The measurement noise $w_k^l$ for sensor $l$ is assumed to be zero-mean white Gaussian with known covariances $R^1 = \text{diag}[q_r, q_{a1}] = \text{diag}[400\text{m}^2, 49\text{mrad}^2]$ with $q_r$ and $q_{a1}$ denoting the variances for the radar range and azimuth measurement noises, respectively, and $R^2 = \text{diag}[q_{a2}, q_e] = \text{diag}[4\text{mrad}^2, 4\text{mrad}^2]$ with $q_{a2}$ and $q_e$ denoting the variances for the infrared sensor azimuth and elevation measurement noises, respectively. Resolutions of both sensors are selected after from [28] (twice of the standard deviations for the corresponding sensor measurement noise): a range resolution of sensor 1 $\alpha^R = 2\times\sqrt{q_r} = 40$m, a angular resolution of sensor 1 $\alpha^{\phi_1} = 2\times\sqrt{q_{a1}} = 14\times10^{-3}$rad, a angular resolution of sensor 2 $\alpha^{\phi_2} = 2\times\sqrt{q_{a2}} = 4\times10^{-3}$rad and a elevation angle resolution of sensor 2 $\alpha^{\theta} = 2\times\sqrt{q_e} = 4\times10^{-3}$rad. The noise for merged measurements $w_k^{J,l,a}$ for sensor $l$ is assumed to be the same with resolved measurement noise $w_k^l$ for sensor $l$. The measurement distance noise $w_k^{l,d}$ for sensor $l$ is assumed to be zero-mean white Gaussian with known covariances $R^{1,d} = \text{diag}[\alpha^R, \alpha^{\phi_1}]$, and $R^{2,d} = \text{diag}[\alpha^{\phi_2}, \alpha^{\theta}]$. To generate the true target trajectories, following (6.28), given the measurements of the two targets at a given sensor, the targets are unresolved with the conditional probability $P_k^{l,a}$ (6.29) and they are merged into one by the linear combination model (6.19) with the signal strength ratio $\beta_k = 0.5$ for all time $k$. (The tracking algorithm does not have this knowledge of how $P_k^{l,a}$ is used to generate data.) Both sensors are assumed to be located at the coordinate system origin. The sampling interval was $T$=1s and it was assumed that the probability of detection $P_D$=0.997 for both sensors.

***The Clutter***: For generating false measurements in simulations, the clutter was assumed to be Poisson distributed with expected number of $\lambda_1 = 20\times10^{-6}$/m-mrad for sensor 1 and $\lambda_2 = 2\times10^{-4}/\text{mrad}^2$ for sensor 2. These statistics were used for generating

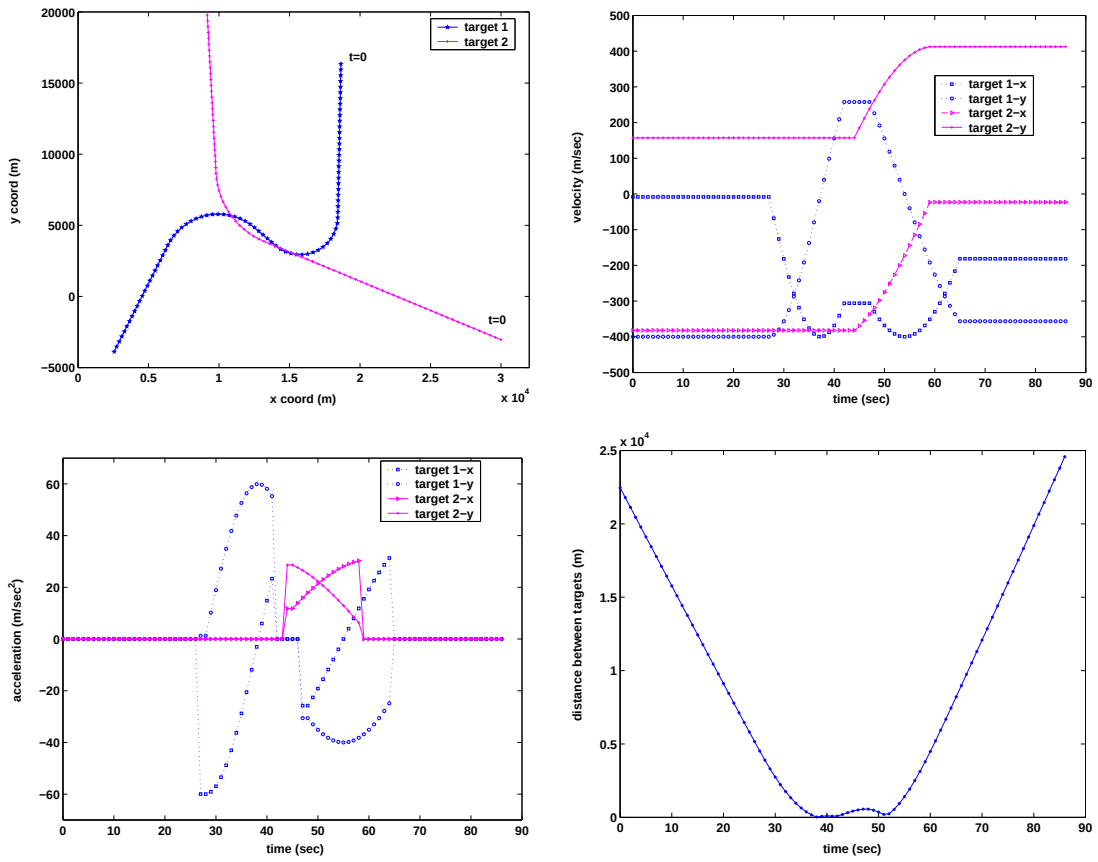


Figure 6.1: The true trajectories of the maneuvering targets (read left to right, top to bottom): (a) Position in $xy$ plane, (b) $x$ and $y$ velocities, (c) $x$ and $y$ accelerations, (d) distance between the targets.

the clutter in all simulations. However, a nonparametric clutter model was used for implementing all the algorithms for target tracking.

***Other Parameters***: The gates for setting up the validation regions for both the sensors were based on the threshold $\gamma$=16 corresponding to a gate probability $P_G$=0.9997.

***Simulation Results***: The results were obtained from 1000 Monte Carlo runs. Fig. 6.1(a)-(d) shows the true trajectory of the two targets and the distance between the two

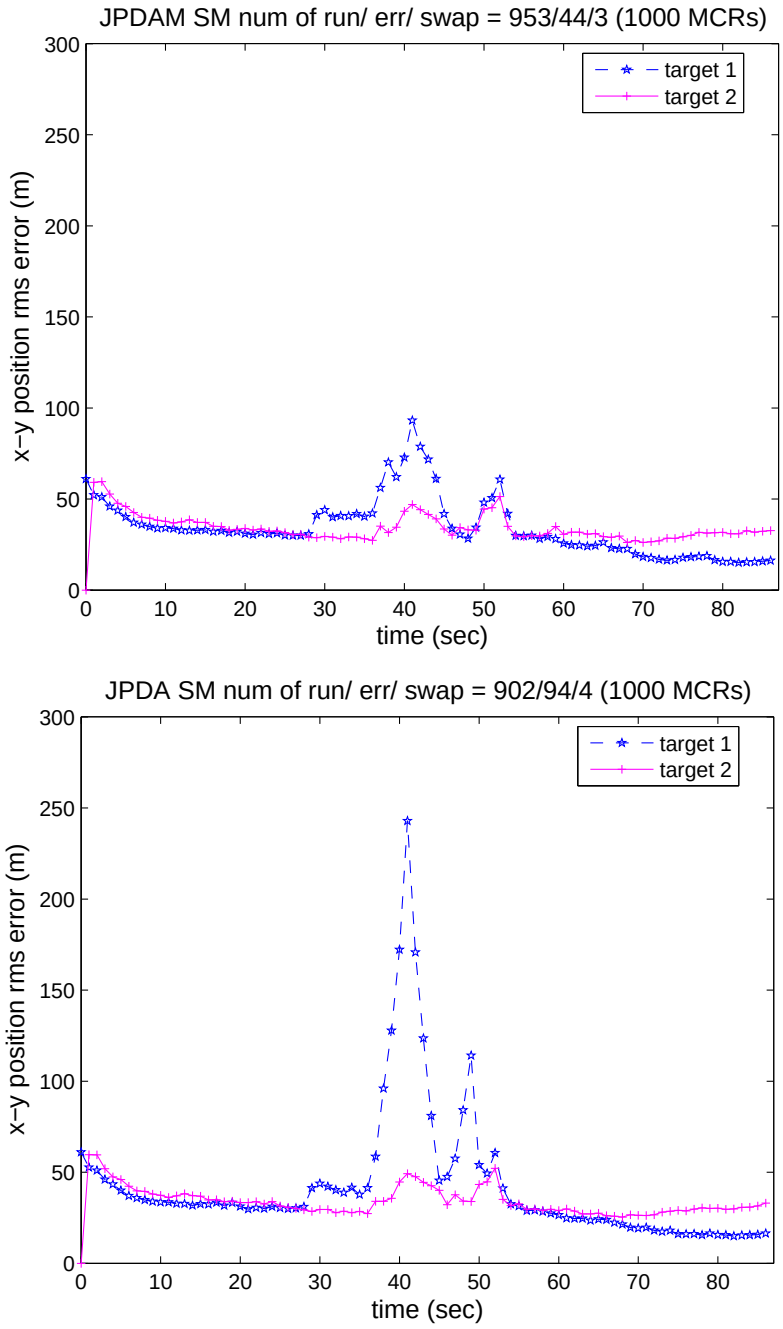


Figure 6.2: Performance (RMSE in position) of the proposed IMM/JPDAMCF and the IMM/JPDACF of [25] based on successful runs (read left to right): (a) proposed IMM/JPDAMCF, (b) standard IMM/JPDACF [25].

| index | proposed IMM/JPDAMCF | standard IMM/JPDACF [25] |
|---|---|---|
| No. of lost tracks | 44/1000 | 94/1000 |
| No. of swapped tracks | 3/1000 | 4/1000 |
| No. of successful tracks | 953/1000 | 902/1000 |

Table 6.1: Simulation results summery based on 1000 runs

targets as a function of time. The two targets start out far apart, move close to each other from 38 to 42 seconds, and then move apart again. Fig. 6.2(a) shows the results of the proposed IMM/JPDAMCF based on 953 successful runs (target swap occurred in 3 runs with 44 track failures). Fig. 6.2(b) shows the standard IMM/JPDACF [25] (the merged target case was not considered) based on 902 successful runs (target swap occurred in 4 runs with 94 track failures) in terms of the RMSE in position. Table 1 shows the number of successful runs (excluding target swapping) for the two approaches IMM/JPDAMCF and IMM/JPDACF. It is seen from Table 1 and Figs. 6.1 and 6.2 that the proposed IMM/JPDAMCF is better than the standard IMM/JPDACF [25] in performance especially in terms of the track estimation accuracy and the loss of tracks.

To assess the computational requirements of the two approaches, we computed the CPU time needed to execute 87 time steps in each run (averaged 100 Monte Carlo runs excluding data/clutter generation) in MATLAB 6.5 on a 2.8 GHz (Mobile) Pentium 4 operating under Windows XP (professional). The standard IMM/JPDACF needs 7.6178 secs (for all 87 time steps) compared to 14.3848 secs required by proposed IMM/JPDAMCF. Thus with a 88.8% increase in computational cost, it is seen that the proposed algorithm can significantly improve the accuracy of track estimation during the periods when targets are temporarily move in close formation.

## 6.6 Conclusions

We investigated on two targets which temporarily move in close formation, giving rise to a single detection due to the resolution limitations of the sensor. We proposed a noble IMM/JPDAMCF algorithm for state estimation for two highly maneuvering targets in clutter. While a past IMM/JPDACF approach [25] applies only to resolved measurements, our proposed approach has extended the multisensor approach of [25] to deal with possibly existing merged measurements arrived from sensors to the central processor.

The proposed algorithm was illustrated via a simulation example and it outperformed a standard IMM/JPDACF algorithm [25] which does not consider the possibility of the data association to the merged measurements, in terms of RMS position error, the number of track losses, and target swappings. The proposed IMM/JPDAMCF resulted in a 25% fewer target swappings and a 54% track losses compared with the standard MM/JPDACF [25]. The improvement in accuracy and track loss comes at the expense of an increase (88.8%) in the computational cost. This improvement in accuracy is seen in our simulation example only during the periods when targets are temporarily move in close formation and gives rise to a single detection due to the resolution limitations of the sensor.

# Chapter 7

# Conclusions and Future Work

## 7.1 Conclusions

In this dissertation, we developed several noble algorithms for maneuvering target tracking in the presence of clutter using multiple sensors. Our main concern was to investigate solutions to the target tracking problems which require the simultaneous completion of two tasks: *estimation* and *data association*. There are many different approaches to both estimation and data association and these are generally the distinguishing features that give rise to different tracking algorithms.

In Chapter 3, a suboptimal filtering algorithm for tracking a highly maneuvering target in a cluttered environment using multiple sensors was proposed. We developed a noble algorithm "simultaneous measurement update using IMMPDA filtering". The existing IMM filtering algorithm and PDA technique were combined with simultaneous measurement update algorithm in our proposed algorithm. This algorithm provides significant improvement over an existing IMMPDA filtering algorithm with sequential sensor processing, because it considers all association hypotheses coupled across multisensor while in the sequential updating considers the separate hypothesis for each sensor. This improvement in accuracy was remarkable especially during the periods following the onset of the target maneuvers. The improvement in accuracy comes at the expense of a slight increase in the computational cost.

In a multisensor central tracking system, asynchronous (delayed) measurements arise due to communication network delays, varying preprocessing times at the sensor platforms and possibly lack of sampling time synchronization among sensor platforms. A state augmented approach was combined with simultaneous measurement update technique to deal with asynchronous (delayed) measurements problem in Chapter 4. In this chapter, we investigated "fixed-but-unknown" delay between sensor network and developed a noble algorithm "simultaneous measurement update using AS-IMMPDA filtering". Compared with an existing IMMPDA filtering algorithm with the assumption of synchronous (no delay) measurements sensor processing, the proposed algorithm achieves considerable improvement (especially in the case of larger delays) in the accuracy of track estimation. Using the proposed AS-IMMPDA algorithm, the smoothed estimate (lag = 1) can be easily obtained from the augmented state estimate and it shows better performance (in terms of RMS error) than the filtered estimate.

In practice, in a multisensor central target tracking system, one can possibly have situations where measurements from the same target do not arrive in correct time order. This OOSM can occur due to communication network delays, varying preprocessing times at the sensor platforms, and lack of sampling time synchronization among sensor platforms. In Chapter 5, the AS-IMMPDA algorithm proposed in Chapter 4 is then extended to deal with "fixed-and-known" delay and possible OOSM between sensor network. Compared with an existing IMMPDA filtering algorithm without dealing with possibly existing OOSM (which assumes only "fixed-and-known" delay), the proposed algorithm achieves considerable improvement in the accuracy of track estimation as the probability of OOSM arrival increases.

In Chapter 6, we considered the problem of tracking multiple maneuvering targets which temporarily operate in close formation in clutter. When multiple targets are close, there might be a single detection originating from more than one target, yielding unresolved (merged) measurements due to a sensor's inherent resolution limitation. The existing IMM/JPDA can not handle data association on the merged measurements. Combining the existing IMM algorithm with JPDAM technique, we presented a noble IMM/JPDAM algorithm for multisensor tracking of multiple maneuvering targets in clutter with possibly merged measurements. The algorithm is illustrated via a simulation example compared with an existing IMM/JPDA filtering algorithm which does not deal with the merged measurements data association hypotheses. The proposed algorithm achieved significant improvement in the accuracy of track estimation especially during target merging period, and caused fewer track losses.

## 7.2 Suggested Future Work

### 7.2.1 Unresolved Measurements with Simultaneous Measurement Update

In Chapters 3, it has been shown that the IMMPDA filtering algorithm with simultaneous measurement update achieves significant improvement in the accuracy of track estimation compared with an existing IMMPDA filtering algorithm with sequential sensor processing. As we have presented proposed IMM/JPDAMCF algorithm to deal with unresolved measurements by sequential updating approach in Chapter 5, we can apply the extension of our IMM/JPDAMCF algorithm by combining with simultaneous measurement update algorithm. This integration of existing IMM/JPDAM algorithms

and simultaneous measurement update algorithms will lead to better performance than earlier algorithms designed for tracking multiple maneuvering targets.

### 7.2.2 Track Initialization

Until now we have limited our investigation to track maintenance in this dissertation (i.e., the initial state of each target is assumed to have been already obtained). In practice, the track formation needs to be done before all the algorithms in this dissertation can be applied. Measurement-to-measurement association is the core requirement for track formation in the presence of measurement uncertainty. Some existing target track formation approaches can be found in [12, 33]. MHT has been recognized as the theoretically best approach to the multitarget tracking problem, yet it requires a considerable amount of computation and memory. Therefore, in the past it was considered unaffordable because of the high computational requirements. Now interest is renewed because of the continuous advances in computer technology and algorithm design. Since MHT approach, unlike IMM/JPDA, is a measurement-oriented approach and considers the track initialization as well, integration of existing track formation algorithms and our track maintenance algorithms is a good challenge for future research topics.

# Bibliography


[1] N. Wax,"Signal-to-noise improvement and the statistics of track populations," *J. of Applied Physics*, Vol. 26, pp. 586-595, May 1955.

[2] R.E. Kalman,"A new approach to linear filtering and prediction problems," *Journal of Basic Engineering*, pp. 35-46, March 1960.

[3] R.W. Sittler,"An optimal data association problem in surveillance theory," *IEEE Trans. Military Electronics*, Vol. MIL-8, pp. 125-139, April 1964.

[4] A.J. Jaffer and Y. Bar-Shalom, "On optimal tracking in multiple target environments," *Proceedings of the Third Symposium on Non-Linear Estimation Theory and Its Applications*,San Diego, CA, pp. 112-117, Sept. 11-13, 1972.

[5] Y. Bar-Shalom and E. Tse, "Tracking in a cluttered environment with probabilistic data association," *Automatica*, Vol. 11, pp. 451-460, Sept. 1975.

[6] R.A. Singer and J.J. Stein, "An optimal tracking filter for processing sensor data of imprecisely determined origin in surveillance system," *Proceedings of the 1971 IEEE Conference on Decision and Control*, Miami Beach, FL, pp. 171-175, Dec. 1971.

[7] R.A. Singer, R.G. Sea, and K.B. Housewright, "Derivation and evaluation of improved tracking filters for use in multi-target environments," *IEEE Transactions on Information Theory*, IT-20, pp. 423-432, July 1974.

[8] D.B. Reid, "A multiple hyphothesis filter for tracking multiple targes in a cluttered environment," *Lockheed Missiles and Space Company Report*, No. LMSC, D-560254, Spet. 1977.

[9] D.B. Reid, "An algorithm for tracking multiple targets," *IEEE Transaction on Automatic Control*, Vol. AC-24, pp. 843-854, Dec. 1979.

[10] T.E. Fortmann, Y. Bar-Shalom, and M. Scheffe "Sonar tracking of multiple targets using joint probabilistic data association", *IEEE Journal of Oceanic Engineering*, Vol. OE-8, pp. 173-184, July 1983.

[11] Kuo-Chu Chang and Y. Bar-Shalom, "Joint probabilistic data association for multitarget tracking with possibly unresolved measurements and maneuvers", *IEEE Transaction on Automatic Control*, Vol. 29, No.7, pp. 585-594, July 1984.

[12] Y. Bar-Shalom and X.R. Li, *Multitarget-Multisensor Tracking: Principles and Techniques*, Storrs, CT: YBS Publishing, 1995.

[13] Y. Bar-Shalom, X.R. Li, and T. Kirubarajan, *Estimation with Applications to Tracking and Navigation*, New York: John Wiley & Sons, 2001.

[14] G.A. Ackerson and K.S. Fu, "On state estimation in swithching environments", *IEEE Trans. on Automatic Control*, Vol. AC-15, pp. 10-17, Feb. 1970.

[15] J.K. Tugnait and A.H. Haddad, "A detection-estimation scheme for state estimation in switching environment", *Automatica*, Vol. 15, pp 477-481, 1979.

[16] H. Akashi and H. Kumamoto, "Random sampling approach to state estimation in switching environments", *Automatica*, Vol. 13, pp 429, 1977.

[17] J.K. Tugnait, "Detection and estimation for abruptly changing systems", *Automatica*, Vol. 18, pp. 607-615, Sept. 1982.

[18] H.A.P. Blom, "An efficient filter for abruptly changing systems," *Proceedings of the 23rd IEEE Conf. on Decision and Control*, pp. 656-658, Las Vegas, NV, 1984.

[19] H.A.P. Blom and Y. Bar-Shalom, "The interacting multiple model algorithm for systems with Markovian switching coefficients," *IEEE Transaction on Automatic Control*, Vol. 33, No 8, pp. 780-783, Aug. 1988.

[20] Y. Bar-Shalom, K.C. Chang, and H.A.P. Blom, "Tracking a maneuvering target using input estimation versus the interacting multiple model algorithm," *IEEE Transaction on Aerospace and Electronic Systems*, Vol. AES-25(2), pp. 296-300, March 1989.

[21] A. Houles and Y. Bar-Shalom, "Multisensor tracking of a maneuvering target in clutter", *IEEE Trans. Aerospace and Electronic Systems*, Vol. AES-25, pp. 176-188, March 1989.

[22] Y. Bar-Shalom and T. E. Fortmann, *Tracking and Data Association*, New York: Academic Press, 1988.

[23] H.A.P. Blom and E.A. Bloem, "Probabilistic data association avoiding track coalescence," *IEEE Trans. Automatic Control*, Vol. AC-45, pp.247-259, Feb. 2000.

[24] H.A.P. Blom and E.A. Bloem, "Combining IMM and JPDA for tracking multiple manuvering targets in clutter," *Proc. 5th Intern. Conf. on Information Fusion*, Annapolis, MD, Vol. 1, pp.705-712, July 8-11. 2002.

[25] J.K. Tugnait, "Tracking of multiple maneuvering targets in clutter using multiple sensors, IMM and JPDA coupled filtering", *IEEE Trans. Aerospace & Electronic Systems*, Vol. AES-40, pp. 320-330, Jan. 2004.

[26] B. Chen and J.K. Tugnait, "Tracking of multiple maneuvering targets in clutter using IMM/JPDA filtering and fixed-lag smoothing", *Automatica*, Vol. 37, pp. 239-249, Feb. 2001.

[27] Y. Bar-Shalom and W.D. Blair, *Multitarget-Multisensor Tracking: Application and Advances*, Vol. III, Artech House, Norwood, MA, 2000.

[28] W. Koch and G.V. Keuk, "Multiple hypothesis Track Maintenance with Possibly Unresolved Measurements", *IEEE Transaction on Aerospace and Electronic Systems*, Vol. 33, No.3, pp. 883-892, July 1997.

[29] X.R. Li and Y. Bar-Shalom, "Design of an interacting multiple algorithm for air traffic control tracking", *IEEE Transactions on Control System Technology*, pp. 186-194, Sept. 1993.

[30] H.A.P. Blom and Y. Bar-Shalom, "The interacting model multiple algorithm for systems with Markovian switching coefficients", *IEEE Trans. Automatic Control*, Vol. AC-33, pp. 780-783, Aug. 1988.

[31] X.R. Li and Y. Bar-Shalom, "Multiple model estimation with variable structure", *IEEE Transaction on Automatic Control*, Vol. 41, No.4, pp. 478-493, April 1996.

[32] X.R. Li, X. Zhi, and Y. Zhang, "Multiple model estimation with variable structure Part III: model group switching algorithm.", *IEEE Transaction on Aerospace and Electronic Systems*, Vol. 351, No.1, pp. 225-240, Jan. 1999.

[33] Y. Bar-Shalom and X.R. Li, *Estimation and Tracking: Principles, Techniques and Software*, Norwood, MA: Artech House, 1993.

[34] D. Willner, C.B. Chang, and K.P. Dunn, "Kalman filter algorithms for a multisensor system.", *Proceedings of 1976 IEEE Conf.on Decision and Control*, Clearwater Beach, FL, Dec. 1976.

[35] Y. Bar-Shalom, "Update with out-of-sequence measurements in tracking: exact solution", *Proc. SPIE Conf. Signal and Data Processing of Small Targets*, Vol. 4048, pp. 541-556, Orlando, FL, April 2000.

[36] Y. Bar-Shalom, M. Mallick, H. Chen, and R. Washburn, "One-step solution for the general out-of-sequence measurement problem in tracking", *Proc. IEEE Aerospace Conference*, Big Sky, MT, Vol. 70, pp. 4.1551-4.1559, March 2002.

[37] M. Mallick, J. Krant, and Y. Bar-Shalom, "Multi-sensor multi-target tracking using out-of-sequence measurements", *Proc. Fifth International Conference on Information Fusion*(Fusion 2002), Annapolis, MD, USA.

[38] S. Jeong and J.K. Tugnait, "Parallel detection fusion for multisensor tracking of a maneuvering target in clutter using IMMPDA filtering," in *Proc. 37th Annual Asilomar Conf. Signals Systems Computers*, Pacific Grove, CA, pp. 1213-1217, Nov. 2003.

[39] B.D.O. Anderson and J.B. Moore, *Optimal Filtering*, Eaglewood Cliffs, NJ: Prentice Hall, 1979.

[40] R.G. Brown and P.Y.C. Hwang, *"Introduction to random signals and applied Kalman filtering: with matlab exercises and solutions"*, John wiley and sons, 1997.

[41] M.S. Grewal and A.P. Andrews, *"Kalman filtering: Theory and Practice"* , Eaglewood Cliffs, NJ: Prentice Hall, 1993.

[42] K.V. Ramachandra, *Kalman Filtering Techniques for Radar Tracking*, New York, NY: Marcel Dekker, 2000.

[43] X.R. Li, "Hybrid estimation Techniques.",*Control and dynamic systems: advances in theory and application*, pp. 1-76, Vol 76, C.T. Leondes(Ed), New York Academic, 1996.

[44] S. Blackman and R. Popoli, *Design and Analysis of Modern Tracking Systems*, Norwood, MA: Artech House, 1999.

[45] F. Dufour and M. Mariton, "Tracking a 3D maneuvering target with passive sensors," *IEEE Trans. Aerospace and Electronic Systems*, Vol. AES-27, pp. 725-738, July 1991.

[46] N.N. Okello and G.W. Pulford, "Simultaneous registration and tracking for multiple radars with cluttered measurements", *Proc. 8th IEEE Workshop on Statistical Signal and Array Processing*, Corfu, Greece, pp. 60-63, June 1996.

[47] B. Chen and J.K. Tugnait, "Multisensor tracking of a maneuvering target in clutter using immpda fixed-lag smoothing", *IEEE Transactions on Aerospace and Electronic Systems*, Vol. 36, no.3, pp. 983-992, July 2000.

[48] G.W. Pulford and R.J. Evans, "Probabilistic sata association for systems with multiple simultaneous measurements", *Automatica*, Vol. 32(9), pp. 1311-1316, Sept. 1996.

[49] Y. Bar-Shalom, H. Chen, and M. Mallick, "One-step solution for the multistep out-of-sequence measurement problem in tracking," *IEEE Trans. Aerospace & Electronic Systems*, Vol. 40, No.1, pp. 27-35, Jan. 2004.

[50] S. Jeong and J.K. Tugnait, "Multisensor tracking of a maneuvering target in clutter with asynchronous measurements using IMMPDA filtering and parallel detection fusion," in *Proc. 2004 American Control Conf.*, Boston, MA, pp. 5350-5355, June 30-July 2, 2004.

[51] S. Challa, R. Evans, and X. Wang "A Bayesian solution and its approximations to out-of-sequence measurement problems," in *Journal of Information Fusion*, Vol. 4, No.3, pp. 185-199, Sept. 2003.

[52] X. Wang and S. Challa, "Augmented state IMM-PDA for OOSM solution to maneuvering target tracking in clutter," in *Radar Conference, 2003. Proceedings of the International*, pp. 479-485, Sept. 2003.

[53] G.W. Pulford and R. J. Evans, "A multipath data association tracker for over-the-horizon radar", *IEEE Transactions on Aerospace and Electronic Systems*, Vol. AES-34, pp. 1165-1183, Oct. 1998.

[54] L.C. Ng and Y. Bar-Shalom, "Modeling of unresolved measurements for multitarget tracking", *Proc. OCEANS '81 Conf.*, Boston, MA, pp. 982-987, Sept. 1981.

[55] G.V. Trunk, "Range resolution of targets using automatic detectors", *IEEE Trans. Aerospace and Electronic Systems*, Vol. AES-14, pp. 750-755, Sept. 1978.

[56] G.V. Trunk and J.D. Wilson, "Track initiation of occasionally unresolved radar targets", *IEEE Trans. Aerospace and Electronic Systems*, Vol. AES-17, pp. 122-130, Jan. 1981.

# Appendices

## Appendix A

## Derivation of the mode-conditioned association event probability Eqn. (3.46)

To evaluate the mode-conditioned association event probabilities, the conditioning is broken down into the past data $Z^{k-1}$ as well as the latest data $Y_k^1$ and $Y_k^2$. A probabilistic interference can be made on both the number of measurements in the validation region (from the clutter density, if known) and on their location. This can be written out as [21]

$$\begin{aligned}
\beta_k^{j,a,b}: &= P[\theta_k^{a,b}|M_k^j, Y_k^1, Y_k^2, Z^{k-1}] = \frac{p(\theta_k^{a,b}, M_k^j, Y_k^1, Y_k^2, Z^{k-1})}{P[M_k^m, Y_k^1, Y_k^2, Z^{k-1}]} \\
&= \frac{p(Y_k^1, Y_k^2|\theta_k^{a,b}, M_k^j, Z^{k-1})P[\theta_k^{a,b}|M_k^j, Z^{k-1}]P[M_k^j, Z^{k-1}]}{\sum_\theta p(Y_k^1, Y_k^2|\theta_k^{a,b}, M_k^j, Z^{k-1})P[\theta_k^{a,b}|M_k^j, Z^{k-1}]P[M_k^j, Z^{k-1}]} \\
&= \frac{p(Y_k^1, Y_k^2|\theta_k^{a,b}, M_k^j, Z^{k-1})P[\theta_k^{a,b}|M_k^j, Z^{k-1}]p[Z^{k-1}|M_k^j]P[M_k^j]}{\sum_\theta p(Y_k^1, Y_k^2|\theta_k^{a,b}, M_k^j, Z^{k-1})P[\theta_k^{a,b}|M_k^j, Z^{k-1}]p[Z^{k-1}|M_k^j]P[M_k^j]} \\
&= \frac{1}{c}p(Y_k^1, Y_k^2|\theta_k^{a,b}, M_k^j, Z^{k-1})P[\theta_k^{a,b}|M_k^j, Z^{k-1}] \qquad \text{(A.1)}
\end{aligned}$$

where $c$ is a normalization constant such that $\sum_{a=0}^{m_1}\sum_{b=0}^{m_2}\beta_k^{j,a,b} = 1$. The first term of the right side of (A.1) is [12, 21]

$$p\{Y_k^1, Y_k^2|\theta_k^{a,b}, M_k^j, Z^{k-1}\}$$

$$= \begin{cases} \left[V_k^1\right]^{-\bar{m}_1} \left[V_k^2\right]^{-\bar{m}_2}, & a=0,\ b=0 \\ P_{G_2}^{-1} \left[V_k^2\right]^{-\bar{m}_2+1} \times \mathcal{N}\left[\nu_k^{j,2(b)}; 0, S_k^{j,2}\right], & a=0,\ b=1,\cdots,\bar{m}_2 \\ P_{G_1}^{-1} \left[V_k^1\right]^{-\bar{m}_1+1} \times \mathcal{N}\left[\nu_k^{j,1(a)}; 0, S_k^{j,1}\right], & a=1,\cdots,\bar{m}_1,\ b=0 \\ P_{G_1}^{-1} \left[V_k^1\right]^{-\bar{m}_1+1} P_{G_2}^{-1} \left[V_k^2\right]^{-\bar{m}_2+1} \times \mathcal{N}\left[\nu_k^{j,a,b}; 0, S_k^{j}\right], & a=1,\cdots,\bar{m}_1,\ b=1,\cdots,\bar{m}_2. \end{cases} \tag{A.2}$$

As in [12, 21], we have

$$P[\theta^{a,b}|M_k^j, Z^{k-1}] = P[\theta^{a,b}|\bar{\mathbf{m}}_1 = \bar{m}_1, \bar{\mathbf{m}}_2 = \bar{m}_2] \tag{A.3}$$

where we have conditioning on the total number of validated measurements obtained from sensor $l$, $\bar{\mathbf{m}}_l = \bar{m}_l$; in this notation $\bar{\mathbf{m}}_l$ is the random variable and $\bar{m}_l$ is its realization. Denoting by $\phi_l$ the number of false measurements, one has

$$\begin{aligned} P[\theta^{a,b}|\bar{\mathbf{m}}_1 = \bar{m}_1, \bar{\mathbf{m}}_2 = \bar{m}_2] &= P[\theta^{a,b}|\phi_1 = \bar{m}_1, \phi_2 = \bar{m}_2] P[\phi_1 = \bar{m}_1, \phi_2 = \bar{m}_2] \\ &+ P[\theta^{a,b}|\phi_1 = \bar{m}_1, \phi_2 = \bar{m}_2 - 1] P[\phi_1 = \bar{m}_1, \phi_2 = \bar{m}_2 - 1] \\ &+ P[\theta^{a,b}|\phi_1 = \bar{m}_1 - 1, \phi_2 = \bar{m}_2] P[\phi_1 = \bar{m}_1 - 1, \phi_2 = \bar{m}_2] \\ &+ P[\theta^{a,b}|\phi_1 = \bar{m}_1 - 1, \phi_2 = \bar{m}_2 - 1] P[\phi_1 = \bar{m}_1 - 1, \phi_2 = \bar{m}_2 - 1] \end{aligned}$$

$$= \begin{cases} 1 \times P\left[\phi_1 = \bar{m}_1, \phi_2 = \bar{m}_2\right] & a=0,\ b=0 \\ \frac{1}{\bar{m}_2} \times P\left[\phi_1 = \bar{m}_1, \phi_2 = \bar{m}_2 - 1\right] & a=0,\ b=1,\cdots,\bar{m}_2 \\ \frac{1}{\bar{m}_1} \times P\left[\phi_1 = \bar{m}_1 - 1, \phi_2 = \bar{m}_2\right] & a=1,\cdots,\bar{m}_1,\ b=0 \\ \frac{1}{\bar{m}_1 \bar{m}_2} \times P\left[\phi_1 = \bar{m}_1 - 1, \phi_2 = \bar{m}_2 - 1\right] & a=1,\cdots,\bar{m}_1,\ b=1,\cdots,\bar{m}_2 \end{cases} \tag{A.4}$$

since $\phi_l$ must be either $\bar{m}_l - 1$ (if the target has been detected from sensor $l$ and its measurement fell in the validation gate) or $\bar{m}_l$. Using Bayes' formula one has

$$
\begin{aligned}
P[\phi_1 = \bar{m}_1, \phi_2 = \bar{m}_2 | \mathbf{m}_1 = \bar{m}_1, \mathbf{m}_2 = \bar{m}_2] &= \frac{\left(1-P_{D_1}P_{G_1}\right)\left(1-P_{D_1}P_{G_1}\right)\mu_F(\bar{m}_1)\mu_F(\bar{m}_2)}{P\{\mathbf{m}_1=\bar{m}_1, \mathbf{m}_2=\bar{m}_2\}} \\
P[\phi_1 = \bar{m}_1, \phi_2 = \bar{m}_2 - 1 | \mathbf{m}_1 = \bar{m}_1, \mathbf{m}_2 = \bar{m}_2] &= \frac{\left(1-P_{D_1}P_{G_1}\right)\left(P_{D_2}P_{G_2}\right)\mu_F(\bar{m}_1)\mu_F(\bar{m}_2-1)}{P\{\mathbf{m}_1=\bar{m}_1, \mathbf{m}_2=\bar{m}_2\}} \\
P[\phi_1 = \bar{m}_1 - 1, \phi_2 = \bar{m}_2 | \mathbf{m}_1 = \bar{m}_1, \mathbf{m}_2 = \bar{m}_2] &= \frac{\left(P_{D_1}P_{G_1}\right)\left(1-P_{D_2}P_{G_2}\right)\mu_F(\bar{m}_1-1)\mu_F(\bar{m}_2)}{P\{\mathbf{m}_1=\bar{m}_1, \mathbf{m}_2=\bar{m}_2\}} \\
P[\phi_1 = \bar{m}_1 - 1, \phi_2 = \bar{m}_2 - 1 | \mathbf{m}_1 = \bar{m}_1, \mathbf{m}_2 = \bar{m}_2] &= \frac{\left(P_{D_1}P_{G_1}\right)\left(P_{D_2}P_{G_2}\right)\mu_F(\bar{m}_1-1)\mu_F(\bar{m}_2-1)}{P\{\mathbf{m}_1=\bar{m}_1, \mathbf{m}_2=\bar{m}_2\}}
\end{aligned}
\tag{A.5}
$$

where $\mu_F(m_l)$ is the probability mass function (pmf) of the number of false measurements and $P_{D_l}P_{G_l}$ is the probability that the target has been detected and its measurements fell in the gate for sensor $l$. The common denominator in (A.5) is

$$
\begin{aligned}
P[\mathbf{m}_1 = \bar{m}_1, \mathbf{m}_2 = \bar{m}_2] \;=\; & \left(1 - P_{D_1}P_{G_1}\right)\left(1 - P_{D_1}P_{G_1}\right)\mu_F(\bar{m}_1)\mu_F(\bar{m}_2) \\
& + \left(1 - P_{D_1}P_{G_1}\right)\left(P_{D_2}P_{G_2}\right)\mu_F(\bar{m}_1)\mu_F(\bar{m}_2 - 1) \\
& + \left(P_{D_1}P_{G_1}\right)\left(1 - P_{D_2}P_{G_2}\right)\mu_F(\bar{m}_1 - 1)\mu_F(\bar{m}_2) \\
& + \left(P_{D_1}P_{G_1}\right)\left(P_{D_2}P_{G_2}\right)\mu_F(\bar{m}_1 - 1)\mu_F(\bar{m}_2 - 1).
\end{aligned}
\tag{A.6}
$$

From (A.5) and (A.6) we have

$$
P[\theta^{a,b} | M_k^j, Z^{k-1}] = P[\theta^{a,b} | \bar{m}_1, \bar{m}_2]
$$

$$
= \begin{cases}
(1-P_{D_1}P_{G_1})\frac{\mu_F(\bar{m}_1)}{\mu_F(\bar{m}_1-1)}\left[P_{D_1}P_{G_1}+(1-P_{D_1}P_{G_1})\frac{\mu_F(\bar{m}_1)}{\mu_F(\bar{m}_1-1)}\right]^{-1} & \\
\quad\times\ (1-P_{D_2}P_{G_2})\frac{\mu_F(\bar{m}_2)}{\mu_F(\bar{m}_2-1)}\left[P_{D_2}P_{G_2}+(1-P_{D_2}P_{G_2})\frac{\mu_F(\bar{m}_2)}{\mu_F(\bar{m}_2-1)}\right]^{-1}, & a=0,\ b=0 \\
(1-P_{D_1}P_{G_1})\frac{\mu_F(\bar{m}_1)}{\mu_F(\bar{m}_1-1)}\left[P_{D_1}P_{G_1}+(1-P_{D_1}P_{G_1})\frac{\mu_F(\bar{m}_1)}{\mu_F(\bar{m}_1-1)}\right]^{-1} & \\
\quad\times\ \frac{1}{\bar{m}_2}P_{D_2}P_{G_2}\left[P_{D_2}P_{G_2}+(1-P_{D_2}P_{G_2})\frac{\mu_F(\bar{m}_2)}{\mu_F(\bar{m}_2-1)}\right]^{-1}, & a=0,\ b=1,\cdots,\bar{m}_2 \\
\frac{1}{\bar{m}_1}P_{D_1}P_{G_1}\left[P_{D_1}P_{G_1}+(1-P_{D_1}P_{G_1})\frac{\mu_F(\bar{m}_1)}{\mu_F(\bar{m}_1-1)}\right]^{-1} & \\
\quad\times\ (1-P_{D_2}P_{G_2})\frac{\mu_F(\bar{m}_2)}{\mu_F(\bar{m}_2-1)}\left[P_{D_2}P_{G_2}+(1-P_{D_2}P_{G_2})\frac{\mu_F(\bar{m}_2)}{\mu_F(\bar{m}_2-1)}\right]^{-1}, & a=1,\cdots,\bar{m}_1,\ b=0 \\
\frac{1}{\bar{m}_1}P_{D_1}P_{G_1}\left[P_{D_1}P_{G_1}+(1-P_{D_1}P_{G_1})\frac{\mu_F(\bar{m}_1)}{\mu_F(\bar{m}_1-1)}\right]^{-1} & \\
\quad\times\ \frac{1}{\bar{m}_2}P_{D_2}P_{G_2}\left[P_{D_2}P_{G_2}+(1-P_{D_2}P_{G_2})\frac{\mu_F(\bar{m}_2)}{\mu_F(\bar{m}_2-1)}\right]^{-1}, & a=1,\cdots,\bar{m}_1,\ b=1,\cdots,\bar{m}_2.
\end{cases} \tag{A.7}
$$

Using the (nonparametric) diffuse prior model [12]

$$
\mu_F(\bar{m}_l) = \mu_F(\bar{m}_l - 1) = \delta \tag{A.8}
$$

where $\delta$ is irrelevant since it cancels out. Exploiting the diffuse model for clutter, we obtain Eqn. (3.46).

## Appendix B

## Derivation of Eqn. (6.62)

For the coupled state vector $x_k$ of a group of two targets defined in (6.2), the conditional probability of unresolved targets given $x_k$ is defined as (6.28)

$$\begin{aligned} P(\mathcal{A}|x_k) &= \exp\left\{-\frac{1}{2}\left[h^l(x_k(1)) - h^l(x_k(2))\right]^T R^{l,d^{-1}}\left[h^l(x_k(1)) - h^l(x_k(2))\right]\right\} \\ &= \left|2\pi R^{l,d}\right|^{1/2}\mathcal{N}\left(0; h^{l,d}(x_k), R^{l,d}\right). \end{aligned} \tag{B.1}$$

From the definition of Eqns. (6.62) and (6.28), $P_k^{J,1,a}$ can be expressed as

$$\begin{aligned} P_k^{J,1,a} &= \int P(\mathcal{A}|x_k)\mathcal{N}(x_k; \hat{x}^J_{k|k-1}, P^J_{k|k-1})dx_k \\ &= \int \left|2\pi R^{l,d}\right|^{1/2}\mathcal{N}\left(0; h^{l,d}(x_k), R^{l,d}\right)\mathcal{N}\left(x_k; \hat{x}^J_{k|k-1}, P^J_{k|k-1}\right)dx_k. \\ &= \frac{1}{\left|2\pi P^k\right|^{1/2}}\int \exp\left\{-\frac{1}{2}\left[(\Pi x_k)^T A^{-1}\Pi x_k + (x_k - \hat{x}_k)^T P_k^{-1}(x_k - \hat{x}_k)\right]\right\}dx_k \end{aligned} \tag{B.2}$$

where we redefine

$$\hat{x}_k := \hat{x}^J_{k|k-1}, \quad P_k := P^J_{k|k-1}, \quad \Pi := H_k^{J,1,d}, \quad A := R^{1,d}. \tag{B.3}$$

Let

$$\Upsilon = \left[(\Pi x_k)^T A^{-1}\Pi x_k + (x_k - \hat{x}_k)^T P_k^{-1}(x_k - \hat{x}_k)\right]. \tag{B.4}$$

Recall that the trace of an $n \times n$ matrix is the sum of its diagonal elements, and, from the elementary properties of trace ('tr' stands for 'trace'):

1. $\mathrm{tr}(A) := \sum_{i=1}^n a_{ii} = \mathrm{tr}(A')$ where $a_{ii}$ is the elements of $A$

2. $\mathrm{tr}(AB) = \mathrm{tr}(BA)$ where $A$ is $m \times n$ and $B$ is $n \times m$

3. $\mathrm{tr}(ABC) = \mathrm{tr}(BCA) = \mathrm{tr}(CAB)$ where $A$, $B$, and $C$ are $n \times n$

4. $x^T Ax = \mathrm{tr}(x^T Ax) = \mathrm{tr}(x^T Ax)$, where $x$ is a $n \times 1$ column vector and $A$ is $n \times n$ matrix,

it is clear that $\Upsilon$ is equal to $\mathrm{tr}(\Upsilon)$. Thus we can manipulate (B.4) as follows;

$$\begin{aligned}
\Upsilon &= \mathrm{tr}\left[(\Pi x_k)^T A^{-1} \Pi x_k + (x_k - \hat{x}_k)^T P_k^{-1} (x_k - \hat{x}_k)\right]_{1\times 1} \\
&= \mathrm{tr}\left[\left(\Pi^T A^{-1}\Pi + P_k^{-1}\right) x_k x_k^T - P_k^{-1}\hat{x}_k x_k^T - \hat{x}_k^T P_k^{-1} x_k + \hat{x}_k^T P_k^{-1}\hat{x}_k\right] \\
&= \mathrm{tr}\left[R^{-1} x_k x_k^T - Q x_k^T - Q^T x_k + \hat{x}_k^T P_k^{-1}\hat{x}_k\right] \\
&= \mathrm{tr}\left[x_k^T R^{-1} x_k - R^{-1} R Q x_k^T - x_k Q^T R R^{-1} + \hat{x}_k^T P_k^{-1}\hat{x}_k\right] \\
&= \mathrm{tr}\left[x_k^T R^{-1} x_k - R^{-1} U x_k^T - x_k U^T R^{-1} + U^T R^{-1} U - U^T R^{-1} U + \hat{x}_k^T P_k^{-1}\hat{x}_k\right] \\
&= \left[x_k^T R^{-1} x_k - R^{-1} U x_k^T - x_k U^T R^{-1} + U^T R^{-1} U - U^T R^{-1} U + \hat{x}_k^T P_k^{-1}\hat{x}_k\right] \\
&= (x_k - U)^T R^{-1} (x_k - U) + \hat{x}_k^T P_k^{-1}\hat{x}_k - U^T R^{-1} U \qquad \text{(B.5)}
\end{aligned}$$

where, for simplicity,

$$\begin{aligned}
&Q := P_k^{-1}\hat{x}_k, \quad R := \left(\Pi^T A^{-1}\Pi + P_k^{-1}\right)^{-1}, \\
&U := RQ = \left(\Pi^T A^{-1}\Pi + P_k^{-1}\right)^{-1} P_k^{-1}\hat{x}_k. \qquad \text{(B.6)}
\end{aligned}$$

Next from (B.3) and (B.5), Eqn. (6.62) can be rewritten as

$$P_k^{J,1,a} = \frac{|2\pi R|^{1/2}}{|2\pi P_k|^{1/2}} \exp\left\{-\frac{1}{2}\left[\hat{x}_k^T P_k^{-1}\hat{x}_k - U^T R^{-1} U\right]\right\}$$

$$\times \int \frac{1}{|2\pi R|^{1/2}} \exp\left\{-\frac{1}{2}\left(x_k - U\right)^T R^{-1}\left(x_k - U\right)\right\} dx_k. \tag{B.7}$$

From the second term (integration part) in (B.7), since $x_k$ is a Gaussian random vector with parameters $U$ and $R$, the integration part of (B.7) turns out to be

$$\int \frac{1}{|2\pi R|^{1/2}} \exp\left\{-\frac{1}{2}\left(x_k - U\right)^T R^{-1}\left(x_k - U\right)\right\} dx_k = 1. \tag{B.8}$$

Therefore, now we get

$$P_k^{J,1,a} = \frac{|2\pi R|^{1/2}}{|2\pi P_k|^{1/2}} \exp\left\{-\frac{1}{2}\left[\hat{x}_k^T P_k^{-1} \hat{x}_k - U^T R^{-1} U\right]\right\}. \tag{B.9}$$

Then from (B.6), the exponential part of (B.9) can be obtained as

$$\begin{aligned}
&\hat{x}_k^T P_k^{-1} \hat{x}_k - U^T R^{-1} U \\
&\quad = \hat{x}_k^T P_k^{-1} \hat{x}_k - Q^T R Q \\
&\quad = \hat{x}_k^T P_k^{-1} \hat{x}_k - \hat{x}_k^T P_k^{-1} R P_k^{-1} \hat{x}_k \\
&\quad = \hat{x}_k^T \left[P_k^{-1} - P_k^{-1}\left[\Pi^T A^{-1} \Pi + P_k^{-1}\right]^{-1} P_k^{-1}\right] \hat{x}_k \\
&\quad = \hat{x}_k^T \left[P_k^{-1} - P_k^{-1}\left[P_k - P_k \Pi^T \left[\Pi P_k \Pi^T + A\right]^{-1} \Pi P_k\right] P_k^{-1}\right] \hat{x}_k \\
&\quad = \hat{x}_k^T \left[\Pi^T \left[\Pi P_k \Pi^T + A\right]^{-1} \Pi\right] \hat{x}_k \\
&\quad = \left(\Pi \hat{x}_k\right)^T \left[\Pi P_k \Pi^T + A\right]^{-1} \Pi \hat{x}_k.
\end{aligned} \tag{B.10}$$

Substituting $\left(\Pi \hat{x}_k\right)^T \left[\Pi P_k \Pi^T + A\right]^{-1} \Pi \hat{x}_k$ for $\hat{x}_k^T P_k^{-1} \hat{x}_k - U^T R^{-1} U$ (B.10) thus yields

$$
\begin{aligned}
P_k^{J,1,a} &= \frac{|R|^{1/2}}{|P_k|^{1/2}} \exp\left\{-\frac{1}{2}\left(\Pi\hat{x}_k\right)^T\left[\Pi P_k\Pi^T + A\right]^{-1}\Pi\hat{x}_k\right\} \\
&= \frac{|R|^{1/2}(2\pi)^{n_z/2}\left|\Pi P_k\Pi^T + A\right|^{1/2}}{|P_k|^{1/2}}\mathcal{N}\left(0;\Pi\hat{x}_k, \Pi P_k\Pi^T + A\right). \qquad \text{(B.11)}
\end{aligned}
$$

Recall the elementary identities of determinants ('det' stands for 'determinant'):

1. $\det(AB) = \det(A)\det(B) = \det(BA)$ where $A$ and $B$ are square matrices

2. $\det(I_n - AB) = \det(I_m - BA)$ where $A$ is $n \times m$ and $B$ is $m \times n$.

The determinant operation part of (B.11) can by simplified as ($|A| = \det(A)$)

$$
\frac{|R|^{1/2}\left|\Pi P_k\Pi^T + A\right|^{1/2}}{|P_k|^{1/2}} = \left(\det\left[\left(\Pi P_k\Pi^T + A\right)RP_k^{-1}\right]\right)^{1/2}. \qquad \text{(B.12)}
$$

Then we also rewrite (B.12) as

$$
\begin{aligned}
&\det\left[\left(\Pi P_k\Pi^T + A\right)RP_k^{-1}\right] \\
&\quad = \det\left[\left(\Pi P_k\Pi^T + A\right)\left(P_k - P_k\Pi^T\left[\Pi P_k\Pi^T + A\right]^{-1}\Pi P\right)P_k^{-1}\right] \\
&\quad = \det\left[\left(\Pi P_k\Pi^T + A\right)\left(I - P_k\Pi^T\left[\Pi P_k\Pi^T + A\right]^{-1}\Pi\right)\right] \\
&\quad = \det\left(\Pi P_k\Pi^T + A\right)\det\left(I - P_k\Pi^T\left[\Pi P_k\Pi^T + A\right]^{-1}\Pi\right) \\
&\quad = \det\left(\Pi P_k\Pi^T + A\right)\det\left(I - \left[\Pi P_k\Pi^T + A\right]^{-1}\Pi P_k\Pi^T\right) \\
&\quad = \det\left(\Pi P_k\Pi^T + A - \Pi P_k\Pi^T\right) = \det(A) = |A|.
\end{aligned} \qquad \text{(B.13)}
$$

From (B.3), (B.11), (B.12), and (B.13), it turns out that

$$
\begin{aligned}
P_k^{J,1,a} &:= (2\pi)^{n_z/2} \left|A\right|^{1/2} \mathcal{N}\left(0;\Pi\hat{x}_k, \Pi P_k \Pi^T + A\right) \\
&= \left|2\pi R^{1,d}\right|^{1/2} \mathcal{N}\left(0; \begin{bmatrix} H_k^{j_1,1} & -H_k^{j_2,1} \end{bmatrix} x_{k|k-1}^J, \begin{bmatrix} H_k^{j_1,1} & -H_k^{j_2,1} \end{bmatrix} P_{k|k-1}^{J,1} \begin{bmatrix} H_k^{j_1,1'} \\ H_k^{j_2,1'} \end{bmatrix} + R^{1,d}\right).
\end{aligned} \tag{B.14}
$$